



Article

Discovery of novel pERK1/2- or #-Arrestin-Preferring 5-HT_{1A} Receptor Biased Agonists: Diversified Therapeutic-Like vs. Side Effects Profile

Joanna Snieciakowska, Monika Guch-Lutwin, Adam Bucki, Anna Wiackowska, Agata Siwek, Magdalena Jastrzbska-Wisek, Anna Partyka, Daria Wilczynska, Karolina Pytko, Gniewomir Latacz, Katarzyna Przejczowska-Pomierny, Elbieta Wyska, Anna Wesoowska, Maciej H. Pawowski, Adrian Newman-Tancredi, and Marcin Koczowski

J. Med. Chem., **Just Accepted Manuscript** • DOI: 10.1021/acs.jmedchem.0c00814 • Publication Date (Web): 04 Sep 2020

Downloaded from pubs.acs.org on September 4, 2020

Just Accepted

"Just Accepted" manuscripts have been peer-reviewed and accepted for publication. They are posted online prior to technical editing, formatting for publication and author proofing. The American Chemical Society provides "Just Accepted" as a service to the research community to expedite the dissemination of scientific material as soon as possible after acceptance. "Just Accepted" manuscripts appear in full in PDF format accompanied by an HTML abstract. "Just Accepted" manuscripts have been fully peer reviewed, but should not be considered the official version of record. They are citable by the Digital Object Identifier (DOI®). "Just Accepted" is an optional service offered to authors. Therefore, the "Just Accepted" Web site may not include all articles that will be published in the journal. After a manuscript is technically edited and formatted, it will be removed from the "Just Accepted" Web site and published as an ASAP article. Note that technical editing may introduce minor changes to the manuscript text and/or graphics which could affect content, and all legal disclaimers and ethical guidelines that apply to the journal pertain. ACS cannot be held responsible for errors or consequences arising from the use of information contained in these "Just Accepted" manuscripts.

Discovery of novel pERK1/2- or β -Arrestin-Preferring 5-HT_{1A} Receptor Biased Agonists: Diversified Therapeutic-Like vs. Side Effects Profile

Joanna Sniecikowska ^a, Monika Gluch-Lutwin ^a, Adam Bucki ^a, Anna Więckowska ^a, Agata Siwek ^a, Magdalena Jastrzebska-Wiesek ^a, Anna Partyka ^a, Daria Wilczyńska ^a, Karolina Pytko ^a, Gniewomir Latacz ^a, Katarzyna Przejczowska-Pomierny ^a, Elżbieta Wyska ^a, Anna Wesołowska ^a, Maciej Pawłowski ^a, Adrian Newman-Tancredi ^b, Marcin Kolaczowski ^{a*}

^a Jagiellonian University Medical College, Faculty of Pharmacy, 9 Medyczna St., 30-688 Kraków, Poland;

^b Neurolix Inc. 251 Little Falls Drive Wilmington, 19808 Delaware, USA

ABSTRACT

Novel 1-(1-benzoylpiperidin-4-yl)methanamine derivatives with high affinity and selectivity for serotonin 5-HT_{1A} receptors were obtained and tested in four functional assays: ERK1/2 phosphorylation, adenylyl cyclase inhibition, calcium mobilization and β -arrestin recruitment. Compounds **44** and **56** (2-methylaminophenoxyethyl and 2-(1H-indol-4-yloxy)ethyl derivatives, respectively) were selected as biased agonists with highly differential “signaling fingerprints” that translated into distinct *in vivo* profiles. *In vitro*, **44** showed biased agonism for ERK1/2 phosphorylation and, *in vivo*, it preferentially exerted antidepressant-like effect in the Porsolt forced swimming test (FST) in rat. In contrast, compound **56** exhibited a first-in-class profile: it preferentially and potently activated β -arrestin recruitment *in vitro* and potently elicited lower lip retraction (LLR) *in vivo*, a component of “serotonergic syndrome”. Both compounds showed promising developability properties. The presented 5-HT_{1A} receptor biased agonists, preferentially targeting various signaling pathways, have the potential to become drug candidates for distinct CNS pathologies and possessing accentuated therapeutic activity and reduced side effects.

INTRODUCTION

Although serotonin 5-HT_{1A} receptors exert major influence in CNS functions such as mood, pain and movement, and were identified several decades ago^{1,2} it is notable that there are still no selective 5-HT_{1A} receptor agonists approved for therapeutic intervention. There are, of course, commercialized drugs that exhibit some agonist properties at 5-HT_{1A} receptors, including the anxiolytic buspirone (Buspar[®]), the antidepressant vortioxetine (Brintellix[®]), the antipsychotic aripiprazole (Abilify[®]), and the antiparkinsonian bromocriptine (Parlodel[®]).^{3–6} However, all of these compounds also interact with other targets, including other monoamine receptors or transporters, and they only partially activate 5-HT_{1A} receptors (i.e. they function as ‘partial agonists’). Moreover, such compounds do not discriminate between subpopulations of 5-HT_{1A} receptors which are expressed in different brain regions and that mediate various, sometimes opposing, physiological and behavioral responses. For example, activation of post-synaptic 5-HT_{1A} heteroreceptors in frontal cortex elicits procognitive and antidepressant effects, whereas activation of pre-synaptic 5-HT_{1A} autoreceptors is associated with pro-depressive effects, notably by inhibiting the release of serotonin in terminal regions.^{7,8} These contrasting effects have long been the object of discussion in the search for more efficacious antidepressants and suggest that indiscriminate activation of multiple 5-HT_{1A} receptor subpopulations may limit the therapeutic efficacy of 5-HT_{1A} receptor agonists or elicit unacceptable side effects. In contrast, recent advances have shown that it is possible to selectively target 5-HT_{1A} receptors in desired brain areas, such as cortex or brain stem, leading to significantly improved and promising therapeutic-like outcomes.

The basis for such preferential brain region targeting is the emerging concept of ‘biased agonism’ at G-protein-coupled receptors. Accumulated studies in recent years provide compelling evidence that different agonists can preferentially activate intracellular signaling via specific effectors, such as different G-protein subtypes or β -arrestins. Given that coupling to particular signaling mechanisms can vary from one brain region to another, this provides a basis for biased agonists to differentially activate particular brain regions. Such differential signaling may be associated with specific

neurochemical, physiological and behavioral responses, and has been proposed in the context of drug discovery at a variety of receptor subtypes as a strategy to achieve superior therapeutic outcomes.^{9–11}

In the case of 5-HT_{1A} receptors, an important advance was the discovery of a first highly selective biased agonist, NLX-101 (aka F15599, **1**), which shows a marked preference for ERK1/2 phosphorylation vs. other signaling pathways (Figure 1).^{12,13} **1** displayed a strikingly superior activity profile in a variety of electrophysiology, microdialysis, behavior and brain imaging studies, as compared to older, canonical 5-HT_{1A} receptor agonists.^{14–16} In particular, **1** exhibited highly promising properties in models of antidepressant and procognitive activity, as well as in models of respiratory deficits in Rett syndrome, an orphan disorder.^{17,18} The discovery of **1** therefore opened the way for drug discovery of novel, selective biased agonists that target 5-HT_{1A} receptors in specific brain areas that control CNS functions and that constitute, potentially, more efficacious and safer pharmacotherapeutics.

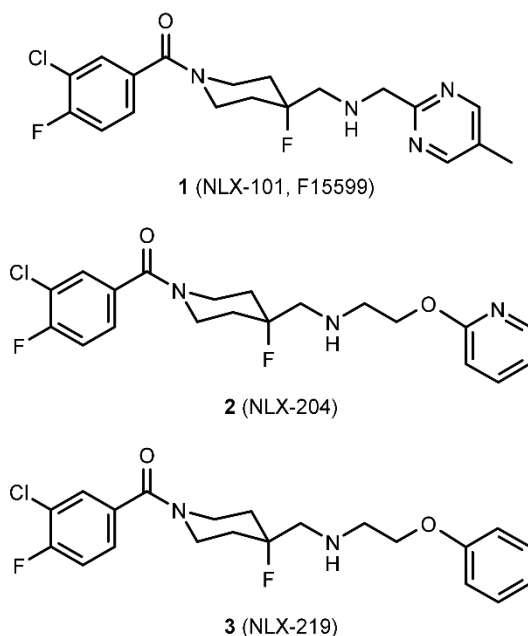


Figure 1. Selective 5-HT_{1A} receptor biased agonists.

However, despite its broad pharmacological characterization, **1** remained isolated as a single example of a biased agonist with a superior pharmacological profile but with no medicinal chemistry

data allowing for rational design of other functionally selective 5-HT_{1A} receptor agonists. In this context, our previous work investigated the SAR and Structure Functional Activity Relationships (SFARs) of novel analogues designed based on the structure of **1**.¹³ In that study, we identified a new, patentable and synthetically versatile chemotype of selective 5-HT_{1A} receptor biased agonists that preferentially activate ERK1/2 phosphorylation *in vitro* and show potent antidepressant-like properties *in vivo*. These findings met our objectives but did not identify structures that may exhibit other biased agonist profiles, notably for β -arrestin recruitment which, as mentioned above, is a major target for GPCR biased agonist studies.

The present study builds upon the conclusion that the pyridine-2-oxy- or phenoxy-ethyl or derivatives of 1-(1-benzoylpiperidin-4-yl)methanamine, represented by lead structures **2** (NLX-204) and **3** (NLX-219), are the most promising chemotypes for obtaining new selective full agonists of the 5-HT_{1A} receptor (Figure 1). Since our previous work studied various unsubstituted derivatives, we focused herein on determining the influence of substitution pattern at the phenyl ring. Based on molecular modeling studies, we observed that phenyl moiety binds in the part of the receptor that is responsible for the stabilization of various bioactive conformations (between transmembrane helices 3, 5 and 6), thus justifying diversification of this fragment to obtain biased agonists with novel profiles of functional selectivity.^{13,19} Specifically, we aimed to obtain, on the one hand, agonists with higher levels of bias for specific signaling pathways (notably pERK1/2) and, on the other hand, agonists exhibiting bias for signaling pathways other than pERK1/2 (notably β -arrestin recruitment). Such biased agonists with diversified functional profiles could prove to be beneficial for different CNS disorders involving serotonergic dysregulation. A series of variously substituted phenoxyethyl derivatives of 1-(1-benzoylpiperidin-4-yl)methanamine was therefore synthesized and extensively tested in a stepwise manner to yield novel, selective and functionally diversified 5-HT_{1A} receptor agonists. As well as broadening our knowledge about the pharmacology of 5-HT_{1A} receptors, such compounds could constitute promising candidates for treatment of different disorders involving serotonergic neurotransmission, some of which (such as depression) may be anticipated to respond

to pERK1/2 biased agonists whereas others may be better treated with β -arrestin biased agonists. Overall, the availability of novel compounds differentially targeting these key signaling mechanisms raises the prospect of achieving increased therapeutic efficacy with reduced side effects in the treatment of CNS disorders.

RESULTS AND DISCUSSION

Design of a novel series of variously substituted phenoxyethyl derivatives of 1-(1-benzoylpiperidin-4-yl)methanamine

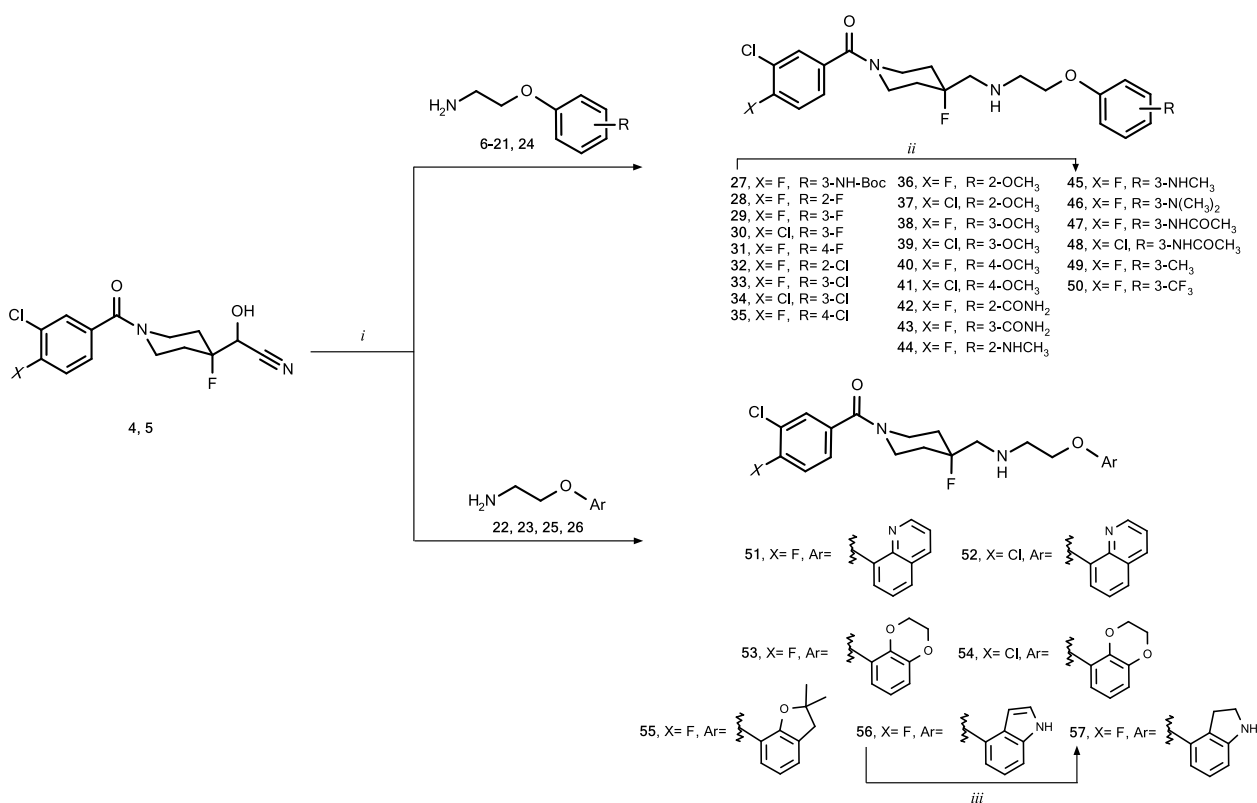
In the present study, we decided to use compound **3**, a previously described unsubstituted phenoxyethyl derivative of 1-(1-benzoylpiperidin-4-yl)methanamine, as a lead structure for modifications. The previously assessed *in silico* developability measures for compound **3**, namely CNS MPO = 4.89, LELP = 6.7 and Fsp3 = 0.38, were considered favorable.¹³ However, to further confirm the properties of this compound as a good lead structure, some *in vitro* studies were applied. They included metabolic stability using rat liver microsomes (RLMs), membrane permeability using PAMPA assay, hepatotoxicity on HepG2 cell line, as well as extended selectivity study on a multitarget panel, including 45 receptors (for the sake of comparison between the lead structure and the most interesting derivatives developed within the present study, the abovementioned data for these compounds was collected in Table 7 and Chart 1 as well as supporting information Table S3). Compound **3** showed acceptable metabolic stability, high permeability, very low potential for hepatotoxicity and significant (at least 500x) selectivity versus the off-targets, including hERG channel, thus proving to be a good starting point for further modifications. The structural diversification was focused on introducing various substituents to the phenoxy moiety, in order to modulate the functional profile, while maintaining favorable developability. The choice of substituents was controlled primarily by molecular weight, number of hydrogen bond donors and

lipophilicity, as well as synthetic feasibility of the final molecules. As a result, a set of 30 novel compounds was proposed for chemical synthesis and pharmacological evaluation.

Synthesis

To prepare the target compounds **28–57** we have utilized a method that we have previously used and described (Scheme 1).¹³ The method is based on a reaction of reductive amination between cyanohydrins **4** or **5** and the appropriate amines (**6–26**). Briefly, cyanohydrins **4** and **5** were prepared in Darzens reaction from benzoylpiperidin-4-on derivatives and chloroacetonitrile, followed by a regioselective ring opening with poly(hydrogen fluoride)pyridine. Amines **6–26** were prepared from the corresponding phenols according to two synthetic pathways depicted in Scheme 2.

Scheme 1. Synthesis of 1-(1-benzoyl-4-fluoropiperidin-4-yl)methanamine derivatives^a

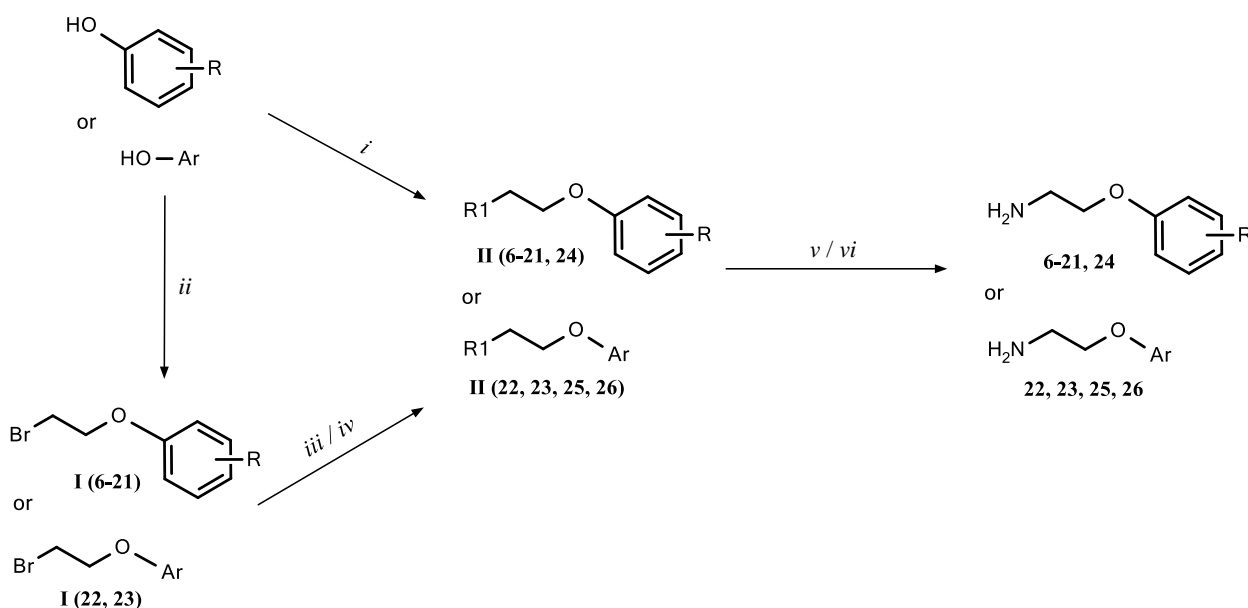


^a Reagents and conditions: (i) DABCO, NaCNBH₃, FeSO₄ × 7H₂O, molecular sieves, MeOH, r.t., 36–72 h, yield: 18–82%; (ii) 1.0 M HCl in EtOAc, r.t., 24 h, yield: 48%; (iii) CH₃COOH, NaCNBH₃, 15 °C – 15 min, then r.t. – 1 h, yield: 67%. X = F or Cl,

Amines **6–23** were synthesized according to a three-step procedure starting with Williamson reaction²⁰ using appropriate phenols and 1,2-dibromoethane. The obtained 2-bromoethoxy derivatives (**I 6–23**) were used in Gabriel's synthesis^{21–23} leading to the desired primary amines. Synthesis of amine **17** (R= 3-NH-CH₃) required additional Boc-protection to prevent reductive amination at a secondary amine group. Deprotection of the amine was performed at the last step of the synthesis of compound **45** (Scheme 1). Amines **24–26** were obtained in Mitsunobu reaction^{24,25} of 2-(methylamino)phenol with *tert*-butyl-2-hydroxyethyl carbamate (**II 24**), and quinolin-8-ol or 1*H*-indol-4-ol with 2-(2-hydroxyethyl)isoindoline-1,3-dione (**II 25** and **II 26**). The following Boc-deprotection or methylaminolysis provided the desired amines. For a detailed description of the synthetic procedures used in the synthesis on amines see the Supporting Information.

The final reaction of reductive amination was carried out in the presence of 1,4-diazabicyclo[2.2.2]octane (DABCO) as a base, sodium cyanoborohydride (NaCNBH₃) as reducing agent and with addition of iron sulfate heptahydrate (FeSO₄ × 7H₂O) that complexes cyanide ions and therefore contributes to the improvement of the reaction yields. In additional step, indole derivative **56** was reduced to indoline analog **57**.

Scheme 2. Synthesis of the amine intermediates (**6–26**)^a



^a Reagents and conditions: (i) for compounds **II 24–26**, *tert*-butyl-2-hydroxyethyl carbamate or 2-(2-hydroxyethyl)isoindoline-1,3-dione, PPh₃, DIAD, THF, 0 °C then r.t., 24 h and 50 °C, 24 h; (ii) 1,2-dibromoethane,

K₂CO₃, acetone, 40–80 °C, 24–72 h; (iii) for compounds **II 6-16, 18-23**, potassium phthalimide, 18-crown-6 ether, DMF, 50 °C, 3 h.; (iv) NaH, CH₃I, THF, 0 °C – 30 min, then r.t – 1 h; for compound **II 17** iv and then iii; (v) for compounds **6-23, 25, 26**, 40% MeNH₂(aq), 10% NaOH, 50 °C, 2 h then r.t., 1 h. (vi) for compound **24**, 1.0 M HCl in EtOAc, r.t., 24 h ; R1= phthalimide or *tert*-butyl carbamate.

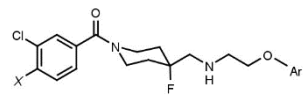
Structure Affinity Relationships (SAfiRs)

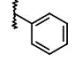
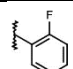
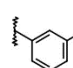
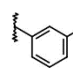
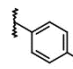
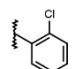
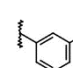
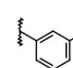
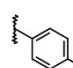
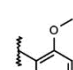
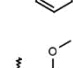
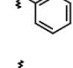
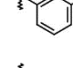
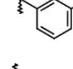
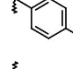
5-HT_{1A} receptor affinity

All the obtained compounds were subjected to affinity determination, using radioligand binding studies. The affinity of the compounds at 5-HT_{1A} receptors was generally high, with p*K*_i values ranging from 8.18 to 12.80 (Table 1, 2). To determine the influence of various phenyl ring substitutions on affinity and exclude the contribution of lipophilicity, we primarily focused on analyzing changes of Ligand-Lipophilicity Efficiency (LLE), calculated as the difference between p*K*_i and ClogD_{7.4}. All the relationships were compared to the unsubstituted phenoxy derivative **3** (LLE 7.59), which was the lead structure for this series (Figure 5).

Firstly, we focused on checking the effect of the substitution site on the phenyl ring, using three commonly used substituents (F, Cl or OCH₃). The substitution in *ortho* position, increased binding affinity, however, the effect was rather modest and did not exceed 0.5 LLE units. The effect of substitution in *meta* position was diversified, ranging from slight increase of affinity for fluoro and methoxy analogs to decrease in the case of the chloro derivative. On the other hand, substitution in *para* position generally decreased the affinity by up to 2 LLE units. The negative effect of a *para* substituent depended on its size, being the least pronounced for the 4-fluoro derivative (LLE 7.34 for **31**) through 4-methoxy derivative (LLE 5.73 for **40**), to reach the lowest value in the case of 4-chloro substituent (LLE 5.19 for **35**).

Table 1. Influence of the substituent position in the phenyl ring on 5-HT_{1A} receptor affinity and selectivity for the most important off-targets.



receptor affinity ^a (pK _i)							
Compd	X	Ar	5-HT _{1A} ^{b,e}	α ₁ ^{c,f}	D ₂ ^{d,g}	ClogD _{7.4} ^h	LLE ⁱ
3	F		10.21 ± 0.20	6.29 ± 0.13	< 6.00	2.62	7.59
28	F		10.80 ± 0.15	< 6.00	< 6.00	2.81	7.99
29	F		10.78 ± 0.18	< 6.00	< 6.00	2.78	8.00
30	Cl		10.69 ± 0.25	6.20 ± 0.06*	< 6.00	3.24	7.45
31	F		10.10 ± 0.15	< 6.00	< 6.00	2.76	7.34
32	F		10.89 ± 0.22	< 6.00	< 6.00	3.25	7.64
33	F		10.32 ± 0.25	< 6.00	< 6.00	3.23	7.08
34	Cl		10.60 ± 0.17	< 6.00	< 6.00	3.70	6.90
35	F		8.41 ± 0.08	< 6.00	< 6.00	3.23	5.19
36	F		10.51 ± 0.09	7.18 ± 0.29*	6.17 ± 0.09	2.49	8.02
37	Cl		9.42 ± 0.01	7.34 ± 0.11*	6.47 ± 0.10	2.95	6.48
38	F		10.22 ± 0.21	< 6.00	< 6.00	2.47	7.75
39	Cl		10.50 ± 0.20	< 6.00	< 6.00	2.93	7.57
40	F		8.18 ± 0.09	< 6.00	< 6.00	2.45	5.73
41	Cl		8.91 ± 0.04	< 6.00	< 6.00	2.91	6.00
1			8.66 ± 0.07	< 6.00	< 6.00	2.29	6.37
(±)8-OH-DPAT			9.09 ± 0.03	NT ^j	NT	1.47	7.68
Buspirone			8.30 ± 0.05	NT	NT	1.35	6.95

^a All binding affinity values are represented as pK_i (i.e. -logK_i) and expressed as means ± SEM from at least 3 experiments performed in duplicate, unless otherwise indicated; Radioligand binding was performed using ^b CHO-K1 cells transfected with 5-HT_{1A} receptors, ^c rat cortex, ^d CHO-K1 cells transfected with D₂ receptors; receptor affinity values were determined by competition binding using ^e [³H]8-OH-DPAT, ^f [³H]-prazosin and ^g [³H]-methylspiperone. In these conditions, pK_i of phentolamine at α₁ receptors was 7.95, and pK_i of haloperidol at D₂ receptors was 8.85;

^h calculated distribution coefficient at pH 7.4; ⁱ Ligand-Lipophilicity Efficiency referring to 5-HT_{1A} receptor; ^j Not tested
* pK_i value was expressed as mean ± range from 2 experiments performed in duplicates.

In support of the observed structure-activity relationships, docking studies showed that, in the group of the derivatives with methoxy substituent (**36**, **38**, **40**), both *ortho* and *meta* substituted compounds took almost the same position in the binding site (Figure 2A). On the other hand, the *para* substituted analog (**40**) was unable to adopt such a position (Figure 2B), probably due to being too sterically hindered, in the area adjacent to the helix 6. In contrast to the above, all the compounds with a smaller fluorine substituent (**28**, **29**, **31**) showed a common binding mode (Figure 3). These results support the conclusion from the binding studies that the affinity of *para* substituted derivatives depends on the size of substituent (the smaller the substituent, the higher the affinity). These structure-activity relationships are consistent with those established for the long-chain arylpiperazines, which suggests a similar binding mode.²⁶

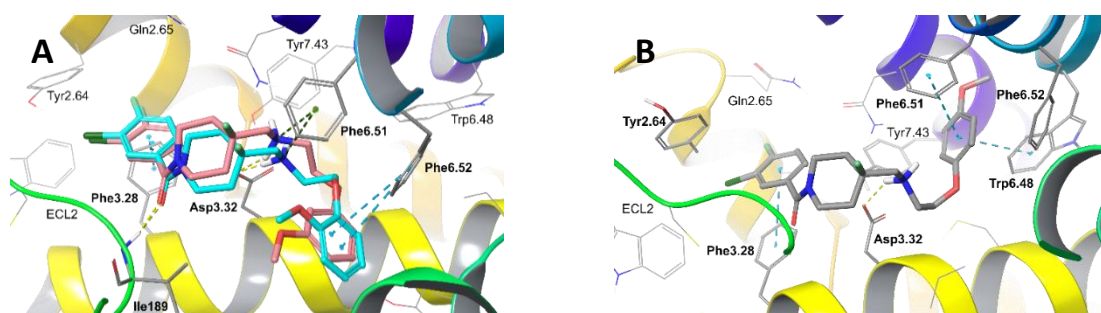


Figure 2. The predicted binding mode of the methoxy derivatives i.e. compound **36** (light teal) together with **38** (pink) (**A**) and compound **40** (gray) (**B**) in the site of serotonin 5-HT_{1A} receptor. Amino acid residues engaged in ligand binding (within 4 Å from the ligand atoms) are displayed as sticks, whereas crucial residues, e.g. forming H-bonds (dotted yellow lines), π - π /CH- π stacking (dotted cyan lines) and cation- π interactions (dotted green line) are represented as thick sticks. ECL2 residues were hidden for clarity; ECL – extracellular loop. The homology model of the 5-HT_{1A} receptor is based on the crystal structure of the 5-HT_{1B} receptor (PDB ID: 4IAR).

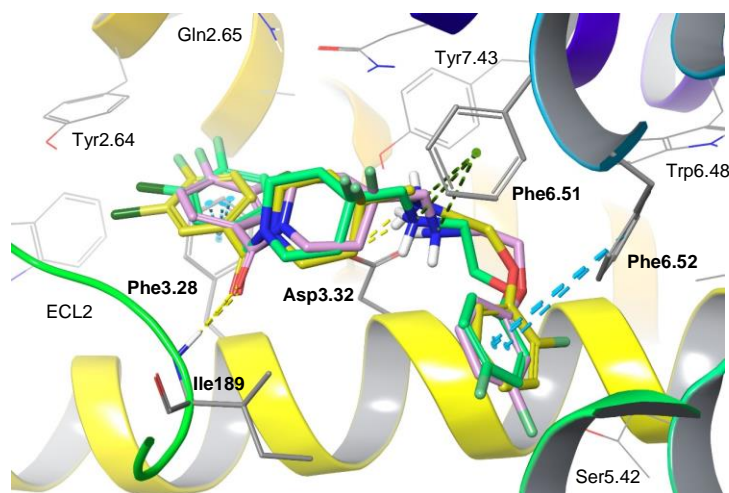


Figure 3. The predicted binding mode of the fluoro derivatives i.e. compound **28** (yellow) together with **29** (pink) and **31** (green) in the site of serotonin 5-HT_{1A} receptor. Amino acid residues engaged in ligand binding (within 4 Å from the ligand atoms) are displayed as sticks, whereas crucial residues, e.g. forming H-bonds (dotted yellow lines), π - π /CH- π stacking (dotted cyan lines) and cation- π interactions (dotted green line) are represented as thick sticks. ECL2 residues were hidden for clarity; ECL – extracellular loop. The homology model of the 5-HT_{1A} receptor is based on the crystal structure of the 5-HT_{1B} receptor (PDB ID: 4IAR).

Further studies focused on exploration of different types of substituents in *meta* and *ortho* positions (well tolerated by the receptor) as well as various benzo-fused heteroaromatic moieties, which can be also considered as a kind of *ortho-meta* substituted derivatives at the phenyl ring (Table 2). All the ligands achieved very high 5-HT_{1A} receptor affinity, with subnanomolar or even picomolar K_i values and generally very high LLE values.

The most pronounced increase in 5-HT_{1A} receptor affinity was noted in the case of derivatives containing HBD moiety at the *meta* position (**45**, **47**, **56** and **57**). Worth mentioning is the fact that one of the *meta*-HBD derivatives, compound **56**, had an exceptionally high affinity, reaching subpicomolar value (pK_i 12.80, K_i 0.16 pM, LLE 10.06). The increase in binding affinity of the derivatives with HBD in the *meta* position can be explained by their ability to create an additional hydrogen bond with serine Ser5.42 in the binding site of the 5-HT_{1A} receptor (Figure 4). This stabilizes the ligand-receptor complex and lowers the binding energy (IFD score for compound **56** = -465.26 compared to -463.69 for compound **3**).

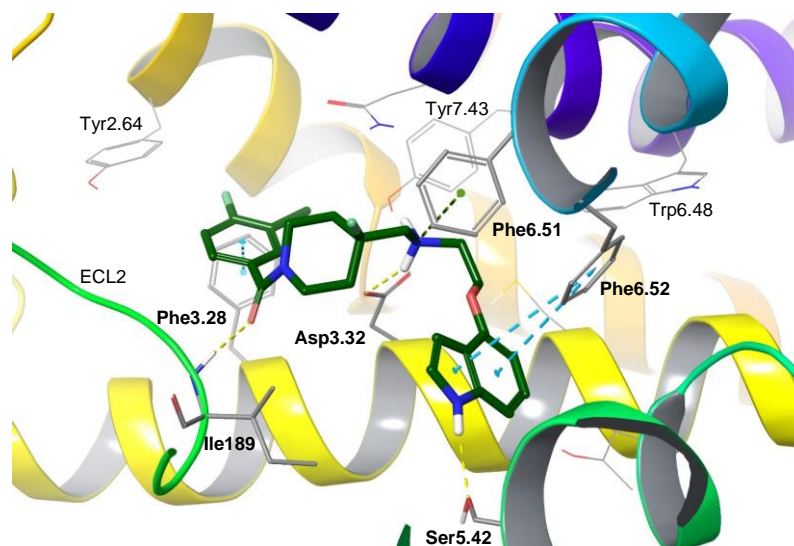


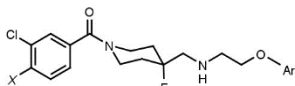
Figure 4. The predicted binding mode of compound **56** (with HBD in *meta* position) in the site of serotonin 5-HT_{1A} receptor. Amino acid residues engaged in ligand binding (within 4 Å from the ligand atoms) are displayed as sticks, whereas crucial residues, e.g. forming H-bonds (dotted yellow lines), π - π /CH- π stacking (dotted cyan lines) and cation- π interactions (dotted green line) are represented as thick sticks. ECL2 residues were hidden for clarity; ECL – extracellular loop. The homology model of the 5-HT_{1A} receptor is based on the crystal structure of the 5-HT_{1B} receptor (PDB ID: 4IAR).

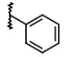
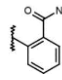
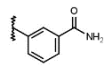
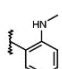
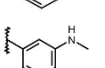
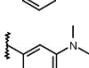
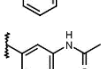
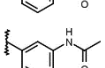
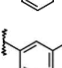
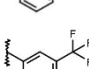
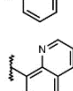
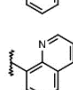
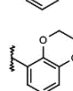
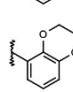
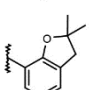
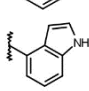
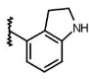
The hypothesis that creating a hydrogen bond in this region improves binding affinity was further supported by the marked increase in LLE for the benzamide derivatives (**42** and **43**), which are also capable of forming this interaction. Moreover, the *meta* derivatives not capable of forming H-bonds (**46**, **49**, **50**), displayed lower affinity, which is consistent with the observation made for compound **33** (a *meta*-chloro derivative) and suggesting that they exert a negative steric contribution (this was, however, less pronounced than in the case of the *para* analogs).

Regarding the substitution at the benzoyl moiety, the 4-chloro analogs had overall lower ligand-lipophilicity efficiencies than their 4-fluoro counterparts, suggesting that this modification is not generally favorable.

1
2
3
4
5
6
7
8
9
10
11
12
13
14
15
16
17
18
19
20
21
22
23
24
25
26
27
28
29
30
31
32
33
34
35
36
37
38
39
40
41
42
43
44
45
46
47
48
49
50
51
52
53
54
55
56
57
58
59
60

Table 2. Influence of the type of substituent in the phenyl ring on 5-HT_{1A} receptor affinity and selectivity for the most important off-targets.



Compd	X	Ar	receptor affinity ^a (pK _i)				
			5-HT _{1A} ^{b,e}	α ₁ ^{c,f}	D ₂ ^{d,g}	ClogD _{7.4} ^h	LLE ⁱ
3	F		10.21 ± 0.20	6.29 ± 0.13	< 6.00	2.62	7.59
42	F		10.22 ± 0.21	< 6.00	< 6.00	1.51	8.71
43	F		10.53 ± 0.24	< 6.00	< 6.00	1.49	9.05
44	F		9.93 ± 0.22	6.04 ± 0.01	< 6.00	2.08	7.86
45	F		10.47 ± 0.19	< 6.00	< 6.00	2.09	8.38
46	F		9.52 ± 0.15	< 6.00	< 6.00	2.72	6.79
47	F		10.08 ± 0.13	< 6.00	< 6.00	1.86	8.21
48	Cl		10.27 ± 0.21	< 6.00	< 6.00	2.33	7.95
49	F		9.85 ± 0.23	< 6.00	< 6.00	3.13	6.72
50	F		9.56 ± 0.02	< 6.00	< 6.00	3.51	6.05
51	F		10.22 ± 0.25	6.76 ± 0.03 [*]	< 6.00	2.82	7.40
52	Cl		9.37 ± 0.03	6.69 ± 0.07	6.36 ± 0.14	3.28	6.09
53	F		9.86 ± 0.11	6.72 ± 0.13 [*]	< 6.00	2.17	7.69
54	Cl		9.71 ± 0.12	6.71 ± 0.02 [*]	6.04 ± 0.12	2.63	7.08
55	F		11.07 ± 0.06	7.76 ± 0.32 [*]	7.54 ± 0.12 [*]	3.22	7.85
56	F		12.80 ± 0.16	7.00 ± 0.05	< 6.00	2.74	10.06
57	F		10.35 ± 0.02	6.36 ± 0.02	< 6.00	2.12	8.23

^a All binding affinity values are represented as pK_i (i.e. -logK_i) and expressed as means ± SEM from at least 3 experiments performed in duplicate, unless otherwise indicated; Radioligand binding was performed using ^b CHO-K1 cells transfected with 5-HT_{1A} receptors, ^c rat cortex, ^d CHO-K1 cells transfected with D₂ receptors; receptor affinity values were determined by competition binding using ^e [³H]8-OH-DPAT, ^f [³H]-prazosin and ^g [³H]-methylspiperone. In these conditions, pK_i of phentolamine at α₁ receptors was 7.95, and pK_i of haloperidol at D₂ receptors was 8.85; ^h calculated distribution coefficient at pH 7.4; ⁱ Ligand-Lipophilicity Efficiency referring to 5-HT_{1A} receptor; ^{*} pK_i value was expressed as mean ± range from 2 experiments performed in duplicates.

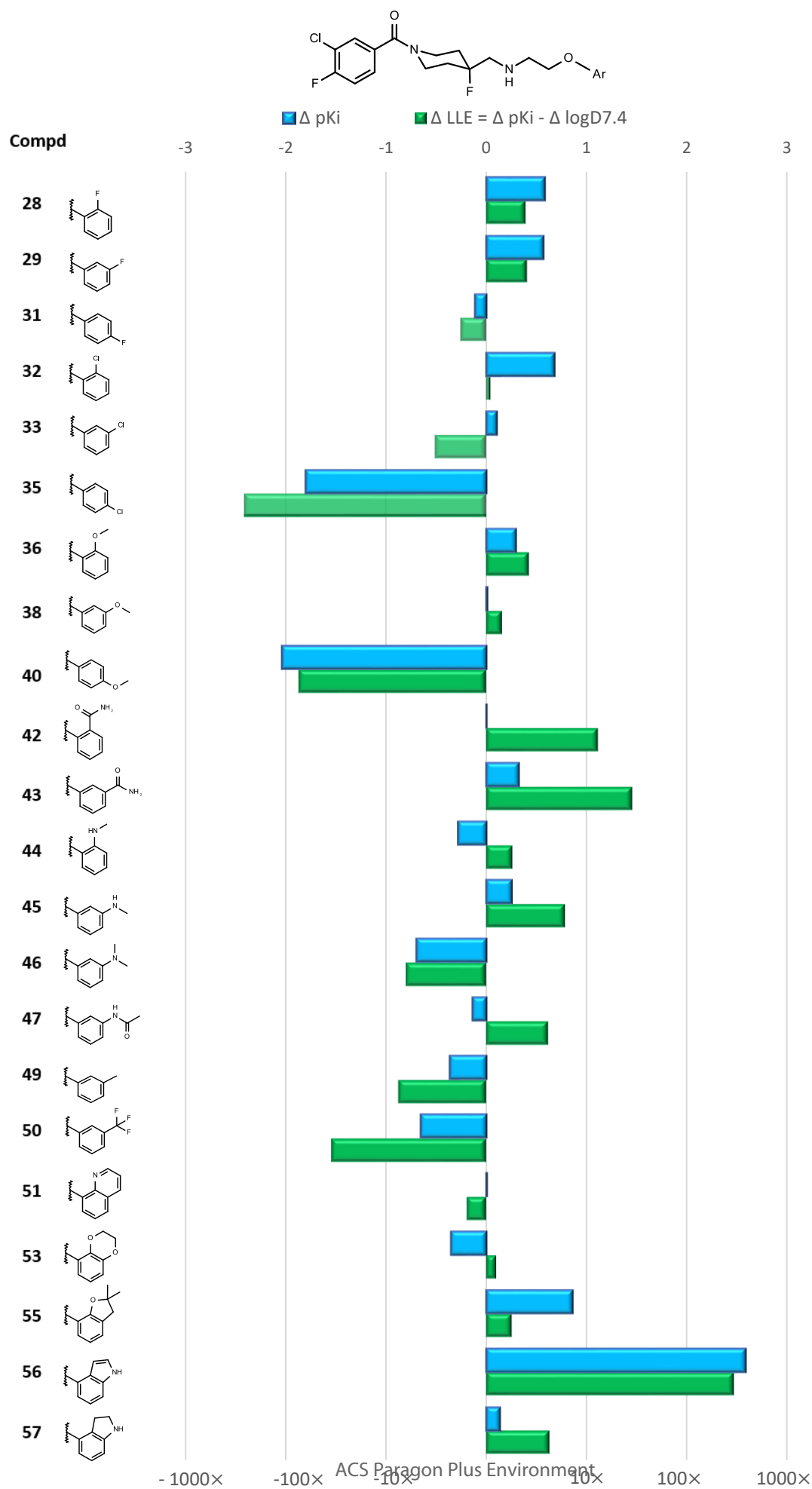
Δ of activity of the novel compounds in relation to the unsubstituted lead structure **3**

Figure 5. Changes in LLE in relation to unsubstituted lead structure **3**, due to substitution at phenyl ring.

Selectivity vs. key antitargets, the adrenergic α_1 and dopaminergic D₂ receptors

Previous studies of 1-(1-benzoylpiperidin-4-yl)methanamine derivatives indicated that the highest risk of off-target interactions is with adrenergic α_1 and dopaminergic D₂ receptors.^{13,27–29} Accordingly, all the novel compounds were tested for binding to these receptors, to confirm their selectivity (Tables 1 and 2).

Concerning α_1 receptor affinity, the majority of the compounds showed very high selectivity for 5-HT_{1A} over α_1 and D₂ receptors (over 1000–10000 times). In general, increased affinity for α_1 receptor was observed for the *ortho* substituted analogs (**36**, **37**, **44**). The highest affinities (pK_i 6.6–7.8) were observed for the derivatives with *ortho*-methoxy substituent (**36**, **37**) and their bicyclic analogs, with oxygen or nitrogen in *ortho* position (**51**, **52**, **53**, **54**, **55**). High α_1 receptor affinity was also observed for the indole derivative **56** (pK_i 7.00). Interestingly, the *ortho*-fluoro- and *ortho*-chloro- derivatives (**28**, **32**) did not show significant affinity for α_1 receptor ($pK_i < 6$) indicating that halogen in this position impairs α_1 receptor binding. In comparison, literature data indicates that *ortho*-methoxy- or *ortho*-ethoxy- substitution in the aryl moiety increase α_1 receptor affinity. For example, in the structure of tamsulosin, a selective α_{1A} receptor antagonist used for the treatment of benign prostatic hyperplasia, a 2-(2-ethoxyphenoxy)ethanamine fragment can be highlighted.³⁰ Nevertheless, it should be noted that selectivity for 5-HT_{1A} vs. α_1 receptors was generally very high, and was less than 1000× for only two compounds (**37**, **52**).

In the case of the D₂ receptor, only one compound (**55**) showed substantial affinity (pK_i D₂ 7.54). This observation is in line with the fact, that the 2,2-dimethyl-2,3-dihydro-1-benzofuran moiety was previously used in the structure of dual acting, 5-HT_{1A}R agonist/D₂R antagonist ligands.³¹ However, the affinity of **55** for D₂ receptor did not significantly affect selectivity, because its affinity for 5-HT_{1A} receptor was still over 3.5 orders of magnitude higher (> 3000×, pK_i 5-HT_{1A} = 11.07).

Summing up, most of the presented compounds showed substantial selectivity versus key antitargets (K_i ratio over 1000-fold), despite the fact that the phenoxyethanamine scaffold is common also for ligands of other monoaminergic receptors. This supports the finding that the 1-[4-(aminomethyl)-4-fluoropiperidin-1-yl]ethan-1-one core is the essential scaffold for providing both high affinity and high selectivity for the 5-HT_{1A} receptor.

Structure Functional Activity Relationships (SFARs)

Based on the results of the studies described above, 25 compounds were selected for functional studies. The functional profiles of the novel compounds were measured at several pathways engaged in 5-HT_{1A} receptor signal transduction. Compounds were tested in four functional assays: ERK1/2 phosphorylation (pERK1/2), adenylyl cyclase inhibition (cAMP), β -arrestin recruitment (β -arrestin) and calcium mobilization (Ca²⁺). To classify the agonist efficacy of the compounds, we assumed that E_{max} values higher than 80% relative to the maximal effect of serotonin, are characteristic of a full agonist, between 79% and 21% of a partial agonist and 20% or less indicating negligible agonist activity. The experiments were carried out using cell lines expressing the recombinant human 5-HT_{1A} receptor.

In terms of potency, the general trends (Tables 3 and 4), were similar to those established in affinity studies. Compared to **3**, the derivatives substituted with the HBD in *meta* position (**43**, **45**, **47**, **48**) were characterized by a rise in potency at all the signaling pathways. The same trend was observed for the bicyclic analogs (**51**, **55**, **56**, **57**), but the other derivatives showed mostly decreased potency in functional assays. The notable exceptions were compound **36** and **38**, the *ortho*- and *meta*-methoxy analogs, respectively, which were characterized by generally higher potency than **3**, as well as compound **42**, an *ortho*-carboxamido analog, which displayed potency similar to **3**, with modest variations in both sides. The extent of potency change varied between individual analogues in terms of signaling pathways, resulting in diversified functional selectivity profile for some of them.

The efficacy of the ligands for the ERK1/2, cAMP and β -arrestin pathways was generally high, falling slightly below 80% in only a few cases. The vast majority of the compounds can therefore be considered as full agonists in those signaling pathways. On the other hand, most of the compounds showed lower efficacies in calcium mobilization assay. Thirteen compounds were classified as partial agonists and two even as negligibly active, as they showed marginal level of stimulation (15%). Both of these compounds were *para*-substituted analogs (**35** and **40**).

Table 3. Functional activity of compounds **28–33**, **35**, **36**, **38–41** at 5-HT_{1A} receptors.

Compd	X	Ar	5-HT _{1A} functional activity ^a							
			ERK1/2 ^b		cAMP ^b		β-arrestin ^c		Ca ²⁺ ^b	
			E _{MAX}	pEC ₅₀	E _{MAX}	pEC ₅₀	E _{MAX}	pEC ₅₀	E _{MAX}	pEC ₅₀
3	F		92%	9.10	90%	8.09	96%	7.98	91%	7.20
28	F		95%	8.24	89%	7.74	97%	7.61*	90%	6.82*
29	F		96%	8.64	99%	7.80	91%	7.46	73%	7.16*
30	Cl		93%	7.70	89%	7.40	104%	6.21*	90%	6.19*
31	F		98%	8.24	96%	7.37	99%	7.06*	73%	7.00
32	F		NT ^d	NT ^d	87%	7.59	94%	7.76	36%	6.26*
33	F		97%	7.99	88%	7.71	99%	6.65*	80%	6.60*
35	F		88%	6.93	63%	6.32	109%	6.01*	15%	5.28
36	F		NT ^d	NT ^d	83%	9.86*	90%	9.43	54%	9.52*
38	F		97%	9.40	89%	8.98	90%	8.64*	64%	7.15
39	Cl		95%	8.14	96%	7.69	95%	6.91	74%	6.50
40	F		86%	7.68	88%	6.25	82%	5.79	15%	6.21
41	Cl		78%	7.32	59%	6.48	65%	5.60	24%	5.88*
1			100%	8.33	92%	7.22	98%	6.71	66%	6.52
(±) 8-OH-DPAT			93%	8.09	63%	7.50	101%	7.84	35%	7.66
Buspirone			44%	7.82	49%	7.14	100%	6.73	8.3%	7.42*
Serotonin^e			100%	7.48	100%	7.51	100%	6.89	100%	7.23

^a All the functional activity values were expressed as means from at least 3 experiments performed in duplicates, unless otherwise indicated. For the sake of clarity, the SEM values were omitted in this table and presented in the supporting information – Table S1; The functional assay was performed using ^b CHO-K1 cells, ^c U2OS cells (Tango LiveBLAzer assay kit); ^d NT – not tested; * value was expressed as mean from 2 experiments performed in duplicates. ^e Data for Serotonin on ERK, cAMP and β-arrestin are reproduced from the previous paper.¹³

Bias factors

The functional selectivity of the ligands was analyzed by calculating bias factors. These compare the efficacy and potency of compounds for pairs of signaling pathways, using the following equation^{32–35}.

$$\text{Bias factor} = \log \left(\frac{\text{relative activity}_{12,\text{lig}}}{\text{relative activity}_{12,\text{ref}}} \right) = \log \left(\left(\frac{E_{\text{max_path1}} \times \text{EC}_{50\text{-path2}}}{\text{EC}_{50\text{-path1}} \times E_{\text{max_path2}}} \right)_{\text{lig}} \div \left(\frac{E_{\text{max_path1}} \times \text{EC}_{50\text{-path2}}}{\text{EC}_{50\text{-path1}} \times E_{\text{max_path2}}} \right)_{\text{ref}} \right)$$

The calculations in the present study follow the same approach as in our previous study.¹³ Briefly, the bias factor provides a measure that integrates E_{max} and EC_{50} values of both a test ligand and a reference compound (i.e., serotonin). Results are presented in Tables 5 and 6 and compounds which displayed significant bias (over 1 log) were highlighted in green (for positive values) or in blue (for negative values). Those compounds which showed significant bias, but with low pEC_{50} values, were marked in gray.

1
2
3
4
5
6
7
8
9
10
11
12
13
14
15
16
17
18
19
20
21
22
23
24
25
26
27
28
29
30
31
32
33
34
35
36
37
38
39
40
41
42
43
44
45
46
47
48
49
50
51
52
53
54
55
56
57
58
59
60

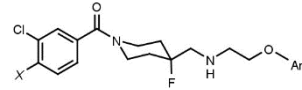
Table 5. Bias factors of compounds (**28–33**, **35**, **36**, **38–41**) and references at 5-HT_{1A} receptors.

Clc1ccc(cc1C(=O)N2CC(F)CCN2CCOAr)X

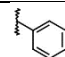
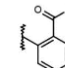
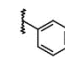
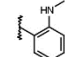
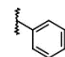
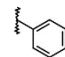
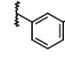
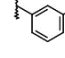
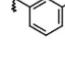
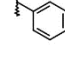
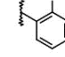
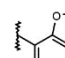
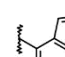
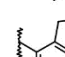
5-HT_{1A} receptor bias factor (logarithmic value)

Compd	X	R	ERK1/2 vs. cAMP	ERK1/2 vs. β-arrestin	ERK1/2 vs. Ca ²⁺	cAMP vs. β-arrestin	cAMP vs. Ca ²⁺	β-arrestin vs. Ca ²⁺
3	F		1.05	0.51	1.65	-0.54	0.60	1.15
28	F		0.56	0.03	1.19	-0.53	0.63	1.16
29	F		0.85	0.60	1.35	-0.25	0.50	0.75
30	Cl		0.35	0.85	1.27	0.50	0.92	0.42
31	F		0.90	0.57	1.11	-0.33	0.20	0.54
32	F		— ^a	— ^a	— ^a	-0.83	1.42	2.25
33	F		0.35	0.73	1.22	0.38	0.86	0.48
35	F		0.78	0.23	2.15	-0.55	1.38	1.92
36	F		— ^a	— ^a	— ^a	-0.23	0.24	0.47
38	F		0.49	0.19	2.17	-0.30	1.68	1.98
39	Cl		0.48	0.63	1.49	0.15	1.02	0.87
40	F		1.44	1.31	1.98	-0.13	0.54	0.67
41	Cl		1.00	1.21	1.70	0.21	0.70	0.49
1			1.17	1.02	1.76	-0.15	0.59	0.74
(±) 8-OH-DPAT			0.79	-0.39	0.59	-1.18	-0.20	0.98
Buspirone			0.66	0.14	0.86	-0.52	0.21	0.73
5-HT			0.00	0.00	0.00	0.00	0.00	0.00

^a- no data for pERK assay

Table 6. Bias factors of compounds **42–51** and **55–57** at 5-HT_{1A} receptors.


5-HT_{1A} receptor bias factor (logarithmic value)

Compd	X	Ar	ERK1/2 vs. cAMP	ERK1/2 vs. β-arrestin	ERK1/2 vs. Ca ²⁺	cAMP vs. β-arrestin	cAMP vs. Ca ²⁺	β-arrestin vs. Ca ²⁺
3	F		1.05	0.51	1.65	-0.54	0.60	1.15
42	F		0.47	-0.04	0.93	-0.51	0.46	0.97
43	F		0.57	0.53	1.98	-0.04	1.42	1.45
44	F		1.13	1.43	1.93	0.31	0.81	0.50
45	F		0.20	-0.60	2.33	-0.80	2.14	2.93
46	F		0.45	0.33	1.12	-0.12	0.67	0.79
47	F		-1.03	-3.49	1.85	-2.47	2.87	5.34
48	Cl		-0.90	-1.95	1.61	-1.06	2.50	3.56
49	F		0.97	0.83	1.84	-0.14	0.87	1.01
50	F		0.73	0.49	1.00	-0.23	0.27	0.50
51	F		-0.17	-3.11	1.33	-2.94	1.50	4.44
55	F		2.80	0.81	3.42	-1.99	0.62	2.61
56	F		0.53	-3.71	2.54	-4.24	2.02	6.25
57	F		0.61	-0.44	2.95	-0.99	2.34	3.39

ERK1/2 vs. cAMP

Most of the compounds showed a preference for ERK1/2 phosphorylation, with the highest bias factors (>1 log) being found for compounds **40**, **44** and **55**. The highest ERK1/2 phosphorylation preference was found for compound **55** with a bias factor of 2.8 log. Three compounds (**47**, **48** and **51**), preferred cAMP pathway and the significant bias was observed for compound **47** (bias factor -1.03).

When comparing 3-chloro-4-fluorobenzoyl (**29**, **38**, **40**, **47**) with their 3,4-dichlorobenzoyl derivatives counterparts (**30**, **39**, **41**, **48**), it is noticeable that the former always show a more pronounced biased profile than the latter compounds.

ERK1/2 vs. β -arrestin

Three compounds preferred ERK1/2 phosphorylation vs β -arrestin, and four compounds preferred β -arrestin recruitment vs ERK1/2 phosphorylation. This is the first time, to our knowledge, that β -arrestin biased agonists have been reported for the selective 5-HT_{1A} receptor ligands. Bias factors for the ERK1/2 biased agonists ranged from 1.21 for compound **41** to 1.43 for compound **44**, whereas in the case of β -arrestin biased agonists, their bias factors were much more pronounced (from -1.95 for **48** to -3.71 log for **56**).

The ERK1/2 preferring compounds were the *para*-methoxy derivatives (**40** and **41**) and the *ortho*-methylamine derivative **44**. On the other hand, the compounds that showed bias for β -arrestin recruitment were either the bicyclic aromatic derivatives (**51** and **56**) or *meta*-acetamido derivatives (**47** and **48**).

It is noticeable that the *ortho*-methylamine-substituted derivative (**44**) showed substantial ERK1/2 bias (1.43), while the *meta*-methylamine-substituted derivative (**45**) showed an opposite preference (bias factor -0.60).

ERK1/2 vs. Ca²⁺

In general, most of the compounds showed substantial bias for ERK1/2 phosphorylation vs. calcium mobilization (Ca^{2+}) and none of the tested compounds showed preference for Ca^{2+} . The highest ERK1/2 preference was found for the benzo-fused, five-membered ring derivatives (**55–57**), reaching bias factor of 3.42 for compound **55**.

cAMP vs. β -arrestin

Only five compounds (**30**, **33**, **39**, **41**, **44**) exhibited some preference towards cAMP inhibition, however not exceeding half a log, whereas the rest of the compounds preferred β -arrestin recruitment. As seen for ERK1/2 vs. cAMP bias, a favorable influence of the 3,4-dichlorobenzoyl moiety on cAMP potency was observed here, as compared to the corresponding 3-chloro-4-fluorobenzoyl analogs.

Among the derivatives with marked β -arrestin recruitment bias, compounds **47**, **48**, **51** and **56** were identified again, as in the case of preference for β -arrestin versus ERK1/2. Interestingly, compound **55** also preferred β -arrestin pathway versus cAMP, despite the fact that previously it exhibited the highest preference for ERK1/2 vs. β -arrestin. This is due to its very high potency in the ERK1/2 assay (pEC_{50} 10.99) and also relatively high β -arrestin potency (pEC_{50} 9.49), as compared to other assays, where its potency was noticeably weaker.

Overall, it should be noted that preference towards β -arrestin recruitment was much higher than for the most biased reference compound, (\pm) 8-OH-DPAT (-1.18) and reached an extremely high value (-4.24) for compound **56**.

Worth mentioning are the previous studies by Stroth and co-workers, where the authors identified 5-HT_{1A} biased ligands with a strong preference for cAMP over β -arrestin signaling³⁶. However, it should be noted that those arylpiperazine derivatives had only partial agonist properties in the cAMP assay (53–73%). They also showed very low E_{max} values in the β -arrestin assay (6–36%). Noteworthy, Stroth et al. reported that the reference agonist (\pm) 8-OH-DPAT achieved only 44% efficacy in β -arrestin assay, while herein it reached 101%, so the observed differences in signaling

bias may be at least partially due to the methodological differences (β -arrestin assay in that study was performed using PathHunter eXpress HTR1A CHO-K1 β -Arrestin GPCR Assay DiscoverX, while in the current study TangoTM HTR1A-bla U2OS LiveBLAzer assay kit, Life Technologies).

cAMP vs. Ca²⁺

Eleven compounds markedly preferred cAMP pathway versus Ca²⁺. Noteworthy, the most biased compounds (with bias factors over 2), had HBD in the *meta* position (**45**, **47**, **48**, **56** and **57**), further indicating the positive influence of this substituent on cAMP inhibition potency. Due to relatively low potency of all the compounds in the calcium mobilization assay, none of them exhibited bias towards this signaling pathway.

β -arrestin vs. Ca²⁺

Thirteen compounds were markedly biased for β -arrestin. Four of the compounds (**47**, **48**, **51** and **56**) showed extremely high bias for β -arrestin (over 3.5 log), reaching 6.25 log value (over 1 000 000 times) for compound **56**. The relatively lower ability of the compounds to stimulate Ca²⁺ mobilization, resulted in a lack of noticeable Ca²⁺-preferring biases.

“Signaling fingerprint” analysis

The functional studies enabled selection of biased agonists that exhibit preference for specific pathways. To describe the pattern of behavior of the compounds in the different pathways, we calculated “signaling fingerprints” based on measures of potency and efficacy, and represented them as bars of particular height and color intensity (heat map), respectively. The potency of each ligand in a particular assay was normalized according to the performance of the native neurotransmitter (i.e. serotonin) in this assay. It was calculated using the following equation:

$$\text{Normalized ligand potency} = -\log \left(\text{EC}_{50 \text{ path}_{\text{lig}}} \div \left(\frac{\text{EC}_{50 \text{ path}}}{\text{EC}_{50 \text{ ref. path}}}_{\text{native ligand}} \right) \right)$$

A ‘signaling fingerprint’ therefore allows for the simultaneous comparison of ligand’s functional profile in all pathways. “Signaling fingerprints” were calculated for both the reference and the novel compounds, including all four tested pathways, with serotonin as the native ligand and cAMP as the reference pathway (due to relatively higher potency of serotonin in this assay). Significant preference of a given pathway was defined in this study as a difference in normalized ligand potency of at least 1 order of magnitude (1 log).

Among the reference compounds (Figure 6) the most biased was compound **1**, showing significant preference for ERK1/2 phosphorylation over all other assays, which is in line with previous studies.^{12,13} On the other hand, (±) 8-OH-DPAT displayed 1 log preference for β-arrestin vs cAMP pathway, but was unbiased with respect to other pathways. Buspirone, consistent with its partial agonist properties, showed low efficacy in all assays but β-arrestin, which was particularly evident for calcium mobilization (E_{max} 8.3%); the potencies, however, didn’t differ significantly.

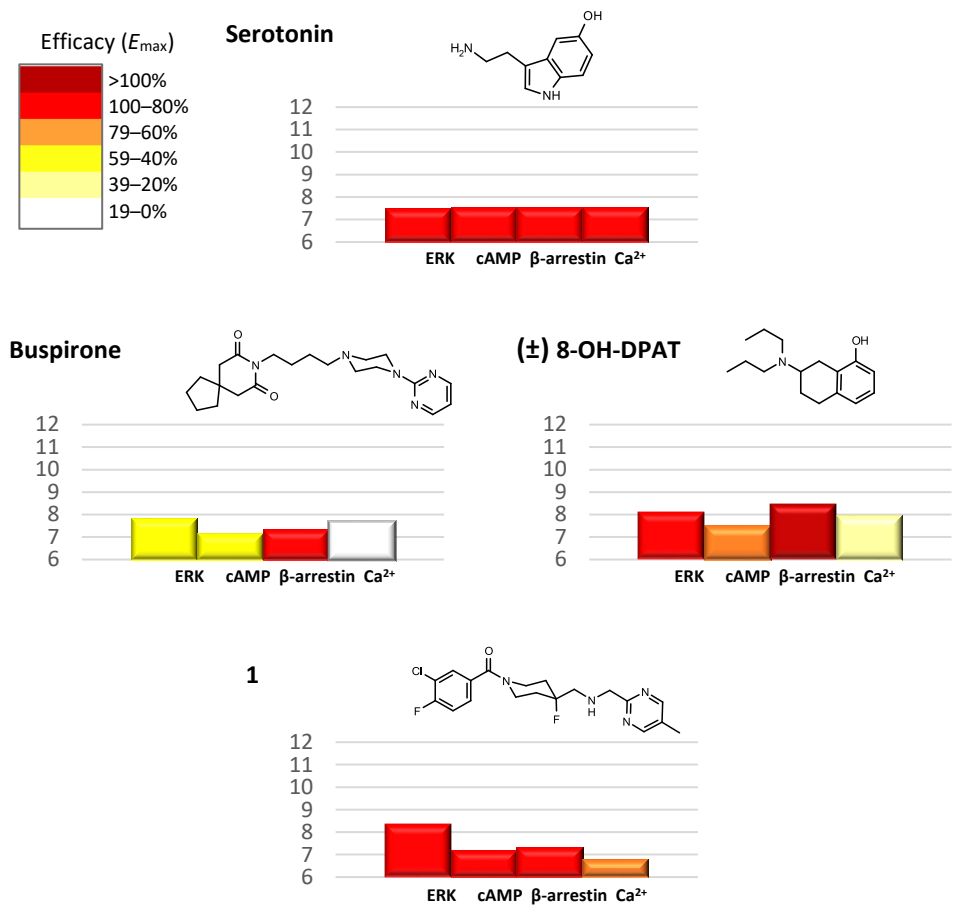


Figure 6. “Signaling fingerprints” for reference compounds (bar height – normalized ligand potency in log scale, bar color – ligand efficacy, as percent E_{\max}).

The “signaling fingerprints” for the most interesting novel compounds, in comparison with the lead structures **2** and **3**, were shown in Figure 7. In the rows, the analogues with structurally closest substituents were collected to show the gradual impact of their modification on changes in the functional profile. The pERK1/2 preferring analogs were shown in the left column, the more balanced in the middle and the β -arrestin biased agonists in the right column.

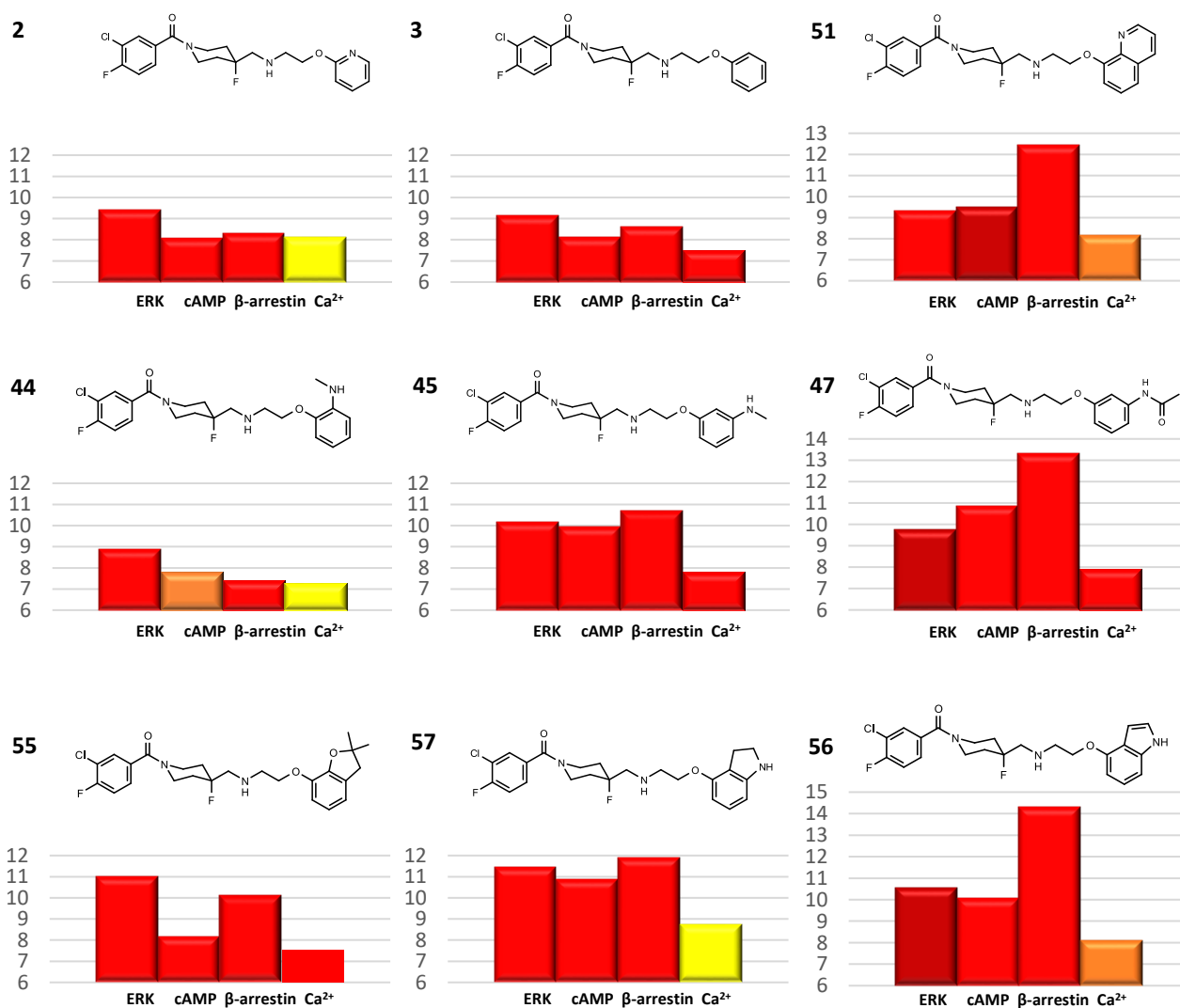


Figure 7. “Signaling fingerprints” for the novel compounds (bar height – normalized ligand potency in log scale, bar color – ligand efficacy, as percent E_{max}). The signaling fingerprints for **2** and **3** are shown for comparison with our previous work.¹³

Based on the more detailed analysis of the “signaling fingerprints”, the novel 5-HT_{1A} receptor agonists can be categorized into three types, divided into five subtypes, each with a different functional selectivity profile. Type I includes ligands with a significant preference for ERK1/2 phosphorylation and a diverse profile of activity in other assays, which is mainly differentiated by the level of activation of β -arrestin recruitment. Type IA, including compounds **44** and **2**, consists of ligands which showed significant preference for ERK1/2 phosphorylation over all other pathways, similarly to the reference biased agonist, **1**. Compounds **3** and **55**, which were classified into type IB, were characterized by a significant preference for ERK1/2 phosphorylation over cAMP and Ca²⁺, but not β -arrestin. Type II includes compounds **45** and **57**, which show a similar level of activity in ERK1/2, cAMP and β -arrestin assays, with a slight preference for the latter.

In contrast to the Type I and II, and of particular interest in the present study, are type III compound: these include first-in-class ligands that strongly prefer β -arrestin recruitment over all other signaling pathways. It is noteworthy, that such a profile was not observed for any of the reference compounds, and, to our knowledge, has not been previously described in the literature, which could imply that these compounds may exhibit novel pharmacological and, potentially, therapeutic properties. Type IIIA (compounds **51** and **56**) includes ligands characterized by the strongest preference of β -arrestin pathway, similar levels of activity in ERK1/2 and cAMP assays and much lower stimulation of Ca²⁺. Type IIIB, represented by compound **47**, is characterized by the high levels of activity in both β -arrestin and cAMP assays (with especially marked activity of β -arrestin pathway), and lower ability to activate ERK1/2 phosphorylation and calcium mobilization. Noteworthy, compound **47** was the only one that showed significant preference for activity (above 1 log) in the cAMP assay over ERK1/2 phosphorylation.

Summing up, the following structure functional selectivity relationships could be inferred:

(1) the presence of an H-bond forming substituent in *ortho* position of the phenoxyethyl moiety (**44**, **55**) or a nitrogen atom built in the aryl ring in the same position (**2**), decreases the ability to activate

1
2 β -arrestin recruitment in the tested group of 5-HT_{1A} receptor agonists, thus relatively enhancing a
3
4 preference for ERK1/2 phosphorylation.
5
6

7 (2) substitution of the H-bond donor (HBD) moiety in *meta* position of the phenoxyethyl moiety
8
9 (45, 57) increases agonist potency in all signaling pathways, with the effect being especially
10
11 pronounced for cAMP inhibition and β -arrestin recruitment. Except for calcium mobilization being
12
13 substantially weaker, those potent agonists do not distinguish significantly between other pathways.
14
15
16

17 (3) in contrast, the derivatives with a bicyclic aromatic moiety (56 and 51) or a flat, π -electron
18
19 containing substituent (e.g. 47), exhibited particular preference for β -arrestin recruitment, yielding
20
21 very strong activity in this assay. Noteworthy, replacement of an aromatic indole moiety of 56 with
22
23 a partially saturated indoline (57) markedly decreased β -arrestin recruitment, resulting in no
24
25 particular preference over ERK1/2 phosphorylation or cAMP inhibition, thus confirming this
26
27 finding. It should be noted that, to our knowledge, these compounds are the first 5-HT_{1A} ligands to
28
29 show such a strong biased agonism for β -arrestin recruitment and this, in itself, constitutes an
30
31 intriguing novel finding in drug discovery at this receptor.
32
33
34
35

36 More broadly, these *in vitro* data strongly indicate that it is possible to identify specific structural
37
38 motifs that are responsible for directing 5-HT_{1A} receptor signaling to distinct intracellular responses.
39
40
41
42
43
44
45
46
47
48
49
50
51
52
53
54
55
56
57
58
59
60

Developability studies

The developability of the novel compounds was initially assessed *in silico* using LELP, Fsp3 and CNS-MPO measures (Table S2). Majority of the compounds showed favorable score values, thus testifying for the overall promising developability potential of the explored series. In order to support the choice of proper candidates for *in vivo* tests, selected *in vitro* developability studies were performed. As a first step, the novel compounds displaying the most interesting functional profiles were tested for preliminary metabolic stability using rat liver microsomes (Table S3). The stability was assessed referring to the marketed drugs of different stability, aripiprazole and verapamil, showing high or low stability in the given conditions, respectively. Various levels of stability were found for the novel compounds, ranging from high stability for compounds **47**, **48**, **51** and **56** (73–87%), through medium stability for compounds **2**, **3** and **44** (54–59%), to low stability for compounds **55** and **57** (21 and 37%). Based on the functional studies and the above results, compound **56**, a β -arrestin recruitment biased agonist with high metabolic stability and compound **44**, an ERK1/2 phosphorylation preferring ligand with medium metabolic stability were selected for further studies. To confirm preliminary metabolic stability data, for the lead structure **3** as well as compounds **44** and **56**, intrinsic clearance was determined in comparison with the reference CNS drugs aripiprazole and diazepam (Table 7). As expected, compound **44** and the lead structure **3** showed the same level of medium metabolic stability (CL_{int} 48.8 and 41.7 mL/min/kg, respectively), similar to diazepam, a reference CNS drug with medium but acceptable stability, whereas compound **56** was more stable, with intrinsic clearance close to aripiprazole, a reference CNS drug showing a very high stability in this experimental setting (CL_{int} 9.6 and 7.2 mL/min/kg, respectively).

As a next step, compounds **44** and **56** were tested for membrane permeability using parallel artificial membrane permeability assay (PAMPA) and for potential hepatotoxicity using HepG2 cells viability (Table 7). Both compounds, similar to the lead structure **3**, showed satisfying permeability ($>1E-06$ cm/s), suggesting good absorption and brain penetration, as well as very low hepatotoxicity, not reaching statistically significant reduction of viability even in concentration as high as 50 μ M.

Table 7. Permeability, hepatotoxicity and intrinsic clearance of compounds **3**, **44** and **56**

Compound	PAMPA <i>Pe</i> [10^{-6} cm/s] \pm SD	Hepatotoxicity 50% viability of HepG2 cells	Intrinsic clearance CL_{int} [mL/min/kg]
3	8.6 \pm 1.4	> 50 μ M	41.7
44	6.7 \pm 1.1	> 50 μ M	48.8
56	4.7 \pm 0.4	> 50 μ M	9.6
References	Caffeine	Doxorubicin	Diazepam
	15.1 \pm 0.40	< 1 μ M	31.0
	Norfloxacin	CCCP	Aripiprazole
	0.56 \pm 0.13	< 10 μ M	7.02

Finally, compounds **44** and **56** were tested for selectivity against a broad group of 45 off-targets, including those structurally and evolutionally closest to the 5-HT_{1A} receptor, as well as the most troublesome for drug development (e.g. hERG channel, Chart 1, Supporting information Tables S4 and S5). In most cases, the affinity for the off-targets proved to be in micromolar range (< 50% binding in 1E-06). For some of the targets, binding was stronger, but considering very high affinity of the tested compounds for the 5-HT_{1A} receptor, the estimated selectivity was still over 3 orders of magnitude (> 1000x), even relatively higher than for the lead structure **3**. Interestingly, compound **56**, which displayed relatively highest affinity for some of the off-targets (reaching $pK_i \sim 8$), proved to be also relatively the most selective (> 10 000x), due to its extremely high affinity for the 5-HT_{1A} receptor ($pK_i = 12.80$). Based on all the data mentioned above, compounds **44** and **56** were ultimately selected for *in vivo* studies.

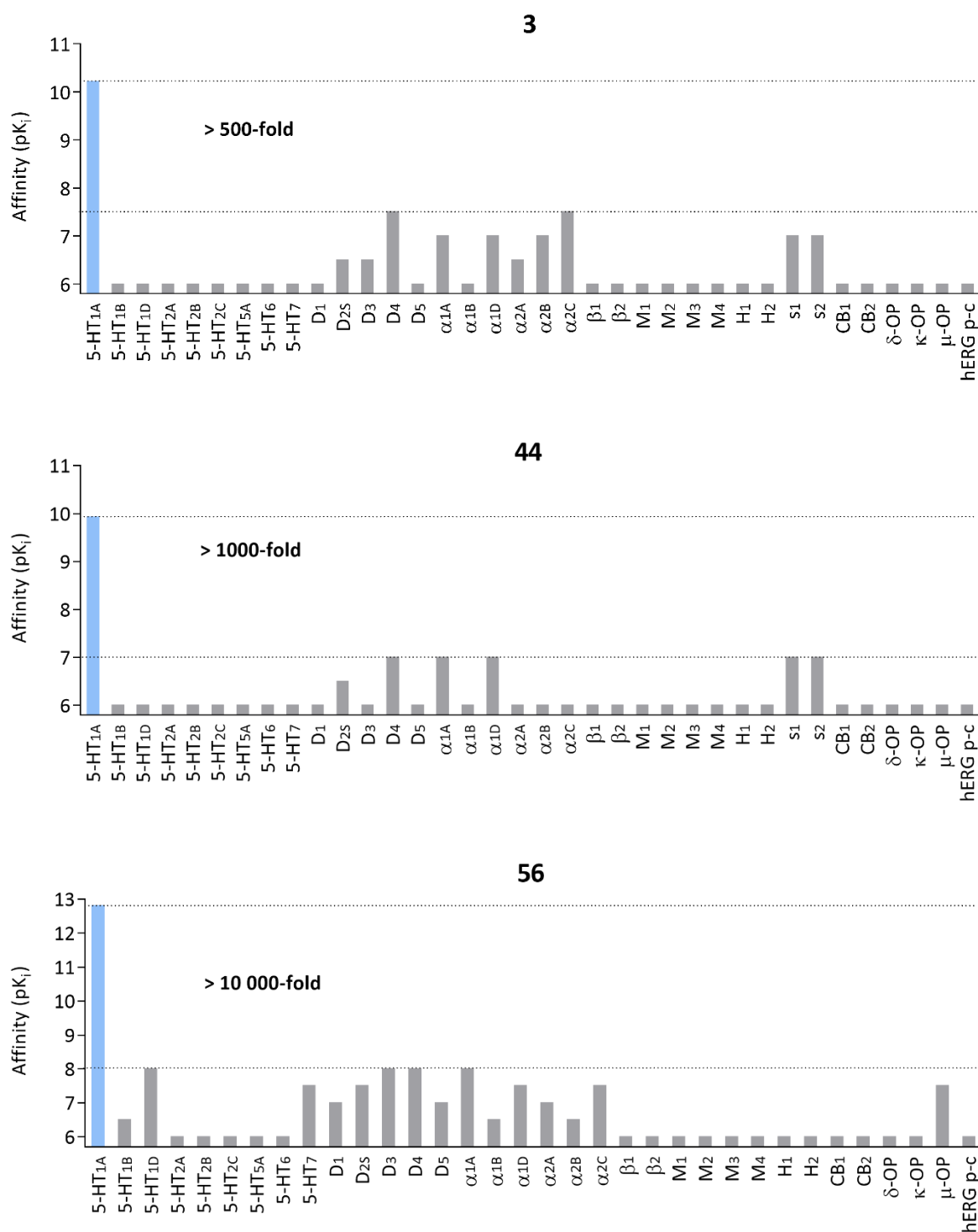
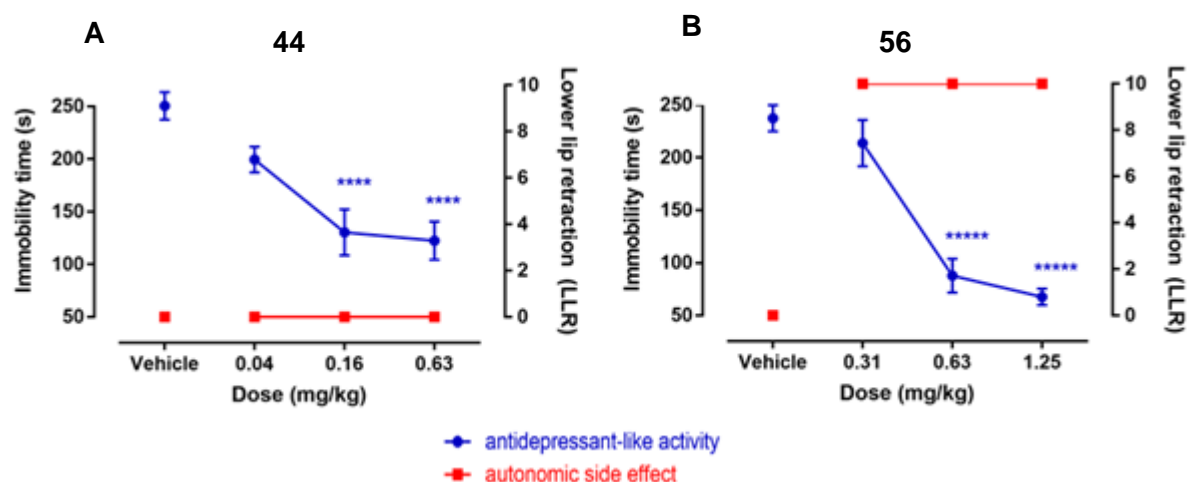


Chart 1. Graphical visualization of selectivity profiles of compounds **3**, **44** and **56**. For the sake of clarity, 34 most important targets are shown out of 46 tested. The pK_i values shown were estimated based on screening data and rounded to the nearest half-log value. For full selectivity data see Supporting information Tables S4 and S5. hERG p-c – hERG blockade determined using patch-clamp method.

***In vivo* studies**

So far, there is only sparse information connecting particular signaling transduction pathways with physiological effects. Evidence indicates that increased cortical ERK1/2 phosphorylation is associated with antidepressant activity,^{37,38} whereas inhibition of cAMP production by hippocampal 5-HT_{1A} receptors may interfere with memory process.^{39,40} On the other hand, it is currently not known what physiological effects are associated with activation of β -arrestin recruitment mediated by 5-HT_{1A} receptors. Nevertheless, it is very important for drug discovery to establish a link between particular functional profiles and the desired pharmacological effects.^{41,42} Therefore, two compounds with significantly differing *in vitro* functional pERK1/2 vs. β -arrestin selectivity profiles were compared in various *in vivo* measures relevant to 5-HT_{1A} receptor agonism. Compound **44** has a pERK1/2 vs. β -arrestin bias factor of 1.43 (i.e. its EC₅₀ is almost 30-fold lower for ERK1/2 phosphorylation than for β -arrestin recruitment), while compound **56** has a bias factor of -3.49, translating to over 3000-fold greater potency for β -arrestin recruitment than for pERK1/2. Interestingly, while both compounds displayed similar effectiveness in the Porsolt forced swimming test (FST) for antidepressant activity, with **44** being slightly more potent (minimal effective dose MED = 0.16 mg/kg p.o. for **44** vs. 0.63 mg/kg p.o. for **56**), they differed significantly in their ability to induce lower lip retraction (LLR). LLR is an autonomic response, a component of the rat “serotonergic syndrome”, attributed to 5-HT_{1A} receptor activation.⁴³ Compound **44** did not induce any significant LLR, even up to a dose 4× higher than the MED for antidepressant activity, while compound **56** elicited a full LLR in a dose 2× lower than the MED in Porsolt test (Chart 2, Supporting information Tables S6 and S8).



s

Chart 2. Differential profiles in the FST (in blue) and LLR (in red) of compounds **44** (A) and **56** (B), the 5-HT_{1A}R biased agonists with contrasting functional selectivity signaling fingerprints (preferential for pERK1/2 and β -arrestin, respectively). **** $p < 0.0001$, ***** $p < 0.00001$.

Noteworthy, at the time point that the *in vivo* effects were observed, we verified that there was a detectable exposure of the tested compounds in both serum and brain (Supporting information Chart S1, Table S10). Moreover, the abovementioned pharmacological effects were reversed by the selective 5-HT_{1A} receptor antagonist WAY100635, thus testifying for their full 5-HT_{1A} receptor dependence (Supporting information Table S7 and S9).

The significance of the LLR effect for human condition is so far unknown. However, it is undoubtedly an autonomic side effect, not connected with the antidepressant-like response in rat, and has previously been considered to be inseparable from the desired therapeutic-like effects resulting of the 5-HT_{1A} receptor activation.⁴⁴ Interestingly, antidepressant-like activity in the FST is mediated by activation of the cortical post-synaptic subpopulation of 5-HT_{1A} receptors, while induction of LLR is thought to be mediated by pre-synaptic 5-HT_{1A} autoreceptors localized in Raphe nuclei.^{45,46} In the case of 5-HT_{1A} receptors, the contrasting roles of pre- and post-synaptic receptors in different brain regions have been extensively investigated, also in the context of therapeutic effectiveness.¹⁶ The diverse pharmacological profiles of **44** and **56** are therefore of considerable interest, because they suggest that different preferences for β -arrestin recruitment relative to ERK1/2

phosphorylation (functional selectivity at the cellular level) may be associated with preferential activation of particular subpopulations of 5-HT_{1A} receptors (brain region selectivity) and thus lead to separate therapeutic and side effects. It should also be considered that such a high level of β -arrestin biased agonism, reported for the first time in the present study, could open the way to novel opportunities for targeting 5-HT_{1A} receptors, with previously unexplored physiological or behavioral outcomes. However, these are preliminary suggestions that need to be carefully and thoroughly evaluated, using more numerous biased agonists and diversified technical approaches. Whilst these observations are promising and warrant further investigation, formal demonstration of superior therapeutic activity by biased agonists ultimately requires appropriately designed clinical trials and a clear understanding linking *in vitro* biased agonism to disease mechanisms. Nevertheless, the present work provides compelling evidence that chemical modifications of 5-HT_{1A} receptor biased agonists allow for their functional diversification, which in turn translates to distinct pharmacological effects *in vivo*.

CONCLUSIONS

The present work describes the SAR and Structure-Functional Activity Relationships (SFAR) of 5-HT_{1A} receptor agonists and proves that novel and highly selective biased agonists can be designed to exhibit distinct and innovative signaling profiles. Thus, a series of 30 novel derivatives of 1-(1-benzoylpiperidin-4-yl)methanamine was synthesized and found to exhibit high affinity for 5-HT_{1A} receptor ($pK_i > 8.0$, LLE > 5.0). 27 of these had subnanomolar affinities ($pK_i > 9.0$, LLE > 6) and 15 compounds possessed higher lipophilic-ligand efficiencies than the lead compound **3**. Noteworthy, compound **56** was found to be extremely potent, one of the highest affinity 5-HT_{1A} receptor ligands discovered to date (based on the ChEMBL database). Moreover, most of the presented compounds showed substantial selectivity versus key anti-targets - the adrenergic α_1 and dopaminergic D₂ receptors (K_i ratio over 1000-fold). 25 compounds were selected and tested in four functional assays connected with the 5-HT_{1A} receptor activation, i.e.: ERK1/2 phosphorylation

(pERK1/2), adenylyl cyclase inhibition (cAMP), calcium mobilization (Ca^{2+}) and β -arrestin recruitment. Based on analysis of SFARs and of bias factors, 9 novel 5-HT_{1A} receptor biased agonists were identified that exhibit diversified functional activity profiles (i.e. ‘signaling fingerprints’). The selected, most interesting biased agonists **44** and **56** displayed high selectivity vs. a panel of 45 off-target sites, as well as promising metabolic stability, high permeability and low hepatotoxicity, thus testifying for their favorable developability profiles. Strikingly, whereas **44** exhibited marked biased agonism for activation of pERK1/2, **56** exhibited the opposite profile, with very potent biased agonism for β -arrestin recruitment. The profile of **56** is, to our knowledge, unprecedented and could constitute a novel class of 5-HT_{1A} receptor biased agonists, an interpretation reinforced by the differential *in vivo* activity of the two compounds in tests of antidepressant-like activity (FST) and behavioral syndrome (LLR). **44** preferentially elicited antidepressant-like effects, whereas **56** more potently elicited LLR, thus suggesting that the balance of β -arrestin recruitment relative to ERK1/2 phosphorylation (functional selectivity) may be associated with accentuated activity in specific physiological and/or behavioral models. As discussed previously, such differences likely reflect activation of particular subpopulations of the 5-HT_{1A} receptors (regional selectivity) and may account for differential separation of therapeutic and side effects.^{16,47,48} The novel 5-HT_{1A} agonists described herein, displaying diversified functional profiles, may constitute promising tool drugs to investigate the activity of 5-HT_{1A} receptor subpopulations and, potentially, could be developed as pharmacotherapeutics to treat CNS disorders involving dysfunctional serotonergic neurotransmission.

EXPERIMENTAL SECTION

Molecular modeling

Computer-aided ligand design and further studies on structure-activity relationships were based on ligand-receptor interactions analysis. The previously built on the template of the 5-HT_{1B} crystal structure (PDB ID 4IAR)⁴⁹ and pre-optimized serotonin 5-HT_{1A} receptor homology model served as a structural target for docking studies.⁵⁰ To capture distinctive binding mode of a variety of functionally biased ligands, the general procedure for developing ligand-optimized models using induced-fit technique⁵¹ served as both ligand-steered binding site optimization method (in terms of amino acid side chains) and routine docking approach, predicting bioactive conformation.¹³ Glide SP flexible docking procedure using OPLS3 force field was set for the induced-fit docking (IFD). H-bond constraint, as well as centroid of a grid box for docking to 5-HT_{1A} receptor, were located on Asp3.32. Ligand structures were sketched in Maestro 2D Sketcher and optimized using LigPrep tool. The aforementioned tools were implemented in Small-Molecule Drug Discovery Suite (Schrödinger, Inc. New York, USA), which was licensed for Jagiellonian University Medical College. Instant JChem was used for structure database management and property prediction, Instant JChem 20.8.0, 2020, ChemAxon (<http://www.chemaxon.com>).

Chemistry

General chemistry information. All the reagents were purchased from commercial suppliers (Sigma-Aldrich, Merck, Chempur, Fluorochem, Enamine, Acros Organics, Manchester Organics, POCh, Activate Scientific, Chem-impex International, Apollo Scientific) and were used without further purification. Analytical thin-layer chromatography (TLC) was performed on Merck Kieselgel 60 F₂₅₄ (0.25 mm) pre-coated aluminum sheets (Merck, Darmstadt, Germany). Compounds were visualized with UV light and by suitable visualization reagents (2.9% solution of ninhydrin in a mixture of 1-propanol and acetic acid (100/3, v/v) and Pancaldi reagent (solution of 12.0 g (NH₄)₆Mo₇O₂₄, 0.5 g Ce(SO₄)₂ and 6.8 mL of 98% H₂SO₄ in 240 mL of water). Flash chromatography was performed on CombiFlash RF (Teledyne Isco), using disposable silica gel flash columns RediSep Rf (silica gel 60, particle size 40–63 μm) and RediSep Gold (silica gel 60, particle size 20–40 μm) purchased from Teledyne Isco. The UPLC-MS or UPLC-MS/MS analyses were done on UPLC-MS/MS system comprising Waters ACQUITY UPLC (Waters Corporation, Milford, MA, USA) coupled with Waters TQD mass spectrometer (electrospray ionization mode ESI with tandem quadrupole). Chromatographic separations were carried out using the ACQUITY UPLC BEH (bridged ethyl hybrid) C18 column: 2.1 × 100 mm and 1.7 μm particle size. The column was maintained at 40 °C and eluted under gradient conditions using 95% to 0% of eluent A over 10 min, at a flow rate of 0.3 mL/min. Eluent A: 0.1% solution of formic acid in water (v/v); eluent B: 0.1% solution of formic acid in acetonitrile (v/v). A total of 10 μL of each sample was injected and chromatograms were recorded using Waters eλ PDA detector. The spectra were analysed in the range of 200–700 nm with 1.2 nm resolution and at a sampling rate of 20 points/s. The UPLC/MS purity of all the test compounds and key intermediates were determined to be >95%. ¹H NMR, ¹³C NMR, and ¹⁹F NMR spectra were obtained in a Varian Mercury spectrometer (Varian Inc., Palo Alto, CA, USA) and JEOL spectrometer (JEOL SAS., Tokyo, Japan), in CDCl₃, CD₃OD or DMSO-*d*₆ operating at 300 MHz (¹H NMR), 75 MHz or 126 MHz (¹³C NMR), and 282 MHz (¹⁹F NMR). Chemical shifts are reported as δ values (ppm) relative to TMS δ = 0 (¹H) as internal standard. The

J values are expressed in Hertz (Hz). Signal multiplicities are represented by the following abbreviations: s (singlet), br s (broad singlet), bd (broad doublet), d (doublet), dd (doublet of doublets), dt (doublet of triplets), t (triplet), td (triplet of doublets), tdd (triplet of doublet of doublets), q (quartet), dq (doublet of quartets), m (multiplet). Melting points were determined on Büchi Melting Point B-540 apparatus using open glass capillaries and are uncorrected.

Synthetic procedures

Previously reported or commercially available compounds:

2-(1-(3-Chloro-4-fluorobenzoyl)-4-fluoropiperidin-4-yl)-2-hydroxyacetonitrile (**4**),¹³

2-(1-(3,4-Dichlorobenzoyl)-4-fluoropiperidin-4-yl)-2-hydroxyacetonitrile (**5**),¹³

2-(2-Chlorophenoxy)ethanamine (**9**).

Detailed procedures for preparation of the amine intermediates 6–26 were described in the Supporting Information.

General procedures for the preparation of 1-(1-benzoylpiperidin-4-yl)methanamine derivatives (27–57).

To appropriate cyanohydrin (**4** or **5**)¹³ (1.0 equiv) dissolved in methanol, DABCO (2.0–12.5 equiv) was added in one portion, followed by the appropriate amine (**6–26**) (1.0–1.6 equiv), 4Å molecular sieves, sodium cyanoborohydride (1.6–7.8 equiv) and iron sulfate heptahydrate ($\text{FeSO}_4 \times 7 \text{H}_2\text{O}$) (1.1 equiv). The mixture was stirred at room temperature until the cyanohydrin was consumed (24–72 h), then the reaction mixture was filtered, concentrated in vacuo and next brine was added. The resulting mixture was extracted with EtOAc (3×), organics were combined and dried over magnesium sulfate, filtered and concentrated. The crude product was purified by flash chromatography.

***tert*-Butyl (3-(2-(((1-(3-chloro-4-fluorobenzoyl)-4-fluoropiperidin-4-yl)methyl)amino)ethoxy)phenyl)(methyl)carbamate (27)**

The title compound was prepared using 2-(1-(3-chloro-4-fluorobenzoyl)-4-fluoropiperidin-4-yl)-2-hydroxyacetonitrile (**4**) (0.110 g, 0.35 mmol) *tert*-butyl (3-(2-aminoethoxy)phenyl)(methyl)carbamate (**17**) (0.120 g, 0.45 mmol), DABCO (0.487 g, 4.34 mmol), sodium cyanoborohydride (0.167 g, 2.71 mmol), molecular sieves (0.900 g) and iron sulfate heptahydrate (0.106 g, 0.38 mmol) in methanol (5 mL). Purification: DCM/methanol/NH_{3(aq)} (9.5/0.5/0.02, v/v/v). Yield: 40%; colorless oil. ¹H NMR (300 MHz, CDCl₃, δ): 7.48 (dd, *J* = 1.8, 7.0 Hz, 1H), 7.33–7.25 (m, 1H), 7.19 (td, *J* = 8.3, 11.6 Hz, 2H), 6.86–6.77 (m, 2H), 6.74–6.65 (m, 1H), 4.51 (br s, 1H), 4.04 (t, *J* = 5.3 Hz, 2H), 3.58 (br s, 1H), 3.35 (br s, 1H), 3.23 (s, 3H), 3.20–3.08 (m, 1H), 3.02 (t, *J* = 5.0 Hz, 2H), 2.91–2.75 (m, 2H), 2.00 (br s, 2H), 1.64 (br s, 3H), 1.45 (s, 9H). Formula: C₂₇H₃₄ClF₂N₃O₄; MS (ESI⁺): *m/z* 538 [M+H⁺]

(3-Chloro-4-fluorophenyl)(4-fluoro-4-(((2-(2-fluorophenoxy)ethyl)amino)methyl)piperidin-1-yl)methanone (28)

The title compound was prepared using 2-(1-(3-chloro-4-fluorobenzoyl)-4-fluoropiperidin-4-yl)-2-hydroxyacetonitrile (**4**) (0.150 g, 0.48 mmol), 2-(2-fluorophenoxy)ethanamine (**6**) (0.118 g, 0.76 mmol), DABCO (0.669 g, 5.97 mmol), sodium cyanoborohydride (0.234 g, 3.73 mmol), molecular sieves (1.043 g) and iron sulfate heptahydrate (0.146 g, 0.53 mmol) in methanol (5 mL). Purification: EtOAc/methanol (9.5/0.5, v/v). Yield: 72%; pale yellow crystallizing oil. ¹H NMR (300 MHz, CDCl₃, δ): 7.51–7.45 (m, 1H), 7.33–7.25 (m, 1H), 7.21–7.13 (m, 1H), 7.11–7.01 (m, 2H), 7.01–6.86 (m, 2H), 4.50 (br s, 1H), 4.13 (t, *J* = 5.0 Hz, 2H), 3.58 (br s, 1H), 3.47–3.14 (m, 2H), 3.05 (t, *J* = 5.0 Hz, 2H), 2.86 (d, *J* = 19.9 Hz, 2H), 2.00 (s, 2H), 1.83–1.51 (m, 3H). ¹³C NMR (75 MHz, CDCl₃, δ): 168.0, 158.8 (d, *J* = 254 Hz), 152.8 (d, *J* = 246.4 Hz), 146.8 (d, *J* = 10.4 Hz), 132.9 (d, *J* = 4.6 Hz), 129.7, 127.1 (d, *J* = 6.9 Hz), 124.3 (d, *J* = 3.5 Hz), 121.5 (d, *J* = 18.4 Hz), 121.5 (d, *J* = 6.9 Hz), 116.8 (d, *J* = 22 Hz), 116.3 (d, *J* = 18.4 Hz), 115.3, 94.4 (d, *J* = 172 Hz), 69.2, 57.2 (d, *J* = 22 Hz), 49.2, 43.6, 38.2, 33.4, 32.6. Formula: C₂₁H₂₂ClF₃N₂O₂; MS (ESI⁺): *m/z* 427 [M+H⁺].

(3-Chloro-4-fluorophenyl)(4-fluoro-4-(((2-(3-fluorophenoxy)ethyl)amino)methyl)piperidin-1-yl)methanone (29)

The title compound was prepared using 2-(1-(3-chloro-4-fluorobenzoyl)-4-fluoropiperidin-4-yl)-2-hydroxyacetonitrile (**4**) (0.150 g, 0.48 mmol), 2-(3-fluorophenoxy)ethanamine (**7**) (0.118 g, 0.76 mmol), DABCO (0.669 g, 5.97 mmol), sodium cyanoborohydride (0.234 g, 3.73 mmol), molecular sieves (1.043 g) and iron sulfate heptahydrate (0.146 g, 0.53 mmol) in methanol (5 mL). Purification: *n*-hexane/EtOAc/methanol/NH_{3(aq)} (5/4.5/0.5/0.02, v/v/v/v). Yield: 40%; white crystalizing oil. ¹H NMR (300 MHz, CDCl₃, δ): 7.48 (dd, *J* = 2.1, 6.9 Hz, 1H), 7.33–7.26 (m, 1H), 7.24–7.13 (m, 2H), 6.67 (tdd, *J* = 1.0, 2.0, 9.5 Hz, 2H), 6.64–6.58 (m, 1H), 4.51 (br s, 1H), 4.04 (t, *J* = 5.0 Hz, 2H), 3.60 (br s, 1H), 3.46–3.10 (m, 2H), 3.03 (t, *J* = 5.1 Hz, 2H), 2.90–2.77 (m, 2H), 2.01 (br s, 2H), 1.63 (br s, 3H). ¹³C NMR (75 MHz, CDCl₃, δ): 168.1, 163.6 (d, *J* = 245 Hz), 160.1 (d, *J* = 11.1 Hz), 158.8 (d, *J* = 254 Hz), 132.9 (d, *J* = 4.4 Hz), 130.2 (d, *J* = 10 Hz), 129.7, 127.1 (d, *J* = 7.7 Hz), 121.5 (d, *J* = 18.2 Hz), 116.8 (d, *J* = 22 Hz), 110.2 (d, *J* = 2.8 Hz), 107.7 (d, *J* = 22 Hz), 102.2 (d, *J* = 24 Hz), 94.4 (d, *J* = 172 Hz), 67.7, 57.3 (d, *J* = 22 Hz), 49.1, 43.9, 38.6, 33.5, 32.8. Formula: C₂₁H₂₂ClF₃N₂O₂; MS (ESI⁺): *m/z* 427 [M+H⁺].

(3,4-Dichlorophenyl)(4-fluoro-4-(((2-(3-fluorophenoxy)ethyl)amino)methyl)piperidin-1-yl)methanone (30)

The title compound was prepared using 2-(1-(3,4-dichlorobenzoyl)-4-fluoropiperidin-4-yl)-2-hydroxyacetonitrile (**5**) (0.150 g, 0.45 mmol), 2-(3-fluorophenoxy)ethanamine (**7**) (0.064 g, 0.41 mmol), DABCO (0.634 g, 5.66 mmol), sodium cyanoborohydride (0.034 g, 0.54 mmol), molecular sieves (0.500 g) and iron sulfate heptahydrate (0.137 g, 0.50 mmol) in methanol (8 mL). Purification: *n*-hexane/Et₂O/DCM/methanol/NH_{3(aq)} (2/2/5.5/0.5/0.02, v/v/v/v/v). Yield: 35%; yellow transparent oil. ¹H NMR (300 MHz, CDCl₃, δ): 7.57–7.42 (m, 2H), 7.26–7.17 (m, 2H), 6.73–6.55 (m, 3H), 4.52 (br s, 1H), 4.04 (t, *J* = 5.1 Hz, 2H), 3.59 (br s, 1H), 3.44–3.10 (m, 2H), 3.03 (t, *J* = 5.0 Hz, 2H), 2.91–2.75 (m, 2H), 2.01 (br s, 2H), 1.62 (br s, 3H). ¹³C NMR (75 MHz, CDCl₃, δ): 167.9, 163.6 (d, *J* = 245.4 Hz), 160.1 (d, *J* = 10.4 Hz), 135.6, 134.1, 133.0, 130.6, 130.2 (d, *J* = 10.4 Hz), 129.1, 126.2, 110.2 (d, *J* = 2.3 Hz), 107.7 (d, *J* = 20 Hz), 102.2 (d, *J* = 24 Hz), 94.3 (d, *J* = 172 Hz), 67.6,

57.3 (d, $J = 22$ Hz), 49.1, 43.5, 38.2, 33.4, 32.6. Formula: $C_{21}H_{22}Cl_2F_2N_2O_2$; MS (ESI⁺): m/z 443 [M+H⁺].

(3-Chloro-4-fluorophenyl)(4-fluoro-4-(((2-(4-fluorophenoxy)ethyl)amino)methyl)piperidin-1-yl)methanone (31)

The title compound was prepared using 2-(1-(3-chloro-4-fluorobenzoyl)-4-fluoropiperidin-4-yl)-2-hydroxyacetonitrile (**4**) (0.100 g, 0.32 mmol), 2-(4-fluorophenoxy)ethanamine (**8**) (0.074 g, 0.48 mmol), DABCO (0.444 g, 3.97 mmol), sodium cyanoborohydride (0.155 g, 2.48 mmol), molecular sieves (0.900 g) and iron sulfate heptahydrate (0.097 g, 0.35 mmol) in methanol (4 mL). Purification *n*-hexane/EtOAc/methanol/NH_{3(aq)} (6/3.5/0.5/0.02, v/v/v/v). Yield: 64%; white crystallizing oil. ¹H NMR (300 MHz, CDCl₃, δ): 7.48 (dd, $J = 2.3, 7.0$ Hz, 1H), 7.33–7.24 (m, 1H), 7.22–7.11 (m, 1H), 7.01–6.90 (m, 2H), 6.88–6.78 (m, 2H), 4.51 (br s, 1H), 4.02 (t, $J = 5.3$ Hz, 2H), 3.62 (d, $J = 19.3$ Hz, 1H), 3.48–3.10 (m, 2H), 3.01 (t, $J = 5.0$ Hz, 2H), 2.83 (d, $J = 19.9$ Hz, 2H), 2.06–1.94 (m, 2H), 1.83–1.45 (m, 3H). ¹³C NMR (75 MHz, CDCl₃, δ): 168.1, 158.8 (d, $J = 253$ Hz), 157.3 (d, $J = 238$ Hz), 154.9, 132.9 (d, $J = 4.6$ Hz), 129.7, 127.1 (d, $J = 6.9$ Hz), 121.5 (d, $J = 18.4$ Hz), 116.8 (d, $J = 22$ Hz), 115.8 (d, $J = 23$ Hz, 2C), 115.5 (d, $J = 8.1$ Hz, 2C), 94.3 (d, $J = 172$ Hz), 68.0, 57.3 (d, $J = 22$ Hz), 49.3, 43.7, 38.3, 33.6, 32.7. Formula: $C_{21}H_{22}ClF_3N_2O_2$; MS (ESI⁺): m/z 427 [M+H⁺].

(3-Chloro-4-fluorophenyl)(4-fluoro-4-(((2-(2-chlorophenoxy)ethyl)amino)methyl)piperidin-1-yl)methanone (32)

The title compound was prepared using 2-(1-(3-chloro-4-fluorobenzoyl)-4-fluoropiperidin-4-yl)-2-hydroxyacetonitrile (**4**) (0.150 g, 0.48 mmol), 2-(2-chlorophenoxy)ethanamine (**9**) (0.131 g, 0.76 mmol), DABCO (0.669 g, 5.97 mmol), sodium cyanoborohydride (0.234 g, 3.73 mmol), molecular sieves (1.043 g) and iron sulfate heptahydrate (0.146 g, 0.53 mmol) in methanol (5 mL). Purification: DCM/methanol (9.5/0.5/0.02, v/v/v) and then *n*-hexane/EtOAc/methanol/NH_{3(aq)} (6/3.5/0.5/0.02, v/v/v/v). Yield: 48%; beige crystallizing oil. ¹H NMR (300 MHz, CDCl₃, δ): 7.47 (dd, $J = 1.8, 7.0$ Hz, 1H), 7.35 (dd, $J = 1.8, 7.6$ Hz, 1H), 7.32–7.26 (m, 1H), 7.24–7.12 (m, 2H), 6.96–6.84 (m, 2H),

4.49 (br s, 1H), 4.12 (t, $J = 5.0$ Hz, 2H), 3.59 (d, $J = 5.9$ Hz, 1H), 3.45–3.12 (m, 2H), 3.07 (t, $J = 5.0$ Hz, 2H), 2.95–2.80 (m, 2H), 2.00 (br s, 2H), 1.84 (s, 1H), 1.77–1.53 (m, 2H). ^{13}C NMR (75 MHz, CDCl_3 , δ): 168.0, 158.8 (d, $J = 254$ Hz), 154.2, 132.9 (d, $J = 4.6$ Hz), 130.3, 129.7, 127.8, 127.1 (d, $J = 6.9$ Hz), 123.0, 121.7, 121.5 (d, $J = 18.4$ Hz), 116.8 (d, $J = 22$ Hz), 113.7, 94.4 (d, $J = 172$ Hz), 68.9, 57.2 (d, $J = 22$ Hz), 49.0, 43.7, 38.2, 33.5, 32.7. Formula: $\text{C}_{21}\text{H}_{22}\text{Cl}_2\text{F}_2\text{N}_2\text{O}_2$; MS (ESI^+): m/z 443 $[\text{M}+\text{H}^+]$.

(3-Chloro-4-fluorophenyl)(4-(((2-(3-chlorophenoxy)ethyl)amino)methyl)-4-fluoropiperidin-1-yl)methanone (33)

The title compound was prepared using 2-(1-(3-chloro-4-fluorobenzoyl)-4-fluoropiperidin-4-yl)-2-hydroxyacetonitrile (**4**) (0.150 g, 0.48 mmol), 2-(3-chlorophenoxy)ethanamine (**10**) (0.131 g, 0.76 mmol), DABCO (0.669 g, 5.97 mmol), sodium cyanoborohydride (0.234 g, 3.73 mmol), molecular sieves (1.043 g) and iron sulfate heptahydrate (0.146 g, 0.53 mmol) in methanol (5 mL). Purification: *n*-hexane/EtOAc/methanol/ $\text{NH}_3(\text{aq})$ (5/4.5/0.5/0.02, v/v/v/v). Yield: 28%; beige crystallizing oil. ^1H NMR (300 MHz, CDCl_3 , δ): 7.48 (dd, $J = 2.1, 6.9$ Hz, 1H), 7.33–7.26 (m, 1H), 7.18 (dt, $J = 5.1, 8.3$ Hz, 2H), 6.96–6.91 (m, 1H), 6.90 (t, $J = 2.1$ Hz, 1H), 6.78 (ddd, $J = 0.8, 2.4, 8.3$ Hz, 1H), 4.52 (br s, 1H), 4.04 (t, $J = 5.0$ Hz, 2H), 3.60 (br s, 1H), 3.37 (br s, 2H), 3.02 (t, $J = 5.1$ Hz, 2H), 2.90–2.77 (m, 2H), 2.02 (br s, 2H), 1.63 (s, 3H). ^{13}C NMR (75 MHz, CDCl_3 , δ): 168.1, 159.5, 158.8 (d, $J = 254$ Hz), 134.9, 132.9 (d, $J = 4.4$ Hz), 130.2, 129.7, 127.1 (d, $J = 7.7$ Hz), 121.7, 121.1, 116.8 (d, $J = 22$ Hz), 114.9, 113.0, 94.3 (d, $J = 172$ Hz), 67.6, 57.3 (d, $J = 22$ Hz), 49.1, 43.3, 39.6, 33.3 (2C). Formula: $\text{C}_{21}\text{H}_{22}\text{Cl}_2\text{F}_2\text{N}_2\text{O}_2$; MS (ESI^+): m/z 443 $[\text{M}+\text{H}^+]$.

(4-(((2-(3-Chlorophenoxy)ethyl)amino)methyl)-4-fluoropiperidin-1-yl)(3,4-dichlorophenyl)methanone (34)

The title compound was prepared using 2-(1-(3,4-dichlorobenzoyl)-4-fluoropiperidin-4-yl)-2-hydroxyacetonitrile (**4**) (0.150 g, 0.45 mmol), 2-(3-chlorophenoxy)ethanamine (**10**) (0.070 g, 0.41 mmol), DABCO (0.634 g, 5.66 mmol), sodium cyanoborohydride (0.034 g, 0.54 mmol), molecular

sieves (0.500 g) and iron sulfate heptahydrate (0.137 g, 0.50 mmol) in methanol (8 mL). Purification: *n*-hexane/EtOAc/methanol/NH_{3(aq)} (4/5.5/0.5/0.02, v/v/v/v). Yield: 36%; yellow oil. ¹H NMR (300 MHz, CDCl₃, δ): 7.53–7.46 (m, 2H), 7.25–7.15 (m, 2H), 6.97–6.87 (m, 2H), 6.78 (ddd, *J* = 1.0, 2.4, 8.3 Hz, 1H), 4.52 (br s, 1H), 4.04 (t, *J* = 5.1 Hz, 2H), 3.59 (br s, 1H), 3.46–3.12 (m, 2H), 3.02 (t, *J* = 5.1 Hz, 2H), 2.91–2.76 (m, 2H), 2.00 (d, *J* = 12.3 Hz, 2H), 1.61 (br s, 3H). ¹³C NMR (75 MHz, CDCl₃, δ): 167.9, 159.5, 135.6, 134.9, 134.1, 133.0, 130.6, 130.2, 129.1, 126.2, 121.1, 114.9, 113.0, 94.3 (d, *J* = 172 Hz), 67.6, 57.2 (d, *J* = 22 Hz), 49.1, 43.5, 38.2, 33.5, 32.9. Formula: C₂₁H₂₂Cl₃FN₂O₂; MS (ESI⁺): *m/z* 459 [M+H⁺].

(3-Chloro-4-fluorophenyl)(4-fluoro-4-(((2-(4-chlorophenoxy)ethyl)amino)methyl)piperidin-1-yl)methanone (35)

The title compound was prepared using 2-(1-(3-chloro-4-fluorobenzoyl)-4-fluoropiperidin-4-yl)-2-hydroxyacetonitrile (**4**) (0.100 g, 0.32 mmol), 2-(4-chlorophenoxy)ethanamine (**11**) (0.082 g, 0.48 mmol), DABCO (0.444 g, 3.97 mmol), sodium cyanoborohydride (0.155 g, 2.48 mmol), molecular sieves (0.900 g) and iron sulfate heptahydrate (0.097 g, 0.35 mmol) in methanol (4 mL). Purification: *n*-hexane/EtOAc/methanol/NH_{3(aq)} (6/3.5/0.5/0.02, v/v/v/v). Yield: 64%; white oil. ¹H NMR (300 MHz, CDCl₃, δ): 7.48 (dd, *J* = 2.1, 6.7 Hz, 1H), 7.34–7.12 (m, 4H), 6.87–6.77 (m, 2H), 4.50 (br s, 1H), 4.02 (t, *J* = 5.0 Hz, 2H), 3.74–3.49 (m, 1H), 3.24 (br s, 2H), 3.02 (t, *J* = 5.0 Hz, 2H), 2.91–2.74 (m, 2H), 2.00 (br s, 2H), 1.88–1.44 (m, 3H). ¹³C NMR (75 MHz, CDCl₃, δ): 168.1, 157.4, 158.8 (d, *J* = 254 Hz), 132.9 (d, *J* = 4.6 Hz), 129.7, 129.3 (2C), 127.1 (d, *J* = 6.9 Hz), 125.8, 121.5 (d, *J* = 18.4 Hz), 116.8 (d, *J* = 22 Hz), 115.7 (2C), 94.3 (d, *J* = 172 Hz), 67.7, 57.3 (d, *J* = 22 Hz), 49.2, 43.7, 38.3, 33.6, 32.8. Formula: C₂₁H₂₂Cl₂F₂N₂O₂; MS (ESI⁺): *m/z* 443 [M+H⁺].

(3-Chloro-4-fluorophenyl)(4-fluoro-4-(((2-(2-methoxyphenoxy)ethyl)amino)methyl)piperidin-1-yl)methanone (36)

The title compound was prepared using 2-(1-(3-chloro-4-fluorobenzoyl)-4-fluoropiperidin-4-yl)-2-hydroxyacetonitrile (**4**) (0.505 g, 1.61 mmol), 2-(2-methoxyphenoxy)ethanamine (**12**) (0.430 g, 2.58

mmol), DABCO (2.256 g, 20.11 mmol), sodium cyanoborohydride (0.788 g, 12.55 mmol), molecular sieves (3.300 g) in methanol (15 mL). Purification: *n*-hexane/EtOAc/methanol/NH_{3(aq)} (6/3.5/0.5/0.02, v/v/v/v). Yield: 35%; pale yellow crystallizing oil. ¹H NMR (300 MHz, CDCl₃, δ): 7.48 (dd, *J* = 2.1, 6.9 Hz, 1H), 7.32–7.26 (m, 1H), 7.20–7.13 (m, 1H), 6.98–6.85 (m, 4H), 4.50 (br s, 1H), 4.12 (t, *J* = 5.3 Hz, 2H), 3.84 (s, 3H), 3.60 (br s, 1H), 3.45–3.13 (m, 2H), 3.04 (t, *J* = 5.3 Hz, 2H), 2.91–2.79 (m, 2H), 2.10–1.92 (m, 2H), 1.70 (br s, 3H). ¹⁹F NMR (282 MHz, CDCl₃, δ): -112.7 (s, 1F), -166.3 (s, 1F). ¹³C NMR (75 MHz, CDCl₃, δ): 168.0, 158.8 (d, *J* = 245 Hz), 149.8, 148.2, 132.9 (d, *J* = 4.4 Hz), 129.7, 127.1 (d, *J* = 7.7 Hz), 121.6, 121.4, 120.9, 116.8 (d, *J* = 22 Hz), 114.2, 111.9, 94.4 (d, *J* = 172 Hz), 69.0, 57.3 (d, *J* = 22 Hz), 55.8, 49.3, 43.8, 38.3, 33.6, 32.8. Formula: C₂₂H₂₅ClF₂N₂O₃; MS (ESI⁺): *m/z* 439 [M+H⁺].

(3,4-Dichlorophenyl)(4-fluoro-4-(((2-(2-methoxyphenoxy)ethyl)amino)methyl)piperidin-1-yl)methanone (37)

The title compound was prepared using 2-(1-(3,4-dichlorobenzoyl)-4-fluoropiperidin-4-yl)-2-hydroxyacetonitrile (**5**) (0.350 g, 1.06 mmol), 2-(2-methoxyphenoxy)ethanamine (**12**) (0.282 g, 1.69 mmol), DABCO (1.479 g, 13.18 mmol), sodium cyanoborohydride (0.518 g, 8.25 mmol), molecular sieves (2.194 g) in methanol (10 mL). Purification: *n*-hexane/EtOAc/methanol/NH_{3(aq)} (6/3.5/0.5/0.02, v/v/v/v). Yield: 30%; pale yellow crystallizing oil. ¹H NMR (300 MHz, CDCl₃, δ): 7.53–7.45 (m, 2H), 7.23 (dd, *J* = 1.8, 8.2 Hz, 1H), 6.99–6.84 (m, 4H), 4.51 (br s, 1H), 4.12 (t, *J* = 5.3 Hz, 2H), 3.84 (s, 3H), 3.57 (br s, 1H), 3.46–3.10 (m, 2H), 3.04 (t, *J* = 5.1 Hz, 2H), 2.91–2.78 (m, 2H), 2.00 (br s, 2H), 1.77 (br s, 3H). ¹³C NMR (75 MHz, CDCl₃, δ): 167.9, 149.7, 148.2, 135.7, 134.1, 133.0, 130.6, 129.1, 126.2, 121.6, 120.9, 114.2, 111.9, 94.3 (d, *J* = 172 Hz), 69.0, 57.3 (d, *J* = 22 Hz), 55.8, 49.3, 43.6, 38.2, 33.4, 32.7. Formula: C₂₂H₂₅Cl₂FN₂O₃; MS (ESI⁺): *m/z* 455 [M+H⁺].

(3-Chloro-4-fluorophenyl)(4-fluoro-4-(((2-(3-methoxyphenoxy)ethyl)amino)methyl)piperidin-1-yl)methanone (38)

The title compound was prepared using 2-(1-(3-chloro-4-fluorobenzoyl)-4-fluoropiperidin-4-yl)-2-hydroxyacetonitrile (**4**) (0.165 g, 0.52 mmol), 2-(3-methoxyphenoxy)ethanamine (**13**) (0.140 g, 0.84 mmol), DABCO (0.734 g, 6.55 mmol), sodium cyanoborohydride (0.256 g, 4.09 mmol), molecular sieves (1.043 g) and iron sulfate heptahydrate (0.165 g, 0.58 mmol) in methanol (5 mL). Purification: *n*-hexane/EtOAc/methanol/NH_{3(aq)} (8/1.5/0.5/0.02, v/v/v/v). Yield: 40%; yellow transparent oil. ¹H NMR (300 MHz, CDCl₃, δ): 7.48 (dd, *J* = 2.1, 6.9 Hz, 1H), 7.33–7.26 (m, 1H), 7.21–7.13 (m, 2H), 6.54–6.48 (m, 2H), 6.47–6.45 (m, 1H), 4.52 (br s, 1H), 4.05 (t, *J* = 5.1 Hz, 2H), 3.78 (s, 3H), 3.59 (br s, 1H), 3.45–3.11 (m, 2H), 3.02 (t, *J* = 5.0 Hz, 2H), 2.91–2.76 (m, 2H), 2.01 (br s, 2H), 1.71 (br s, 3H). ¹³C NMR (75 MHz, CDCl₃, δ): 168.1, 160.8, 160.0, 158.8 (d, *J* = 254 Hz), 132.9 (d, *J* = 4.4 Hz), 129.9, 129.7, 127.1 (d, *J* = 7.7 Hz), 121.5 (d, *J* = 18.2 Hz), 116.8 (d, *J* = 22 Hz), 106.7, 106.4, 101.0, 94.3 (d, *J* = 172 Hz), 67.3, 57.3 (d, *J* = 22 Hz), 55.3, 49.3, 43.6, 38.2, 33.6, 32.8. Formula: C₂₂H₂₅ClF₂N₂O₃; MS (ESI⁺): *m/z* 439 [M+H⁺].

(3,4-Dichlorophenyl)(4-fluoro-4-(((2-(3-methoxyphenoxy)ethyl)amino)methyl)piperidin-1-yl)methanone (39)

The title compound was prepared using 2-(1-(3,4-dichlorobenzoyl)-4-fluoropiperidin-4-yl)-2-hydroxyacetonitrile (**5**) (0.124 g, 0.37 mmol), 2-(3-methoxyphenoxy)ethanamine (**13**) (0.100 g, 0.60 mmol), DABCO (0.524 g, 4.68 mmol), sodium cyanoborohydride (0.183 g, 2.91 mmol), molecular sieves (0.776 g) in methanol (4 mL). Purification: *n*-hexane/EtOAc/methanol/NH_{3(aq)} (8/1.5/0.5/0.02, v/v/v/v). Yield: 30%; yellow oil. ¹H NMR (300 MHz, CDCl₃, δ): 7.53–7.47 (m, 2H), 7.23 (dd, *J* = 1.8, 8.2 Hz, 1H), 7.18 (t, *J* = 8.1 Hz, 1H), 6.56–6.43 (m, 3H), 4.51 (br s, 1H), 4.05 (t, *J* = 5.1 Hz, 2H), 3.79 (s, 3H), 3.60 (br s, 1H), 3.38 (br s, 2H), 3.02 (t, *J* = 5.0 Hz, 2H), 2.90–2.78 (m, 2H), 2.01 (br s, 2H), 1.59 (br s, 3H). ¹³C NMR (126 MHz, CDCl₃, δ) 168.0, 160.9, 160.1, 135.7, 134.2, 133.1, 130.7, 130.0, 129.2, 126.3, 106.8, 106.5, 101.1, 94.4 (d, *J* = 172.6 Hz), 67.4, 57.4 (d, *J* = 21.7 Hz), 55.4, 49.4, 43.7, 38.2, 33.7 (d, *J* = 22.9 Hz), 32.8 (d, *J* = 21.1 Hz). Formula: C₂₂H₂₅Cl₂FN₂O₃; MS (ESI⁺): *m/z* 455 [M+H⁺].

(3-Chloro-4-fluorophenyl)(4-fluoro-4-(((2-(4-methoxyphenoxy)ethyl)amino)methyl)piperidin-1-yl)methanone (40)

The title compound was prepared using 2-(1-(3-chloro-4-fluorobenzoyl)-4-fluoropiperidin-4-yl)-2-hydroxyacetonitrile (**4**) (0.150 g, 0.48 mmol), 2-(4-methoxyphenoxy)ethanamine (**14**) (0.128 g, 0.77 mmol), DABCO (0.669 g, 5.97 mmol), sodium cyanoborohydride (0.234 g, 3.73 mmol), molecular sieves (1.043 g) and iron sulfate heptahydrate (0.146 g, 0.53 mmol) in methanol (5 mL). Purification: *n*-hexane/EtOAc/methanol/NH_{3(aq)} (6/3.5/0.5/0.02, v/v/v/v) and then EtOAc/methanol (9/1, v/v). Yield: 51%; colorless oil. ¹H NMR (300 MHz, CDCl₃, δ): 7.48 (dd, *J* = 2.1, 6.9 Hz, 1H), 7.33–7.26 (m, 1H), 7.22–7.14 (m, 1H), 6.83 (s, 4H), 4.50 (br s, 1H), 4.01 (t, *J* = 5.1 Hz, 2H), 3.76 (s, 3H), 3.60 (br s, 1H), 3.44–3.13 (m, 2H), 3.00 (t, *J* = 5.1 Hz, 2H), 2.90–2.78 (m, 2H), 2.02 (s, 2H), 1.64 (br s, 3H). ¹³C NMR (75 MHz, CDCl₃, δ): 168.1, 158.8 (d, *J* = 254 Hz), 154.0, 152.9, 132.9 (d, *J* = 4.4 Hz), 129.7, 127.1 (d, *J* = 7.7 Hz), 121.5 (d, *J* = 18.2 Hz), 116.8 (d, *J* = 22 Hz), 115.5 (2C), 114.7 (2C), 94.3 (d, *J* = 172 Hz), 68.0, 57.3 (d, *J* = 22 Hz), 55.7, 49.4, 43.8, 38.2, 33.8, 33.1. Formula: C₂₂H₂₅ClF₂N₂O₃; MS (ESI⁺): *m/z* 439 [M+H⁺].

(3,4-Dichlorophenyl)(4-fluoro-4-(((2-(4-methoxyphenoxy)ethyl)amino)methyl)piperidin-1-yl)methanone (41)

The title compound was prepared using 2-(1-(3,4-dichlorobenzoyl)-4-fluoropiperidin-4-yl)-2-hydroxyacetonitrile (**5**) (0.350 g, 1.06 mmol), 2-(4-methoxyphenoxy)ethanamine, (**14**) (0.265 g, 1.59 mmol), DABCO (1.479 g, 13.18 mmol), sodium cyanoborohydride (0.518 g, 8.25 mmol), molecular sieves (2.194 g), in methanol (10 mL). Purification: EtOAc/methanol (9.9/0.1, v/v). Yield: 30%; pale yellow crystallizing oil. ¹H NMR (300 MHz, CDCl₃, δ): 7.54–7.44 (m, 2H), 7.23 (dd, *J* = 2.1, 8.2 Hz, 1H), 6.83 (s, 4H), 4.52 (br s, 1H), 4.01 (t, *J* = 5.1 Hz, 2H), 3.76 (s, 3H), 3.57 (br s, 1H), 3.45–3.10 (m, 2H), 3.00 (t, *J* = 5.0 Hz, 2H), 2.88–2.77 (m, 2H), 2.02 (m, 2H), 1.61 (br s, 3H). ¹⁹F NMR (282 MHz, CDCl₃, δ): -166.5 (s, 1F). ¹³C NMR (75 MHz, CDCl₃, δ): 167.9, 154.0, 152.9, 135.7, 134.1, 133.0, 130.6, 129.1, 126.2, 115.5 (2C), 114.6 (2C), 94.3 (d, *J* = 172 Hz), 68.0, 57.3

(d, $J = 22$ Hz), 55.7, 49.4, 43.6, 38.2, 33.5, 32.5. Formula: $C_{22}H_{25}Cl_2FN_2O_3$; MS (ESI⁺): m/z 455 [M+H⁺].

2-(2-(((1-(3-Chloro-4-fluorobenzoyl)-4-fluoropiperidin-4-yl)methyl)amino)ethoxy)benzamide (42)

The title compound was prepared using 2-(1-(3-chloro-4-fluorobenzoyl)-4-fluoropiperidin-4-yl)-2-hydroxyacetonitrile (**4**) (0.163 g, 0.52 mmol), 2-(2-aminoethoxy)benzamide (**15**) (0.140 g, 0.78 mmol), DABCO (0.725 g, 6.48 mmol), sodium cyanoborohydride (0.253 g, 4.04 mmol), molecular sieves (0.900 g) and iron sulfate heptahydrate (0.158 g, 0.57 mmol) in methanol (5 mL). Purification: *n*-hexane/Et₂O/DCM/methanol/NH_{3(aq)} (3/2/4.5/0.5/0.02, v/v/v/v/v). Yield: 29%; white powder. ¹H NMR (300 MHz, DMSO-*d*₆, δ): 7.95 (s, 1H), 7.81 (dd, $J = 1.8, 7.6$ Hz, 1H), 7.65 (dd, $J = 1.8, 7.0$ Hz, 1H), 7.54 (br s, 1H), 7.50–7.37 (m, 3H), 7.12 (d, $J = 8.2$ Hz, 1H), 7.00 (t, $J = 7.9$ Hz, 1H), 4.33–4.07 (m, 3H), 3.38 (br s, 1H), 3.27–2.97 (m, 2H), 2.93 (t, $J = 5.3$ Hz, 2H), 2.81–2.66 (m, 2H), 2.13 (br s, 1H), 1.96–1.64 (m, 4H). ¹³C NMR (75 MHz, DMSO-*d*₆, δ): 167.2, 166.7, 157.2, 158.1 (d, $J = 248.7$ Hz), 134.4, 132.9, 131.3, 129.7, 128.2 (d, $J = 6.9$ Hz), 123.1, 121.0, 120.2 (d, $J = 18.3$ Hz), 117.4 (d, $J = 21$ Hz), 113.8, 95.6 (d, $J = 172$ Hz), 68.5, 56.7 (d, $J = 22$ Hz), 49.0, 43.4, 38.0, 33.1, 32.3. Formula: $C_{22}H_{24}ClF_2N_3O_3$; MS (ESI⁺): m/z 452 [M+H⁺]. Melting point: 180.5–181.0 °C.

3-(2-(((1-(3-Chloro-4-fluorobenzoyl)-4-fluoropiperidin-4-yl)methyl)amino)ethoxy)benzamide (43)

The title compound was prepared using 2-(1-(3-chloro-4-fluorobenzoyl)-4-fluoropiperidin-4-yl)-2-hydroxyacetonitrile (**4**) (0.100 g, 0.32 mmol), 3-(2-aminoethoxy)benzamide (**16**) (0.080 g, 0.41 mmol), DABCO (0.444 g, 3.97 mmol), sodium cyanoborohydride (0.155 g, 2.48 mmol), molecular sieves (0.900 g) and iron sulfate heptahydrate (0.097 g, 0.35 mmol) in methanol (5 mL). Purification: EtOAc/methanol (9/1, v/v). Yield: 42%; yellow transparent oil. ¹H NMR (300 MHz, CDCl₃, δ): 7.46 (dd, $J = 1.8, 7.0$ Hz, 1H), 7.42–7.37 (m, 1H), 7.35–7.23 (m, 3H), 7.20–7.11 (m, 1H), 7.04 (td, $J = 2.9, 5.9$ Hz, 1H), 6.43–6.04 (m, 2H), 4.49 (br s, 1H), 4.09 (t, $J = 5.3$ Hz, 2H), 3.58 (br s, 1H), 3.45–

3.08 (m, 2H), 3.02 (t, $J = 5.3$ Hz, 2H), 2.83 (d, $J = 19.9$ Hz, 2H), 1.98 (br s, 3H), 1.81–1.48 (m, 2H). ^{19}F NMR (282 MHz, CDCl_3 , δ): -112.6 (s, 1F), -166.4 (s, 1F). ^{13}C NMR (75 MHz, CDCl_3 , δ): 169.4, 168.1, 159.0, 158.8 (d, $J = 254$ Hz), 134.8, 132.8 (d, $J = 3.5$ Hz), 129.7, 129.6, 127.1 (d, $J = 7.7$ Hz), 121.5 (d, $J = 17.3$ Hz), 119.5, 118.6, 116.8 (d, $J = 22$ Hz), 113.3, 94.3 (d, $J = 172$ Hz), 67.5, 57.2 (d, $J = 22$ Hz), 49.1, 43.7, 38.3, 33.6, 32.8. Formula: $\text{C}_{22}\text{H}_{24}\text{ClF}_2\text{N}_3\text{O}_3$; MS (ESI $^+$): m/z 452 [$\text{M}+\text{H}^+$].

(3-Chloro-4-fluorophenyl)(4-fluoro-4-(((2-(2-(methylamino)phenoxy)ethyl)amino)methyl)piperidin-1-yl)methanone (44)

The title compound was prepared using 2-(1-(3-chloro-4-fluorobenzoyl)-4-fluoropiperidin-4-yl)-2-hydroxyacetonitrile (**4**) (0.120 g, 0.38 mmol), 2-(2-aminoethoxy)-*N*-methylaniline (**24**) (0.076 g, 0.46 mmol), DABCO (0.084 g, 0.76 mmol), sodium cyanoborohydride (0.038 g, 0.61 mmol), molecular sieves (0.900 g) and iron sulfate heptahydrate (0.117 g, 0.42 mmol) in methanol (5 mL). Purification: EtOAc/methanol (9.5/0.5, v/v). Yield: 29%; yellow transparent oil. ^1H NMR (300 MHz, CDCl_3 , δ): 7.52–7.44 (m, 1H), 7.34–7.26 (m, 1H), 7.23–7.12 (m, 1H), 6.96–6.87 (m, 1H), 6.78 (dd, $J = 1.5, 7.9$ Hz, 1H), 6.64 (dq, $J = 1.8, 7.8$ Hz, 2H), 4.50 (br s, 1H), 4.09 (t, $J = 5.3$ Hz, 2H), 3.60 (br s, 1H), 3.45–3.13 (m, 2H), 3.05 (t, $J = 5.0$ Hz, 2H), 2.90–2.75 (m, 5H), 2.00 (br s, 3H), 1.64 (m., 3H). ^{19}F NMR (282 MHz, CDCl_3 , δ): -112.6 (s, 1F), -166.6 (s, 1F). ^{13}C NMR (126 MHz, CDCl_3 , δ) 168.2, 158.9 (d, $J = 252.3$ Hz), 145.9, 139.7, 132.9 (d, $J = 4.2$ Hz), 129.8, 127.2 (d, $J = 7.8$ Hz), 122.1, 121.7 (d, $J = 18.1$ Hz), 116.9 (d, $J = 21.1$ Hz), 116.4, 111.1, 109.8, 94.3 (d, $J = 172.6$ Hz), 67.6 (s), 57.1 (d, $J = 21.7$ Hz), 49.4, 43.6, 38.2, 33.6, 32.9, 30.4. Formula: $\text{C}_{22}\text{H}_{26}\text{ClF}_2\text{N}_3\text{O}_2$; MS (ESI $^+$): m/z 438 [$\text{M}+\text{H}^+$].

(3-Chloro-4-fluorophenyl)(4-fluoro-4-(((2-(3-(methylamino)phenoxy)ethyl)amino)methyl)piperidin-1-yl)methanone (45)

The title compound was prepared by Boc-deprotection of *tert*-butyl (3-(2-(((1-(3-chloro-4-fluorobenzoyl)-4-fluoropiperidin-4-yl)methyl)amino)ethoxy)phenyl)(methyl)carbamate (**27**).

Compound **27** (1.0 equiv, 0.075 g, 0.14 mmol) was mixed with 1.0 M HCl in EtOAc (5 mL) and stirred at room temperature for 24 h. Then, the mixture was filtered to give the product as a hydrochloride salt. The obtained hydrochloride salt was turned into a free base (using 10% aqueous solution of sodium carbonate) before purification. Purification: DCM/methanol/NH_{3(aq)} (9.5/0.5/0.02, v/v/v). Yield: 48%; white-gray crystallizing oil. ¹H NMR (300 MHz, CD₃OD, δ): 7.73–7.00 (m, 7H), 4.46 (br s, 3H), 3.77–3.34 (m, 6H), 3.22 (br s, 1H), 3.08 (s, 3H), 2.19–1.81 (m, 4H), NH protons not detected. ¹⁹F NMR (282 MHz, CDCl₃, δ): -114.8 (s, 1F), -166.6 (s, 1F). ¹³C NMR (75 MHz, CDCl₃, δ): 169.0, 160.0 (d, *J* = 3.5 Hz), 156.1, 150.7 (d, *J* = 4.7 Hz), 129.7 (d, *J* = 8.5 Hz), 129.3, 128.8, 127.1, 122.5, 111.6, 105.9, 102.8, 98.9, 94.5 (d, *J* = 172 Hz), 67.0, 57.3 (d, *J* = 22 Hz), 56.2, 49.4, 43.9, 38.4, 33.7, 32.9. Formula: C₂₂H₂₆ClF₂N₃O₂; MS (ESI⁺): *m/z* 438 [M+H⁺].

(3-Chloro-4-fluorophenyl)(4-(((2-(3-(dimethylamino)phenoxy)ethyl)amino)methyl)-4-fluoropiperidin-1-yl)methanone (46)

The title compound was prepared using 2-(1-(3-chloro-4-fluorobenzoyl)-4-fluoropiperidin-4-yl)-2-hydroxyacetonitrile (**4**) (0.166 g, 0.53 mmol), 3-(2-aminoethoxy)-*N,N*-dimethylaniline (**18**) (0.133 g, 0.74 mmol), DABCO (0.740 g, 6.61 mmol), sodium cyanoborohydride (0.277 g, 4.13 mmol), molecular sieves (1.043 g) and iron sulfate heptahydrate (0.162 g, 0.58 mmol) in methanol (5 mL). Purification: DCM/methanol/NH_{3(aq)} (9.5/0.5/0.02, v/v/v) and then *n*-hexane/EtOAc/methanol/NH_{3(aq)} (4/5.5/0.5/0.02, v/v/v/v). Yield: 42%; colorless oil. ¹H NMR (300 MHz, CDCl₃, δ): 7.48 (dd, *J* = 2.1, 6.7 Hz, 1H), 7.34–7.25 (m, 1H), 7.22–7.07 (m, 2H), 6.40–6.32 (m, 1H), 6.31–6.22 (m, 2H), 4.50 (br s, 1H), 4.06 (t, *J* = 5.0 Hz, 2H), 3.60 (br s, 1H), 3.47–3.08 (m, 2H), 3.02 (t, *J* = 5.0 Hz, 2H), 2.93 (s, 6H), 2.84 (d, *J* = 19.9 Hz, 2H), 2.00 (br s, 2H), 1.87–1.47 (m, 3H). ¹³C NMR (75 MHz, CDCl₃, δ): 168.0, 159.8, 158.8 (d, *J* = 254 Hz), 152.0, 132.9 (d, *J* = 4.4 Hz), 129.7 (d, *J* = 2.3 Hz, 2C), 127.1 (d, *J* = 6.9 Hz), 121.5 (d, *J* = 18.4 Hz), 116.8 (d, *J* = 22 Hz), 105.9, 101.9, 99.6, 94.4 (d, *J* = 172 Hz), 67.0, 57.3 (d, *J* = 22 Hz), 49.4, 43.7, 40.6 (2C), 38.1, 33.7, 32.9. Formula: C₂₃H₂₈ClF₂N₃O₂; MS (ESI⁺): *m/z* 452 [M+H⁺].

***N*-(3-(2-(((1-(3-Chloro-4-fluorobenzoyl)-4-fluoropiperidin-4-yl)methyl)amino)ethoxy)phenyl)acetamide (47)**

The title compound was prepared using 2-(1-(3-chloro-4-fluorobenzoyl)-4-fluoropiperidin-4-yl)-2-hydroxyacetonitrile (**4**) (0.150 g, 0.48 mmol), *N*-[3-(2-aminoethoxy)phenyl]acetamide (**19**) (0.148 g, 0.76 mmol), DABCO (0.669 g, 5.97 mmol,), sodium cyanoborohydride (0.234 g, 3.73 mmol), molecular sieves (1.043 g) and iron sulfate heptahydrate (0.146 g, 0.53 mmol) in methanol (5 mL). Purification: EtOAc/methanol (9.5/0.5, v/v). Yield: 82%; colorless oil. ¹H NMR (500 MHz, CDCl₃, δ): 7.54 (br s, 1H), 7.47 (dd, *J* = 1.9, 7.0 Hz, 1H), 7.31–7.26 (m, 2H), 7.20–7.13 (m, 2H), 6.94 (br d, *J* = 8.0 Hz, 1H), 6.62 (br d, *J* = 7.2 Hz, 1H), 4.50 (br s, 1H), 4.13–4.06 (m, 2H), 3.59 (br s, 1H), 3.43–3.19 (m, 2H), 3.09 (br s, 2H), 2.93 (br d, *J* = 19.8 Hz, 2H), 2.14 (s, 3H), 2.11–1.91 (m, 3H), 1.83–1.58 (m, 2H). ¹³C NMR (75 MHz, CDCl₃, δ): 173.0, 168.7, 168.1, 159.2, 158.7 (d, *J* = 254 Hz), 139.4, 132.8 (d, *J* = 4.4 Hz), 129.6 (d, *J* = 6.1 Hz), 127.1 (d, *J* = 7.7 Hz), 121.5 (d, *J* = 17.7 Hz), 116.8 (d, *J* = 22 Hz), 112.2, 110.2, 106.4, 94.3 (d, *J* = 172 Hz), 67.3, 57.2 (d, *J* = 22 Hz), 49.2, 43.5, 38.1, 33.4, 32.5, 22.6. Formula: C₂₃H₂₆ClF₂N₃O₃; MS (ESI⁺): *m/z* 466 [M+H⁺].

***N*-(3-(2-(((1-(3,4-Dichlorobenzoyl)-4-fluoropiperidin-4-yl)methyl)amino)ethoxy)phenyl)acetamide (48)**

The title compound was prepared using 2-(1-(3,4-dichlorobenzoyl)-4-fluoropiperidin-4-yl)-2-hydroxyacetonitrile (**5**) (0.075 g, 0.23 mmol), *N*-[3-(2-aminoethoxy)phenyl]acetamide (**19**) (0.070 g, 0.36 mmol), DABCO (0.317 g, 2.83 mmol), sodium cyanoborohydride (0.111 g, 1.76 mmol), molecular sieves (0.47 g) in methanol (3 mL). Purification: EtOAc/methanol (9/1 v/v). Yield: 18%; yellow oil. ¹H NMR (500 MHz, CDCl₃, δ): 7.66 (br s, 1H), 7.52–7.41 (m, 2H), 7.31 (br s, 1H), 7.21 (dd, *J* = 1.7, 8.0 Hz, 1H), 7.15 (br t, *J* = 8.2 Hz, 1H), 6.92 (br d, *J* = 7.7 Hz, 1H), 6.61 (br d, *J* = 7.2 Hz, 1H), 4.50 (br s, 1H), 4.06 (br t, *J* = 4.9 Hz, 2H), 3.56 (br s, 1H), 3.36 (br s, 1H), 3.12 (br s, 1H), 3.05 (br t, *J* = 4.0 Hz, 2H), 2.88 (br d, *J* = 17.5 Hz, 2H), 2.60 (br s, 1H), 2.13 (s, 3H), 2.08–1.88 (m, 2H), 1.66 (br s, 2H). ¹³C NMR (126 MHz, CDCl₃, δ) 168.5, 168.1, 159.4, 139.3, 135.7, 134.2, 133.1, 130.7, 129.7, 129.2, 126.3, 112.2, 110.4, 106.5, 94.4 (d, *J* = 172.6 Hz), 67.4, 57.3 (d, *J* = 22.3 Hz),

49.3, 43.7, 38.2, 33.7 (d, $J = 16.9$ Hz), 32.79 (d, $J = 17.5$ Hz), 24.8. Formula: $C_{23}H_{26}Cl_2FN_3O_3$; MS (ESI⁺): m/z 482 [M+H⁺].

(3-Chloro-4-fluorophenyl)(4-fluoro-4-(((2-(*m*-tolylloxy)ethyl)amino)methyl)piperidin-1-yl)methanone (49)

The title compound was prepared using 2-(1-(3-chloro-4-fluorobenzoyl)-4-fluoropiperidin-4-yl)-2-hydroxyacetonitrile (**4**) (0.120 g, 0.38 mmol), 2-(*m*-tolylloxy)ethanamine (**20**) (0.081 g, 0.54 mmol), DABCO (0.535 g, 4.78 mmol), sodium cyanoborohydride (0.178 g, 2.98 mmol), molecular sieves (0.900 g) and iron sulfate heptahydrate (0.117 g, 0.42 mmol) in methanol (5 mL). Purification: *n*-hexane/Et₂O/DCM/methanol/NH_{3(aq)} (3/2/4.5/0.5/0.02, v/v/v/v/v). Yield: 53%; white crystallizing oil. ¹H NMR (300 MHz, CD₃OD, δ): 7.59 (dd, $J = 1.8, 7.0$ Hz, 1H), 7.45–7.37 (m, 1H), 7.36–7.28 (m, 1H), 7.17–7.06 (m, 1H), 6.78–6.66 (m, 3H), 4.43 (br s, 1H), 4.05 (t, $J = 5.3$ Hz, 2H), 3.68–3.49 (m, 1H), 3.39 (br s, 1H), 3.28–3.09 (m, $J = 5.3$ Hz, 1H), 3.00 (t, $J = 5.6$ Hz, 2H), 2.91–2.79 (m, 2H), 2.29 (s, 3H), 2.06–1.62 (m, 4H), *NH* proton not detected. ¹³C NMR (75 MHz, CD₃OD, δ): 168.6, 158.8, 158.7 (d, $J = 251$ Hz), 139.2, 133.0 (d, $J = 4.6$ Hz), 129.3, 128.8, 127.3 (d, $J = 6.9$ Hz), 121.3, 120.9 (d, $J = 18.4$ Hz), 116.6 (d, $J = 21.8$ Hz), 114.9, 111.1, 93.8 (d, $J = 172.7$ Hz), 66.5, 56.5 (d, $J = 21.9$ Hz), 48.8, 43.6, 38.1, 32.9, 32.2, 20.2. Formula: $C_{22}H_{25}ClF_2N_2O_2$; MS (ESI⁺): m/z 423 [M+H⁺].

(3-Chloro-4-fluorophenyl)(4-fluoro-4-(((2-(3-(trifluoromethyl)phenoxy)ethyl)amino)methyl)piperidin-1-yl)methanone (50)

The title compound was prepared using 2-(1-(3-chloro-4-fluorobenzoyl)-4-fluoropiperidin-4-yl)-2-hydroxyacetonitrile (**4**) (0.150 g, 0.48 mmol), 2-(3-(trifluoromethyl)phenoxy)ethanamine (**21**) (0.156 g, 0.76 mmol), DABCO (0.669 g, 5.97 mmol), sodium cyanoborohydride (0.234 g, 3.73 mmol), molecular sieves (1.043 g) and iron sulfate heptahydrate (0.146 g, 0.53 mmol) in methanol (5 mL). Purification: EtOAc/methanol (9.5/0.5, v/v) and then *n*-hexane/EtOAc (3/7, v/v). Yield: 49%; yellow transparent oil. ¹H NMR (300 MHz, CDCl₃, δ): 7.48 (dd, $J = 2.1, 6.7$ Hz, 1H), 7.42–

7.34 (m, 1H), 7.33–7.26 (m, 1H), 7.24–7.16 (m, 2H), 7.13 (d, $J = 3.5$ Hz, 1H), 7.06 (dd, $J = 2.9, 8.2$ Hz, 1H), 4.48 (br s, 1H), 4.09 (t, $J = 5.0$ Hz, 2H), 3.75–3.48 (m, 1H), 3.47–3.10 (m, 2H), 3.05 (t, $J = 5.0$ Hz, 2H), 2.91–2.76 (m, 2H), 2.07–1.95 (m, 2H), 1.83–1.44 (m, 3H). ^{13}C NMR (75 MHz, CDCl_3 , δ): 168.1, 158.9, 158.8 (d, $J = 254$ Hz), 132.9 (d, $J = 4.6$ Hz), 131.8 (d, $J = 32.3$ Hz), 130.0, 129.7, 127.1 (d, $J = 8.1$ Hz), 123.9 (q, $J = 272$ Hz), 121.5 (d, $J = 18.2$ Hz), 117.9, 117.6 (q, $J = 3.9$ Hz), 116.8 (d, $J = 22$ Hz), 111.3 (q, $J = 3.9$ Hz), 94.3 (d, $J = 172$ Hz), 67.7, 57.3 (d, $J = 22$ Hz), 49.1, 43.5, 38.3, 33.7, 32.8. Formula: $\text{C}_{22}\text{H}_{22}\text{ClF}_5\text{N}_2\text{O}_2$; MS (ESI^+): m/z 477 $[\text{M}+\text{H}^+]$.

(3-Chloro-4-fluorophenyl)(4-fluoro-4-(((2-(quinolin-8-yloxy)ethyl)amino)methyl)piperidin-1-yl)methanone (51)

The title compound was prepared using 2-(1-(3-chloro-4-fluorobenzoyl)-4-fluoropiperidin-4-yl)-2-hydroxyacetonitrile (**4**) (0.200 g, 0.64 mmol), 2-(quinolin-8-yloxy)ethanamine (**25**) (0.192 g, 1.02 mmol), DABCO (0.892 g, 7.96 mmol), sodium cyanoborohydride (0.311 g, 4.99 mmol), molecular sieves (1.400 g) and iron sulfate heptahydrate (0.195 g, 0.70 mmol) in methanol (7 mL). Purification: EtOAc/methanol (9.5/0.5, v/v). Yield: 69%; beige crystallizing oil. ^1H NMR (300 MHz, CDCl_3 , δ): 8.92 (dd, $J = 1.8, 4.1$ Hz, 1H), 8.15 (dd, $J = 1.7, 8.3$ Hz, 1H), 7.50–7.38 (m, 4H), 7.28 (dd, $J = 2.1, 4.6$ Hz, 1H), 7.19–7.12 (m, 1H), 7.09 (dd, $J = 1.7, 7.3$ Hz, 1H), 4.50 (br s, 1H), 4.34 (t, $J = 5.3$ Hz, 2H), 3.58 (br s, 1H), 3.39–3.13 (m, 4H), 2.98–2.86 (m, 2H), 2.06–1.97 (m, 2H), 1.66 (br s, 3H). ^{13}C NMR (75 MHz, CDCl_3 , δ): 168.0, 158.7 (d, $J = 254$ Hz), 154.5, 149.2, 140.2, 136.1, 132.9 (d, $J = 4.4$ Hz), 129.7, 129.5, 127.1 (d, $J = 7.2$ Hz), 126.7, 121.7, 121.4, 120.1, 116.7 (d, $J = 22$ Hz), 109.4, 94.3 (d, $J = 172$ Hz), 68.7, 57.3 (d, $J = 22$ Hz), 49.1, 43.6, 38.3, 33.6, 32.9. Formula: $\text{C}_{24}\text{H}_{24}\text{ClF}_2\text{N}_3\text{O}_2$; MS (ESI^+): m/z 460 $[\text{M}+\text{H}^+]$.

(3,4-Dichlorophenyl)(4-fluoro-4-(((2-(quinolin-8-yloxy)ethyl)amino)methyl)piperidin-1-yl)methanone fumarate salt (52)

The title compound was prepared using 2-(1-(3,4-dichlorobenzoyl)-4-fluoropiperidin-4-yl)-2-hydroxyacetonitrile (**5**) (0.597 g, 1.90 mmol), 2-(quinolin-8-yloxy)ethanamine (**25**) (0.395 g, 2.11

mmol), DABCO (2.660 g, 23.75 mmol), sodium cyanoborohydride (0.932 g, 14.82 mmol), molecular sieves (3.200 g) in methanol (18 mL). Purification: EtOAc/methanol/NH_{3(aq)} (9.5/0.5/0, 02, v/v/v). Yield: 15%; white oil. The compound was prepared as fumarate salt by adding a solution on fumaric acid in methanol (0.034 g in 2 ml methanol). ¹H NMR (500 MHz, CD₃OD, δ): 8.88 (dd, *J* = 1.7, 4.3 Hz, 1H), 8.37 (dd, *J* = 1.6, 8.4 Hz, 1H), 7.64–7.51 (m, 5H), 7.34 (dd, *J* = 2.0, 8.3 Hz, 1H), 7.27–7.22 (m, 1H), 6.66 (s, 2H), 4.53 (br s, 1H), 4.49 (t, *J* = 4.8 Hz, 2H), 3.68–3.54 (m, 3H), 3.50–3.37 (m, 3H), 3.20 (br s, 1H), 2.23–1.74 (m, 4H), *NH* protons not detected. ¹³C NMR (126 MHz, CD₃OD, δ) 169.6 (2C), 168.5, 152.9, 148.9, 138.8, 137.3, 135.6, 134.8 (2C), 133.9, 132.6, 130.8, 129.8, 128.9, 127.1, 126.4, 122.0, 120.6, 109.3, 91.8 (d, *J* = 175.6 Hz), 63.4, 53.9 (d, *J* = 21.1 Hz), 47.2, 42.9, 37.5, 32.5 (d, *J* = 19.3 Hz), 31.8 (d, *J* = 26.6 Hz). Formula: C₂₄H₂₄Cl₂FN₃O₂ · C₄H₄O₄; MS (ESI⁺): *m/z* 476 [M+H⁺].

(3-Chloro-4-fluorophenyl)(4-(((2-((2,3-dihydrobenzo[b][1,4]dioxin-5-yl)oxy)ethyl)amino)methyl)-4-fluoropiperidin-1-yl)methanone (53)

The title compound was prepared using 2-(1-(3-chloro-4-fluorobenzoyl)-4-fluoropiperidin-4-yl)-2-hydroxyacetonitrile (**4**) (0.081 g, 0.26 mmol), 2-(2, 3-dihydro-1, 4-benzodioxin-6-yloxy)ethanamine (**22**) (0.080 g, 0.41 mmol), DABCO (0.359 g, 3.20 mmol), sodium cyanoborohydride (0.125 g, 2.00 mmol), molecular sieves (0.531 g) in methanol (3 mL). Purification: EtOAc/methanol (9.5/0.5, v/v). Yield: 19%, colorless oil. ¹H NMR (300 MHz, CDCl₃, δ): 7.48 (dd, *J* = 2.1, 6.9 Hz, 1H), 7.32–7.26 (m, 1H), 7.21–7.14 (m, 1H), 6.78–6.71 (m, 1H), 6.53 (ddd, *J* = 1.3, 8.2, 10.8 Hz, 2H), 4.50 (br s, 1H), 4.32–4.27 (m, 2H), 4.27–4.23 (m, 2H), 4.16–4.07 (m, 2H), 3.60 (br s, 1H), 3.34 (br s, 2H), 3.05 (t, *J* = 5.3 Hz, 2H), 2.91–2.78 (m, 2H), 2.02 (s, 2H), 1.63 (br s, 3H). Formula: C₂₃H₂₅ClF₂N₂O₄; MS (ESI⁺): *m/z* 467 [M+H⁺].

(3,4-Dichlorophenyl)(4-(((2-((2,3-dihydrobenzo[b][1,4]dioxin-5-yl)oxy)ethyl)amino)methyl)-4-fluoropiperidin-1-yl)methanone (54)

The title compound was prepared using 2-(1-(3,4-chlorobenzoyl)-4-fluoropiperidin-4-yl)-2-hydroxyacetonitrile (**5**) (0.200 g, 0.60 mmol), 2-(2,3-dihydro-1,4-benzodioxin-6-yloxy)ethanamine (**22**) (0.189 g, 0.97 mmol), DABCO (0.847 g, 7.55 mmol), sodium cyanoborohydride (0.296 g, 4.71 mmol), molecular sieves (1.254 g) in methanol (6 mL). Purification: EtOAc/methanol (9.9/0.1, v/v) and then *n*-hexane/EtOAc/ methanol/NH_{3(aq)} (4/5.5/0.5/0.02, v/v/v/v). Yield: 30%; pale yellow oil. ¹H NMR (300 MHz, CDCl₃, δ): 7.53–7.46 (m, 2H), 7.23 (dd, *J* = 1.8, 8.2 Hz, 1H), 6.78–6.71 (m, 1H), 6.52 (ddd, *J* = 1.4, 8.3, 10.8 Hz, 2H), 4.51 (br s, 1H), 4.31–4.27 (m, 2H), 4.27–4.23 (m, 2H), 4.11 (t, *J* = 5.4 Hz, 2H), 3.56 (br s, 1H), 3.45–3.11 (m, 2H), 3.04 (t, *J* = 5.1 Hz, 2H), 2.90–2.79 (m, 2H), 2.08–1.92 (m, 2H), 1.67 (br s, 3H). ¹⁹F NMR (282 MHz, CDCl₃, δ): -166.3 (s, 1F). ¹³C NMR (75 MHz, CDCl₃, δ): 167.9, 148.2, 144.4, 135.7, 134.1, 133.9, 133.0, 130.6, 129.1, 126.2, 120.2, 110.5, 106.3, 95.5 (d, *J* = 172 Hz), 69.0, 64.4, 64.2, 57.3 (d, *J* = 22 Hz), 49.2, 43.5, 39.0, 33.6, 32.6. Formula: C₂₃H₂₅Cl₂FN₂O₄; MS (ESI⁺): *m/z* 483 [M+H⁺].

(3-Chloro-4-fluorophenyl)(4-(((2,2-dimethyl-2,3-dihydrobenzofuran-7-yl)oxy)ethyl)amino)methyl)-4-fluoropiperidin-1-yl)methanone (55**)**

The title compound was prepared using 2-(1-(3-chloro-4-fluorobenzoyl)-4-fluoropiperidin-4-yl)-2-hydroxyacetonitrile (**4**) (0.100 g, 0.32 mmol), 2-(((2,2-dimethyl-2,3-dihydrobenzofuran-7-yl)oxy)ethanamine (**23**) (0.092 g, 0.45 mmol), DABCO (0.444 g, 3.97 mmol), sodium cyanoborohydride (0.155 g, 2.48 mmol), molecular sieves (0.900 g) and iron sulfate heptahydrate (0.097 g, 0.35 mmol) in methanol (5 mL). Purification: *n*-hexane/DCM/methanol/NH_{3(aq)} (4/5.5/0.5/0.02, v/v/v/v). Yield: 33%; yellow oil. ¹H NMR (300 MHz, CDCl₃, δ): 7.48 (dd, *J* = 1.8, 7.0 Hz, 1H), 7.32–7.25 (m, 1H), 7.22–7.13 (m, 1H), 6.81–6.70 (m, 3H), 4.50 (br s, 1H), 4.15 (t, *J* = 5.0 Hz, 2H), 3.71–3.50 (m, 1H), 3.48–3.08 (m, 2H), 3.06–2.96 (m, 4H), 2.83 (d, *J* = 19.9 Hz, 2H), 1.99 (br s, 2H), 1.83 (br s, 3H), 1.49 (s, 6H). ¹³C NMR (75 MHz, CDCl₃, δ): 168.0, 158.8 (d, *J* = 254 Hz), 147.9, 143.5, 132.9 (d, *J* = 3.5 Hz), 129.7, 128.6, 127.1 (d, *J* = 8.1 Hz), 121.5 (d, *J* = 18.4 Hz), 120.3, 118.1, 116.8 (d, *J* = 22 Hz), 113.7, 94.3 (d, *J* = 172 Hz), 87.3, 69.0, 57.2 (d, *J* = 22 Hz),

49.2, 43.6, 43.2, 38.3, 33.5, 32.8, 28.3 (2C). Formula: $C_{25}H_{29}ClF_2N_2O_3$; MS (ESI⁺): m/z 479 [M+H⁺].

(4-(((2-((1*H*-Indol-4-yl)oxy)ethyl)amino)methyl)-4-fluoropiperidin-1-yl)(3-chloro-4-fluorophenyl)methanone fumarate salt (56)

The title compound was prepared using 2-(1-(3-chloro-4-fluorobenzoyl)-4-fluoropiperidin-4-yl)-2-hydroxyacetonitrile (**4**) (0.150 g, 0.48 mmol), 2-((1*H*-indol-4-yl)oxy)ethanamine (**26**) (0.126 g, 0.72 mmol), DABCO (0.669 g, 5.97 mmol), sodium cyanoborohydride (0.234 g, 3.73 mmol), molecular sieves (1.043 g) and iron sulfate heptahydrate (0.146 g, 0.53 mmol) in methanol (5 mL). Purification: *n*-hexane/EtOAc/methanol/NH_{3(aq)} (3/6.5/0.5/0.02, v/v/v/v). Yield: 64%; beige powder. The compound was prepared as fumarate salt by adding a solution on fumaric acid in methanol (0.035 g in 2 ml methanol). ¹H NMR (500 MHz, CD₃OD, δ): 7.58 (dd, *J* = 2.0, 7.2 Hz, 1H), 7.40–7.35 (m, 1H), 7.35–7.30 (m, 1H), 7.14 (d, *J* = 3.2 Hz, 1H), 7.08–6.99 (m, 2H), 6.71 (s, 2H), 6.58 (d, *J* = 2.9 Hz, 1H), 6.54 (d, *J* = 7.4 Hz, 1H), 4.49 (br s, 1H), 4.43 (t, *J* = 5.2 Hz, 2H), 3.60 (br s, 1H), 3.56 (t, *J* = 5.0 Hz, 2H), 3.48–3.35 (m, 3H), 3.19 (br s, 1H), 2.09 (br s, 1H), 1.98 (s, 2H), 1.91–1.72 (m, 2H), *NH* protons not detected. ¹³C NMR (126 MHz, CD₃OD, δ): 170.0 (2C), 169.6, 159.8 (d, *J* = 251.1 Hz), 152.2, 138.9, 135.5 (2C), 133.7 (d, *J* = 4.2 Hz), 130.4, 128.3 (d, *J* = 7.8 Hz), 123.9, 122.5, 121.9 (d, *J* = 18.1 Hz), 119.6, 117.7 (d, *J* = 22.3 Hz), 106.4, 100.9, 99.1, 92.9 (d, *J* = 175.0 Hz), 64.1, 55.1 (d, *J* = 20.5 Hz), 48.9, 43.9, 38.5, 33.3, 32.6. Formula: $C_{23}H_{24}ClF_2N_3O_2 \cdot C_4H_4O_4$; MS (ESI⁺): m/z 448 [M+H⁺].

(3-Chloro-4-fluorophenyl)(4-fluoro-4-(((2-(indolin-4-yloxy)ethyl)amino)methyl)piperidin-1-yl)methanone (57)

The title compound was prepared by the reduction of ((4-(((2-((1*H*-indol-4-yl)oxy)ethyl)amino)methyl)-4-fluoropiperidin-1-yl)(3-chloro-4-fluorophenyl)methanone) (**56**).

To a solution of compound **56** (1.0 equiv, 0.177 g, 0.40 mmol) in acetic acid (1.0 equiv, 0.23 mL, 0.40 mmol) sodium cyanoborohydride (2.0 equiv 0.051 g, 0.80 mmol) was added in portions at 15

1
2 °C. Then the mixture was warmed up to room temperature and stirred for an hour. The reaction
3
4 mixture was then cooled to 0 °C, quenched and adjusted to pH 8 with a saturated aqueous solution
5
6 of sodium bicarbonate and extracted with EtOAc (3×). The organic layers were combined and dried
7
8 over magnesium sulfate, filtered and concentrated to yield the crude product that was purified by
9
10 flash chromatography in *n*-hexane/EtOAc/methanol/NH_{3(aq)} (6/3/1/0.02, v/v/v/v). Yield: 67%; pale
11
12 pink transparent oil. ¹H NMR (300 MHz, CDCl₃, δ): 7.48 (dd, *J* = 2.3, 7.0 Hz, 1H), 7.35–7.26 (m,
13
14 1H), 7.23–7.11 (m, 1H), 6.97 (t, *J* = 7.9 Hz, 1H), 6.29 (dd, *J* = 7.9, 14.4 Hz, 2H), 4.51 (br s, 1H),
15
16 4.08 (t, *J* = 5.0 Hz, 2H), 3.56 (t, *J* = 8.5 Hz, 3H), 3.47–3.08 (m, 2H), 3.06–2.93 (m, 4H), 2.91–2.76
17
18 (m, 2H), 2.02 (br s, 2H), 1.85–1.44 (m, 2H), *NH* protons not detected. ¹⁹F NMR (282 MHz, CDCl₃,
19
20 δ): -112.6 (s, 1F), -166.7 (s, 1F). ¹³C NMR (75 MHz, CDCl₃, δ): 168.0, 158.8 (d, *J* = 254 Hz), 155.6,
21
22 153.5, 132.9 (d, *J* = 3.5 Hz), 129.7, 128.6, 127.1 (d, *J* = 6.9 Hz), 121.5 (d, *J* = 18 Hz), 116.8 (d, *J*
23
24 = 22 Hz), 116.0, 103.3, 102.6, 94.4 (d, *J* = 172 Hz), 67.2, 57.2 (d, *J* = 22 Hz), 49.3, 47.4, 43.5, 38.2,
25
26 33.5, 32.7, 26.9. Formula: C₂₃H₂₆ClF₂N₃O₂; MS (ESI⁺): *m/z* 450 [M+H⁺].
27
28
29
30
31
32
33
34
35
36
37
38
39
40
41
42
43
44
45
46
47
48
49
50
51
52
53
54
55
56
57
58
59
60

***In vitro* studies**

The tested compounds were examined for known classes of assay interference compounds. None of the compounds contain substructural features recognized as pan assay interference compounds (PAINS), according to SwissADME tool.⁵²

Radioligand Binding Assays for 5-HT_{1A}R, α_1 R, D₂R

Preparation of solutions of test and reference compounds

1 mM stock solutions of tested compounds were prepared in DMSO. Serial dilutions of compounds were prepared in 96-well microplate in assay buffers using automated pipetting system epMotion 5070 (Eppendorf). The final concentration of DMSO in the test solutions was 0.1%. Each compound was tested in 10 concentrations from 1.0E-06 to 1.0E-12 M (final concentration).

Serotonin 5-HT_{1A} Receptor Binding Assay

Radioligand binding was performed using membranes from CHO-K1 cells stably transfected with the human 5-HT_{1A} receptor (PerkinElmer). All assays were carried out in duplicates. 50 μ L working solution of the tested compounds, 50 μ L [³H]-8-OH-DPAT (final concentration 1 nM) and 150 μ L diluted membranes (10 μ g protein per well) prepared in assay buffer (50 mM Tris, pH 7.4, 10 mM MgSO₄, 0, 5 mM EDTA, 0.1% ascorbic acid) were transferred to polypropylene 96-well microplate using 96-wells pipetting station Rainin Liquidator (MettlerToledo). Serotonin (10 μ M) was used to define nonspecific binding. Microplate was covered with a sealing tape, mixed and incubated for 60 minutes at 27 °C. The reaction was terminated by rapid filtration through GF/C filter mate presoaked with 0.3% polyethyleneimine for 30 minutes. Ten rapid washes with 200 μ L 50 mM Tris buffer (4 °C, pH 7.4) were performed using automated harvester system Harvester-96 MACH III FM (Tomtec). The filter mates were dried at 37 °C in forced air fan incubator and then solid scintillator MeltiLex was melted on filter mates at 90 °C for 4 minutes. Radioactivity was counted in

MicroBeta2 scintillation counter (PerkinElmer). Data were fitted to a one-site curve-fitting equation with Prism 6 (GraphPad Software) and K_i values were estimated from the Cheng–Prusoff equation.

Adrenergic α_1 Receptor Binding Assay

Radioligand binding was performed using rat cortex. Tissue was homogenized in 20 volumes of ice-cold 50 mM Tris-HCl buffer, pH 7.6 using an Ultra Turrax T25B (IKA) homogenizer. The homogenate was centrifuged at 20,000 \times g for 20 min. The resulting supernatant was decanted and pellet was resuspended in the same buffer and centrifuged again in the same conditions. The final pellet was resuspended in appropriate volume of buffer (10 mg/1ml). All assays were carried out in duplicates. 50 μ L working solution of the tested compounds, 50 μ L [3 H]-prazosin (final concentration 0.2 nM) and 150 μ L tissue suspension were transferred to polypropylene 96-well microplate using 96-wells pipetting station Rainin Liquidator (MettlerToledo). Phentolamine (10 μ M) was used to define nonspecific binding. Microplate was covered with a sealing tape, mixed and incubated for 30 minutes at 30 $^{\circ}$ C. The incubation was terminated by rapid filtration over glass fiber filters FilterMate B (PerkinElmer, USA) using 96-well FilterMate harvester (PerkinElmer, USA). Five rapid washes were performed with ice-cold 50 mM Tris-HCl buffer, pH 7.6. The filter mates were dried at 37 $^{\circ}$ C in forced air fan incubator and then solid scintillator MeltiLex was melted on filter mates at 90 $^{\circ}$ C for 5 minutes. Radioactivity was counted in MicroBeta2 scintillation counter (PerkinElmer). Data were fitted to a one-site curve-fitting equation with Prism 6 (GraphPad Software) and K_i values were estimated from the Cheng–Prusoff equation.

Dopamine D_2 Receptor Binding Assay

Radioligand binding was performed using membranes from CHO-K1 cells stably transfected with the human D_2 receptor (PerkinElmer). All assays were carried out in duplicates. 50 μ L working solution of the tested compounds, 50 μ L [3 H]-methylnpipерone (final concentration 0.4 nM) and 150 μ L diluted membranes (3 μ g protein per well) prepared in assay buffer (50 mM Tris, pH 7.4, 50 mM HEPES, 50 mM NaCl, 5 mM $MgCl_2$, 0.5 mM EDTA) were transferred to polypropylene 96-well

microplate using 96-wells pipetting station Rainin Liquidator (MettlerToledo). Haloperidol (10 μ M) was used to define nonspecific binding. Microplate was covered with a sealing tape, mixed and incubated for 60 minutes at 37 °C. The reaction was terminated by rapid filtration through GF/B filter mate presoaked with 0.5% polyethyleneimine for 30 minutes. Ten rapid washes with 200 μ L 50 mM Tris buffer (4 °C, pH 7.4) were performed using automated harvester system Harvester-96 MACH III FM (Tomtec). The filter mates were dried at 37 °C in forced air fan incubator and then solid scintillator MeltiLex was melted on filter mates at 90 °C for 5 minutes. Radioactivity was counted in MicroBeta2 scintillation counter (PerkinElmer). Data were fitted to a one-site curve-fitting equation with Prism 6 (GraphPad Software) and K_i values were estimated from the Cheng–Prusoff equation.

Functional assays for the 5-HT_{1A} receptor

ERK1/2 phosphorylation

Test and reference compounds were dissolved in dimethyl sulfoxide (DMSO) at a concentration of 10 mM. Serial dilutions were prepared in 96-well microplate in HBSS with 0.1% BSA added and 8 concentrations were tested. The final concentration of DMSO in the test solutions was 0.1%.

The CHO-5HT_{1A} receptor cells were tested for agonist-induced ERK1/2-phosphorylation using the SureFire ERK1/2-Phosphorylation Alpha LISA assay kit according to the manufacturer's instruction (Perkin Elmer). After thawing, cells were cultured in medium (Advanced DMEM/F12 with 1% FBS dialyzed, 400 μ g/mL G-418, 4 mM L-Glutamine). At the experiment cells were plated at 50, 000 cells/well of 96-well tissue culture plate and grown 7 hours in incubator (5% CO₂, 37 °C), after this time the cells were starving (DMEM/F12 with 0, 1% BSA (immunoglobulin- and protease-free) for 12 hours. The serial dilutions of compounds were added and incubated for 15 minutes in 37 °C. The medium was removed, "lysis buffer" (70 μ L) was added and the plate gently agitated on a plate shaker (10 minutes). The plates were freezing in -80 °C. The next day, plate were thawing on plate shaker for 10 minutes and 10 μ L were transferred to assay plates (384-OptiPlate, Perkin Elmer) in

duplicate and 10 μ L of reaction mix AlphaLISA SureFire Ultra assay (Perkin Elmer) were added. The plate were incubated for 2 hours in 22 °C. After incubation, the assay plate were measured in an EnVision multifunction plate reader (Perkin Elmer Life Science). E_{\max} values were defined as the response of the ligand expressed as a percentage of the maximal response elicited by serotonin, determined by nonlinear regression using GraphPad Prism 6.0 software. pEC_{50} values correspond to the ligand concentration at which 50% of its own maximal response was measured.

cAMP inhibition

Tested and reference compounds were dissolved in dimethyl sulfoxide (DMSO) to the concentration of 10 mM. Dilutions were prepared in 96-well microplate in assay buffers. For 5-HT_{1A} receptors, adenylyl cyclase activity was determined using cryopreserved CHO-K1 cells with expression of the human serotonin 5-HT_{1A} receptor. The final concentration of DMSO in the test solutions was 0.1%. The functional assay was performed with the CHO-K1 cells with expression of the 5-HT_{1A} human serotonin receptor where plasmid containing the coding sequence was transfected in. The cells were cultured under selective conditions (400 μ g/mL Geneticin G418) (Perkin Elmer). Thawed cells were resuspended in stimulation buffer (HBSS, 5 mM HEPES, 0.5 IBMX, and 0.1% BSA at pH 7.4) at 2×10^5 cells/mL. The same volume (10 μ L) of cell suspension was added to tested compounds with 10 μ M forskolin. Samples were loaded onto a white opaque half area 96-well microplate. Cell stimulation was performed for 40 min at room temperature. After incubation, cAMP measurements were performed with homogeneous TR-FRET immunoassay using the LANCE Ultra cAMP kit (PerkinElmer, USA). 10 μ L of EucAMP Tracer Working Solution and 10 μ L of ULight-anti-cAMP Tracer Working Solution were added, mixed, and incubated for 1 h. The TR-FRET signal was read on an EnVision microplate reader (PerkinElmer, USA). E_{\max} values were defined as the response of the ligand expressed as a percentage of the maximal response elicited by serotonin, determined by nonlinear regression using GraphPad Prism 6.0 software. pEC_{50} values correspond to the ligand concentration at which 50% of its own maximal response was measured.

β-arrestin recruitment

Test and reference compounds were dissolved in dimethyl sulfoxide (DMSO) at a concentration of 10 mM. Serial dilutions were prepared in 96-well microplate in DMEM medium with 10% FBS added and 8 concentrations were tested. The final concentration of DMSO in the test solutions was 0.1%.

The HTR1A-bla U2OS receptor cells contain the human Serotonin Type 1A receptor linked to a TEV protease site and a Gal4-VP16 transcription factor, were tested for agonist-induced using the Tango LiveBLAzer assay kit according to the manufacturer's instruction (Life Technologies). After thawing, cells were cultured in medium (McCoy's 5A with 10% FBS dialyzed, 0.1 mM NEAA, 25 mM HEPES, 1mM Sodium Pyruvate, 100 µg/mL G-418, 100 U/mL Penicillin/Streptomycin Antibiotic, 200 µg/mL Zeocin, 50 µg/mL Hygromycin). At the experiment cells were plated at 10,000 cells/well of 384-well black, clear bottom, tissue culture plate and grown 12 hours in incubator (5% CO₂, 37 °C) in DMEM medium with 10% FBS added. The serial dilutions of compounds were added and incubated for 5 hours (5% CO₂, 37 °C). After this time, 8 µL of reaction mix were added. The plate were incubated for 2 hours in 22 °C. After incubation, the assay plate were measured in an FLUOstar Optima a multifunction plate reader (Perkin Elmer Life Science). E_{\max} values were defined as the response of the ligand expressed as a percentage of the maximal response elicited by serotonin, determined by nonlinear regression using GraphPad Prism 6.0 software. pEC₅₀ values correspond to the ligand concentration at which 50% of its own maximal response was measured.

Calcium mobilization assay

Test and reference compounds were dissolved in dimethyl sulfoxide (DMSO) at a concentration of 10 mM. Serial dilutions were prepared in 96-well microplate in assay buffer and 8 to 10 concentrations were tested. The final concentration of DMSO in the test solutions was 0.1%.

A cellular aequorin-based functional assay was performed with recombinant CHO-K1 cells expressing mitochondrially targeted aequorin, human GPCR and the promiscuous G protein α_{16} for

5-HT_{1A} receptor. Assay was executed according to previously described protocol. After thawing, cells were transferred to assay buffer (DMEM/HAM's F12 with 0.1% protease free BSA) and centrifuged. The cell pellet was resuspended in assay buffer and coelenterazine h was added at final concentrations of 5 μ M. The cells suspension was incubated at 16 °C, protected from light with constant agitation for 16 h and then diluted with assay buffer to the concentration of 100, 000 cells/ml. After 1 h of incubation, 50 μ l of the cells suspension was dispensed using automatic injectors built into the radiometric and luminescence plate counter MicroBeta2 LumiJET (PerkinElmer, USA) into white opaque 96-well microplates preloaded with test compounds. Immediate light emission generated following calcium mobilization was recorded for 30 s. In antagonist mode, after 25 min of incubation the reference agonist was added to the above assay mix and light emission was recorded again. Final concentration of the reference agonist was equal to EC80 (300 nM serotonin).

Developability studies

Preliminary metabolic stability assesment

The in vitro evaluation of metabolic stability of phenoxyethyl derivatives of 1-(1-benzoyl-4-fluoropiperidin-4-yl)methanamine was performed by using rat liver microsomes (RLMs) (Sigma-Aldrich, St. Louis, MO, USA) according to described previously methods and protocols.^{53–55} The reaction mixtures were prepared first, consisted of 50 μ M of tested compound, microsomes (1 mg/mL) and 10 mM tris-HCl buffer pH = 7.4. Reaction mixtures were preliminary incubated for 5 minutes in temperature 37 °C. After preincubation the 50 μ L of NADPH Regeneration System (Promega, Madison, WI, USA) was added to initiate the reaction. The reaction mixtures were incubated for 2 hours at temperature 37 °C. In order to terminate the reaction, 200 μ L of cold extra pure methanol was added. Then, the mixtures were centrifuged (14000 rpm, 15 min) and the supernatants were analyzed using LC/MS Waters ACQUITY™ TQD system with the TQ Detector (Waters, Milford, USA).

The in silico prediction of metabolic biotransformations was performed by MetaSite 6.0.1 software (Molecular Discovery Ltd, Hertfordshire, UK).⁵⁶ The computational liver model of metabolism was used for determination of the most probable sites of metabolism and identification of structures of obtained in vitro metabolites.

Intrinsic clearance

For determination of the intrinsic clearance (CL_{int}) parameter five independent reactions were terminated by the addition of cold methanol containing internal standard (IS) at different time points: 0, 5, 15, 30, 45 min. The reaction mixtures were next centrifuged at 14 500 r.p.m for 10 min. The course of reaction was followed by using the analyte/IS peak height ratio values. In the determination of in vitro $t_{1/2}$ value the slope of linear regression from log concentration remaining versus time relationships ($-k$) was used according to R.S. Obach (1999). The supernatants with **3**, **44** and **56** were analyzed by HPLC system (LaChrom Elite, Merck-Hitachi, Germany) consisted of an L-2130 pump, an L-2200 autosampler, and an L-2420 UV-VIS detector. EZChrome Elite v. 3.2 (Merck-Hitachi, Germany) computer program was used for data acquisition and integration. The separation of studied compounds was performed using a 250×4.6 mm Supelcosil LC-CN column with a particle size of $5 \mu\text{m}$ (Sigma Aldrich, Germany) protected with a guard column (20×4 mm) with the same packing material. The mobile phase consisted of 50 mM potassium dihydrogen phosphate (pH=4.6), methanol and acetonitrile mixed at a ratio of 51:40:9, v/v/v and run at 1 ml/min. Chromatographic analysis was carried out at 25°C and the analytical wavelength was 205 nm.

PAMPA assay

The ability to passive transport across a cell membrane was determined by Pre-coated PAMPA Plate System GentestTM (Corning, Tewksbury, MA, USA) according to described previously protocols.^{54,55} The compounds' concentrations in acceptor and donor wells were estimated by the UPLC-MS analyses, which were performed by LC/MS Waters ACQUITYTM TQD system with the

1
2 TQ Detector (Waters, Milford, USA). The permeability coefficients (P_e , cm/s) were calculated
3
4 according described previously formulas.⁵⁷
5
6

7 The substrates of Pgp were determined by the luminescent Pgp-Glo™ Assay System (Promega,
8 Madison, WI, USA). The test measures luminescently the ATP consuming by Pgp in the presence
9
10 of substrates. The assay was performed in triplicate as described previously.⁵⁵ Tested compounds
11
12 (100 μ M) were incubated with Pgp membranes for 40 minutes at 37 °C. The positive (VL) and
13
14 negative (CFN) controls were incubated at 200 and 100 μ M, respectively. Basal activity of Pgp was
15
16 considered as the difference in the luminescent signal between samples treated with 100 μ M of the
17
18 potent and selective Pgp inhibitor (Na_3VO_4) and untreated samples. The luminescence signal was
19
20 measured by microplate reader EnSpire PerkinElmer (Waltham, MA, USA). Caffeine (CFN) and
21
22 norfloxacin (NFX) were purchased from Sigma-Aldrich (St. Louis, MO, USA).
23
24
25
26
27
28

29 **Hepatotoxicity**

30
31 The hepatotoxicity was investigated with use of hepatoma HepG2 (ATCC® HB-8065™) cell line.
32
33 Cells were grown under described previously conditions.⁵⁴ The cells viability was determined by
34
35 CellTiter 96® AQueous Non-Radioactive Cell Proliferation Assay (Promega, Madison, WI, USA)
36
37 after 72h of incubation with tested compounds at final concentration range (0.1–100 μ M). The
38
39 reference toxins CCCP and DX were used at 10 μ M and 1 μ M, respectively. The absorbance was
40
41 measured using a microplate reader EnSpire (PerkinElmer, Waltham, MA USA) at 490 nm. The
42
43 compounds and references were tested in quadruplicate. Doxorubicin (DX) was purchased from
44
45 Sigma-Aldrich (St. Louis, MO, USA).
46
47
48
49

50 **Extended selectivity studies**

51
52 The off-target receptor screen and cardiac toxicity (hERG automated patch-clamp method) assays
53
54 were performed by Eurofins Pharma Discovery Services according to the well-known methods.
55
56 Further methodological details are available on the company Web site
57
58 (www.eurofinsdiscoveryservices.com) and the appropriate publications.^{58–65}
59
60

***In vivo* pharmacodynamics studies**

Animals

The experiments were performed on male Wistar rats (170–200 g) obtained from an accredited animal facility at the Jagiellonian University Medical College, Krakow, Poland. The animals were housed in group of four in controlled environment (ambient temperature 21 ± 2 °C; relative humidity 50–60%; 12 h light/dark cycles (lights on at 8:00). Standard laboratory food (LSM-B) and filtered water were freely available. Animals were housed for a period of 6 days in polycarbonate Makrolon type 3 cages (dimensions 26.5×15×42 cm, ‘open top’) without enrichment environment (only wooden shavings litter). Each animal was assigned randomly to treatment groups and only used once (no repeated use of animals). All the experiments were performed by two observers unaware of the treatment applied between 9:00 and 14:00 on separate groups of animals. All experimental procedures involving animals were conducted in accordance with European Union (Directive 2010/63/EU) and Polish legislation acts concerning animal experimentation and approved by the II Local Ethics Committee for Experiments on Animals in Cracow, Poland (approval number: 108/2016). All efforts were made to minimize suffering and to reduce the number of animals used in the experiments and to use only the number of animals necessary to produce reliable scientific data. Each experimental group consisted of 6-8 animals

Drugs

All drugs were dissolved in distilled water immediately before administration in a volume of 2 mL/kg. The examined compounds were administered orally 60 min. before tests. In antagonism experiments, WAY100635 (Tocris, UK) was administered subcutaneously (s.c.) 75 min. before testing. Control animals received vehicle (distilled water) according to the same schedule.

Porsolt forced swimming test (FST)

The experiment was carried out according to method of Porsolt et.al.⁶⁶ On the first day of an experiment, the animals were individually gently placed in Plexiglas cylinders (40 cm high, 18 cm in diameter) containing 17 cm of water maintained at 23–25 °C for 15 min. On removal from water, the rats were placed for 30 min in a Plexiglas box under a 60 W bulb to dry. On the following day (24 h later), the rats were re-placed in the cylinder after administration of test compounds and the total duration of immobility was recorded during the 5-min test period. Immobility was considered to occur when no additional activity was observed other than that necessary to keep the rat's head above the water.⁶⁷ Fresh water was used for each animal.

Lower Lip Retraction (LLR)

Observations were made according to the method described by Kleven et al.⁶⁸ Animals were observed individually during 10 min period, for 10 s of observation per animal. During each of these observation periods, the uninterrupted presence for at least 3 s (1) or absence (0) of lower lip retraction (LLR) was recorded. This cycle was repeated 10 times over a 10-min period; thus, the incidence of a particular behavior could vary from 0 to 10.

Statistical analysis

The data of behavioral studies were evaluated by an analysis of variance: one-way ANOVA (when one drug was given) or two-way ANOVA (when two drugs were used) followed by Bonferroni's post hoc test (statistical significance set at $p < 0.05$).

***In vivo* pharmacokinetics studies**

Animals

Male Wistar rats weighing 200-250 g were used in this study. The investigated compounds were dissolved in water and administered orally at three different doses, i.e. 0.31, 0.63, and 1.25 mg/kg (**56**) and 0.04, 0.16, 0.63 mg/kg (**44**). One hour following compound administration, the animals were sacrificed by decapitation and blood and brains were harvested. The blood was allowed to clot

at room temperature and subsequently centrifuged at 3000 rpm for 10 min (Universal 32 centrifuge, Hettich, Germany) to obtain serum. All collected samples were frozen at -80 °C until assayed.

Determination of **56** and **44** in serum and brain tissue

Serum and brain concentrations of the studied compounds were measured by HPLC with UV detection. The brains were homogenized in distilled water (1:4, w/v) with a tissue homogenizer TH220 (Omni International, Inc., Warrenton, VA, USA). The extraction of both compounds from serum and brain homogenates was performed using a mixture of ethyl acetate and hexane (30:70, v/v). The internal standard (IS) for **56** was 6-[(1-(3-chloro-4-fluorobenzoyl)-4-fluoropiperidin-4-yl)methyl]amino)methyl]-*N*,3-dimethylpyridin-2-amine (0.5 µg/mL for serum samples and 2 µg/mL for brain homogenates) and for **44** it was (3-chloro-4-fluorophenyl)(4-fluoro-4-((5-methylpyridin-2-yl)methyl)amino)methyl)piperidin-1-yl)methanone (2 µg/mL for both serum and brain samples) as methanolic solutions.

To isolate **56** and **44** from serum (1.5 mL) or brain homogenate (2 mL) containing these compounds, an appropriate IS (10 µL) was added and the samples were alkalized with 100 µL of 4 M NaOH. Then the samples were extracted with 6 mL of the extraction reagent by shaking for 20 min (IKA Vibrax VXR, Germany). After centrifugation at 3 000 rpm for 20 min (Universal 32, Hettich, Germany), the organic layers were transferred to new tubes containing 150 µL solution of 0.1 M H₂SO₄ and methanol (90:10 v/v). The mixtures were shaken for 20 min and centrifuged for 20 min (3 000 rpm). The organic layer was discarded and 60-80 µL aliquots of the acidic solutions were injected into the HPLC system.

The analytical procedure for ultrafiltrate was similar to that described above, with the exception that 300 µL of this matrix was used for analysis, the volumes of 4 M NaOH and the extraction solvent were 20 µL and 1 mL, respectively, and the organic layers were transferred to 100 µL of the acidic solution.

The HPLC system (LaChrom Elite, Merck-Hitachi, Germany) consisted of an L-2130 pump, an L-2200 autosampler, and an L-2420 UV-VIS detector. EZChrome Elite v. 3.2 (Merck-Hitachi, Germany) computer program was used for data acquisition and integration. The separation of studied compounds was performed using a 250 × 4.6 mm Supelcosil LC-CN column with a particle size of 5 μm (Sigma Aldrich, Germany) protected with a guard column (20 × 4 mm) with the same packing material. The mobile phase consisted of 50 mM potassium dihydrogen phosphate (pH = 4.6), methanol, and acetonitrile mixed at a ratio of 51:40:9, v/v/v and run at 1 mL/min. Chromatographic analysis was carried out at 25 °C and the analytical wavelength was 205 nm.

The calibration curves were constructed by plotting the ratio of peak areas of the studied compound to that of an appropriate IS versus the compound concentration. They were linear in the concentration range of 0.5 – 5 ng/mL for **56** and 0.25 – 5 ng/mL for **44** in serum and 1 – 50 ng/g for **56** and 5 – 100 ng/g for **44** in brain homogenate. In the case of ultrafiltrate, the calibration curves were linear in the range of 5-700 ng/mL for both compounds. The lower limit of quantification (LLOQ) for all biological matrices studied was the lowest calibration standard on the calibration curve, which after extraction procedure were analyzed with a coefficient of variation (CV) of ≤ 20% and a relative error (RE) of ≤ 20%. No interfering peaks were observed in the chromatograms. The assays were reproducible with low intra- and inter-day variation (CV < 10%). The concentrations were expressed in ng/mL of serum or ultrafiltrate and ng/g of wet brain tissue.

Determination of *in vitro* rat plasma protein binding

Fresh blood was harvested from male adult Wistar rats that were sacrificed by exsanguination. The blood was allowed to clot for 20 min at room temperature and then centrifuged at 3000 rpm for 10 min (Universal 32, Hettich, Germany). **56** and **44** dissolved in water were added in volume of 10 μL to separate glass tubes containing 1 mL aliquots of rat serum to achieve final concentrations of 3 and 30 μg/mL each. All tests were run in triplicates. After vortexing, the serum samples were incubated in a water bath at 37 °C for 30 minutes with gentle shaking. Following this incubation

1
2 period, 100 μ L of serum samples from each tube were transferred to Eppendorf tubes and frozen at
3
4 -80 $^{\circ}$ C for analysis. The remaining serum was transferred into Centrifree[®] ultrafiltration devices
5
6 with Ultracel[®] regenerated cellulose membrane (Merck, Darmstadt, Germany) and centrifuged at
7
8 1000 x g for 15 minutes (EBA III centrifuge, Hettich, Germany). The collected ultrafiltrates were
9
10 frozen (-80 $^{\circ}$ C) for further analysis.
11
12
13
14
15
16
17
18
19
20
21
22
23
24
25
26
27
28
29
30
31
32
33
34
35
36
37
38
39
40
41
42
43
44
45
46
47
48
49
50
51
52
53
54
55
56
57
58
59
60

ASSOCIATED CONTENT

Supporting information

Molecular Formula Strings (MFS), functional activity data with SEM/range values, dose-response curves for functional activity, developability parameters of the target compounds (Fsp3, LELP, CNS-MPO), metabolic stability data, the UPLC chromatograms of the reaction mixtures, in silico prediction and the proposed structures of metabolites, the selectivity of **3**, **44** and **56** against a broad panel of off-targets, results of the in vivo pharmacodynamics studies of **44** and **56**, serum and brain exposure of **44** and **56**, detailed procedures for preparation of the amine intermediates 6–8 and 10–26. Spectra of the target compounds (¹H NMR, ¹⁹F NMR, ¹³C NMR, HPLC). This material is available free of charge on the ACS Publications website at <http://pubs.acs.org>.

AUTHOR INFORMATION

Corresponding Author

Phone: (48)126205460 Fax: (48)126205458.

E-mail: marcin.kolaczkowski@uj.edu.pl

Author Contributions

All authors have contributed and have given approval to the final version of the manuscript.

Notes

The authors declare the following competing financial interest(s): A.N.-T. is an employee and a shareholder of Neurolix Inc.

ACKNOWLEDGEMENT

This study was financially supported by The National Science Centre (NCN) Grant No. 2015/19/B/NZ7/03543.

1
2
3
4
5
6
7
8
9
10
11
12
13
14
15
16
17
18
19
20
21
22
23
24
25
26
27
28
29
30
31
32
33
34
35
36
37
38
39
40
41
42
43
44
45
46
47
48
49
50
51
52
53
54
55
56
57
58
59
60

ABBREVIATIONS

SAfiRs, Structure Affinity Relationships; SFARs, Structure Functional Activity Relationships; cAMP – cyclic adenosine monophosphate; ERK1/2, extracellular signal–regulated kinase 1/2; **1** (F15599), {[1-(3-chloro-4-fluorobenzoyl)-4-fluoropiperidin-4-yl]methyl}[(5-methylpyrimidin-2-yl)methyl]amine; FST, forced swimming test (Porsolt test); LLR, Lower Lip Retraction; IFD, induced fit docking, LLE, lipophilic ligand efficiency; PAINS, pan-assay interference compounds; WAY-100635, *N*-[2-[4-(2-methoxyphenyl)piperazin-1-yl]ethyl]-*N*-pyridin-2-ylcyclohexanecarboxamide; RLM, Rat Liver Microsomes;

References

- (1) Pazos, A.; Palacios, J. M. Quantitative Autoradiographic Mapping of Serotonin Receptors in the Rat Brain. I. Serotonin-1 Receptors. *Brain Research* **1985**, *346*, 205–230.
- (2) Fargin, A.; Raymond, J. R.; Lohse, M. J.; Kobilka, B. K.; Caron, M. G.; Lefkowitz, R. J. The Genomic Clone G-21 Which Resembles a β -Adrenergic Receptor Sequence Encodes the 5-HT 1A Receptor. *Nature* **1988**, *335*, 358–360.
- (3) Peroutka, S. J. Selective Interaction of Novel Anxiolytics with 5-Hydroxytryptamine 1A Receptors. *Biological Psychiatry* **1985**, *20*, 971–979.
- (4) Jordan, S.; Koprivica, V.; Chen, R.; Tottori, K.; Kikuchi, T.; Altar, C. A. The Antipsychotic Aripiprazole Is a Potent, Partial Agonist at the Human 5-HT_{1A} Receptor. *European Journal of Pharmacology* **2002**, *441*, 137–140.
- (5) Adell, A. Lu-AA21004, a Multimodal Serotonergic Agent, for the Potential Treatment of Depression and Anxiety. *IDrugs* **2010**, *12*, 900–910.
- (6) Newman-Tancredi, A.; Cussac, D.; Quentric, Y.; Touzard, M.; Verri  le, L.; Carpentier, N.; Millan, M. J. Differential Actions of Antiparkinson Agents at Multiple Classes of Monoaminergic Receptor. III. Agonist and Antagonist Properties at Serotonin, 5-HT₁ and 5-HT₂, Receptor Subtypes. *J Pharmacol Exp Ther* **2002**, *303*, 815–822.
- (7) Sniecikowska, J.; Newman-Tancredi, A.; Kolaczowski, M. From Receptor Selectivity to Functional Selectivity: The Rise of Biased Agonism in 5-HT_{1A} Receptor Drug Discovery. *Curr Top Med Chem* **2019**, *19*, 2393–2420.
- (8) Artigas, F.; Bortolozzi, A.; Celada, P. Can We Increase Speed and Efficacy of Antidepressant Treatments? Part I: General Aspects and Monoamine-Based Strategies. *Eur Neuropsychopharmacol* **2018**, *28*, 445–456.
- (9) Bologna, Z.; Teoh, J.-P.; Bayoumi, A. S.; Tang, Y.; Kim, I.-M. Biased G Protein-Coupled Receptor Signaling: New Player in Modulating Physiology and Pathology. *Biomol Ther* **2017**, *25*, 12–25.

- (10) Rodríguez-Espigares, I.; Kaczor, A. A.; Stepniewski, T. M.; Selent, J. Challenges and Opportunities in Drug Discovery of Biased Ligands. *Methods Mol. Biol.* **2018**, *1705*, 321–334.
- (11) Seyedabadi, M.; Ghahremani, M. H.; Albert, P. R. Biased Signaling of G Protein Coupled Receptors (GPCRs): Molecular Determinants of GPCR/Transducer Selectivity and Therapeutic Potential. *Pharmacol. Ther.* **2019**, *200*, 148–178.
- (12) Newman-Tancredi, A.; Martel, J.-C.; Assié, M.-B.; Buritova, J.; Laressergues, E.; Cosi, C.; Heusler, P.; Slot, L. B.; Colpaert, F. C.; Vacher, B.; Cussac, D. Signal Transduction and Functional Selectivity of F15599, a Preferential Post-Synaptic 5-HT_{1A} Receptor Agonist. *British Journal of Pharmacology* **2009**, *156*, 338.
- (13) Sniecikowska, J.; Gluch-Lutwin, M.; Bucki, A.; Więckowska, A.; Siwek, A.; Jastrzebska-Wiesek, M.; Partyka, A.; Wilczyńska, D.; Pytka, K.; Pociecha, K.; Cios, A.; Wyska, E.; Wesołowska, A.; Pawłowski, M.; Varney, M. A.; Newman-Tancredi, A.; Kolaczowski, M. Novel Aryloxyethyl Derivatives of 1-(1-Benzoylpiperidin-4-yl)Methanamine as the Extracellular Regulated Kinases 1/2 (ERK1/2) Phosphorylation-Preferring Serotonin 5-HT_{1A} Receptor-Biased Agonists with Robust Antidepressant-like Activity. *J. Med. Chem.* **2019**, *62*, 2750–2771.
- (14) Becker, G.; Bolbos, R.; Costes, N.; Redouté, J.; Newman-Tancredi, A.; Zimmer, L. Selective Serotonin 5-HT_{1A} Receptor Biased Agonists Elicit distinct Brain Activation Patterns: A PharmacMRI Study. *Scientific Reports* **2016**, *6*, 1-12.
- (15) Sniecikowska, J.; Newman-Tancredi, A.; Kolaczowski, M. From Receptor Selectivity to Functional Selectivity: The Rise of Biased Agonism in 5-HT_{1A} Receptor Drug Discovery. *Curr Top Med Chem* **2019**, *19*, 2393–2420.
- (16) Newman-Tancredi, A. Biased Agonism at Serotonin 5HT_{1A} Receptors: Preferential Postsynaptic Activity for Improved Therapy of CNS Disorders. *Neuropsychiatry* **2011**, *1*, 149–164.

- (17) Abdala, A. P.; Bissonnette, J. M.; Newman-Tancredi, A. Pinpointing Brainstem Mechanisms Responsible for Autonomic Dysfunction in Rett Syndrome: Therapeutic Perspectives for 5-HT_{1A} Agonists. *Frontiers in Physiology* **2014**, *5*, 205.
- (18) Depoortère, R.; Papp, M.; Gruca, P.; Lason-Tyburkiewicz, M.; Niemczyk, M.; Varney, M. A.; Newman-Tancredi, A. Cortical 5-Hydroxytryptamine 1A Receptor Biased Agonist, NLX-101, Displays Rapid-Acting Antidepressant-like Properties in the Rat Chronic Mild Stress Model. *J. Psychopharmacol. (Oxford)* **2019**, *33*, 1456–1466.
- (19) Zhou, Q.; Yang, D.; Wu, M.; Guo, Y.; Guo, W.; Zhong, L.; Cai, X.; Dai, A.; Jang, W.; Shakhnovich, E. I.; Liu, Z.-J.; Stevens, R. C.; Lambert, N. A.; Babu, M. M.; Wang, M.-W.; Zhao, S. Common Activation Mechanism of Class A GPCRs. *eLife* **2019**, *8*, e50279.
- (20) Williamson, A. XLV. Theory of Ætherification. *The London, Edinburgh, and Dublin Philosophical Magazine and Journal of Science* **1850**, *37*, 350–356.
- (21) Gabriel, S. Ueber Eine Darstellungsweise Primärer Amine Aus Den Entsprechenden Halogenverbindungen. *Ber. Dtsch. Chem. Ges.* **1887**, *20*, 2224–2236.
- (22) Wolfe, S.; Hasan, S. K. Five-Membered Rings. II. Inter and Intramolecular Reactions of Simple Amines with N-Substituted Phthalimides. Methylamine as a Reagent for Removal of a Phthaloyl Group from Nitrogen. *Can. J. Chem.* **1970**, *48*, 3572–3579.
- (23) Kołaczkowski, M.; Marcinkowska, M.; Bucki, A.; Pawłowski, M.; Mitka, K.; Jaśkowska, J.; Kowalski, P.; Kazek, G.; Siwek, A.; Wasik, A.; Wesołowska, A.; Mierzejewski, P.; Bienkowski, P. Novel Arylsulfonamide Derivatives with 5-HT₆/5-HT₇ Receptor Antagonism Targeting Behavioral and Psychological Symptoms of Dementia. *J. Med. Chem.* **2014**, *57*, 4543–4557.
- (24) Mitsunobu, O.; Yamada, M.; Mukaiyama, T. Preparation of Esters of Phosphoric Acid by the Reaction of Trivalent Phosphorus Compounds with Diethyl Azodicarboxylate in the Presence of Alcohols. *BCSJ* **1967**, *40*, 935–939.

- (25) Mitsunobu, O.; Yamada, M. Preparation of Esters of Carboxylic and Phosphoric Acid via Quaternary Phosphonium Salts. *BCSJ* **1967**, *40*, 2380–2382.
- (26) Nowak, M.; Kołaczkowski, M.; Pawłowski, M.; Bojarski, A. J. Homology Modeling of the Serotonin 5-HT_{1A} Receptor Using Automated Docking of Bioactive Compounds with Defined Geometry. *J. Med. Chem.* **2006**, *49*, 205–214.
- (27) van Wijngaarden, I.; Tulp, M. T.; Soudijn, W. The Concept of Selectivity in 5-HT Receptor Research. *Eur. J. Pharmacol.* **1990**, *188*, 301–312.
- (28) Hamon, M.; Fattaccini, C. M.; Adrien, J.; Gallissot, M. C.; Martin, P.; Gozlan, H. Alterations of Central Serotonin and Dopamine Turnover in Rats Treated with Ipsapirone and Other 5-Hydroxytryptamine_{1A} Agonists with Potential Anxiolytic Properties. *J. Pharmacol. Exp. Ther.* **1988**, *246*, 745–752.
- (29) Foreman, M. M.; Fuller, R. W.; Leander, J. D.; Benvenga, M. J.; Wong, D. T.; Nelson, D. L.; Calligaro, D. O.; Swanson, S. P.; Lucot, J. B.; Flaugh, M. E. Preclinical Studies on LY228729: A Potent and Selective Serotonin_{1A} Agonist. *J. Pharmacol. Exp. Ther.* **1993**, *267*, 58–71.
- (30) Harada, K.; Kawaguchi, A.; Ohmori, M.; Fujimura, A. Antagonistic Activity of Tamsulosin against Human Vascular Alpha₁-Adrenergic Receptors. *Clin. Pharmacol. Ther.* **2000**, *67*, 405–412.
- (31) Newman-Tancredi, A.; Assié, M.-B.; Martel, J.-C.; Cosi, C.; Slot, L. B.; Palmier, C.; Raully-Lestienne, I.; Colpaert, F.; Vacher, B.; Cussac, D. F15063, a Potential Antipsychotic with D₂/D₃ Antagonist, 5-HT_{1A} Agonist and D₄ Partial Agonist Properties. I. In Vitro Receptor Affinity and Efficacy Profile. *Br. J. Pharmacol.* **2007**, *151*, 237–252.
- (32) Brust, T. F.; Hayes, M. P.; Roman, D. L.; Burris, K. D.; Watts, V. J. Bias Analyses of Preclinical and Clinical D₂ Dopamine Ligands: Studies with Immediate and Complex Signaling Pathways. *J. Pharmacol. Exp. Ther.* **2015**, *352*, 480–493.

- (33) Griffin, M. T.; Figueroa, K. W.; Liller, S.; Ehlert, F. J. Estimation of Agonist Activity at G Protein-Coupled Receptors: Analysis of M2 Muscarinic Receptor Signaling through Gi/o, Gs, and G15. *J Pharmacol Exp Ther* **2007**, *321*, 1193–1207.
- (34) Ehlert, F. J. On the Analysis of Ligand-Directed Signaling at G Protein-Coupled Receptors. *Naunyn-Schmied Arch Pharmacol* **2008**, *377*, 549–577.
- (35) Rajagopal, S.; Ahn, S.; Rominger, D. H.; Gowen-MacDonald, W.; Lam, C. M.; Dewire, S. M.; Violin, J. D.; Lefkowitz, R. J. Quantifying Ligand Bias at Seven-Transmembrane Receptors. *Mol. Pharmacol.* **2011**, *80*, 367–377.
- (36) Stroth, N.; Niso, M.; Colabufo, N. A.; Perrone, R.; Svenningsson, P.; Lacivita, E.; Leopoldo, M. Arylpiperazine Agonists of the Serotonin 5-HT1A Receptor Preferentially Activate CAMP Signaling versus Recruitment of β -Arrestin-2. *Bioorg. Med. Chem.* **2015**, *23*, 4824–4830.
- (37) Depoortère, R.; Auclair, A. L.; Bardin, L.; Colpaert, F. C.; Vacher, B.; Newman-Tancredi, A. F15599, a Preferential Post-Synaptic 5-HT1A Receptor Agonist: Activity in Models of Cognition in Comparison with Reference 5-HT1A Receptor Agonists. *Eur Neuropsychopharmacol* **2010**, *20*, 641–654.
- (38) Dwivedi, Y.; Rizavi, H. S.; Teppen, T.; Sasaki, N.; Chen, H.; Zhang, H.; Roberts, R. C.; Conley, R. R.; Pandey, G. N. Aberrant Extracellular Signal-Regulated Kinase (ERK) 5 Signaling in Hippocampus of Suicide Subjects. *Neuropsychopharmacology* **2007**, *32*, 2338–2350.
- (39) Yasuno, F.; Suhara, T.; Nakayama, T.; Ichimiya, T.; Okubo, Y.; Takano, A.; Ando, T.; Inoue, M.; Maeda, J.; Suzuki, K. Inhibitory Effect of Hippocampal 5-HT1A Receptors on Human Explicit Memory. *AJP* **2003**, *160*, 334–340.
- (40) Luo, Y.; Kuang, S.; Li, H.; Ran, D.; Yang, J. CAMP/PKA-CREB-BDNF Signaling Pathway in Hippocampus Mediates Cyclooxygenase 2-Induced Learning/Memory Deficits of Rats Subjected to Chronic Unpredictable Mild Stress. *Oncotarget* **2017**, *8*, 35558–35572.

- (41) Albert, P. R.; Vahid-Ansari, F. The 5-HT_{1A} Receptor: Signaling to Behavior. *Biochimie* **2019**, *161*, 34–45.
- (42) Michel, M. C.; Charlton, S. J. Biased Agonism in Drug Discovery-Is It Too Soon to Choose a Path? *Mol. Pharmacol.* **2018**, *93*, 259–265.
- (43) Haberzettl, R.; Bert, B.; Fink, H.; Fox, M. A. Animal Models of the Serotonin Syndrome: A Systematic Review. *Behavioural Brain Research* **2013**, *256*, 328–345.
- (44) Jastrzębska-Więsek, M.; Partyka, A.; Rychtyk, J.; Śniecikowska, J.; Kołaczkowski, M.; Wesołowska, A.; Varney, M. A.; Newman-Tancredi, A. Activity of Serotonin 5-HT_{1A} Receptor Biased Agonists in Rat: Anxiolytic and Antidepressant-like Properties. *ACS Chem. Neurosci.* **2018**, *9*, 1040–1050.
- (45) Berendsen, H. H.; Bourgondien, F. G.; Broekkamp, C. L. Role of Dorsal and Median Raphe Nuclei in Lower Lip Retraction in Rats. *Eur. J. Pharmacol.* **1994**, *263*, 315–318.
- (46) Celada, P.; Bortolozzi, A.; Artigas, F. Serotonin 5-HT_{1A} Receptors as Targets for Agents to Treat Psychiatric Disorders: Rationale and Current Status of Research. *CNS Drugs* **2013**, *27*, 703–716.
- (47) Levigoureux, E.; Vidal, B.; Fieux, S.; Bouillot, C.; Emery, S.; Newman-Tancredi, A.; Zimmer, L. Serotonin 5-HT_{1A} Receptor Biased Agonists Induce Different Cerebral Metabolic Responses: A [18F]-Fluorodesoxyglucose Positron Emission Tomography Study in Conscious and Anesthetized Rats. *ACS Chem Neurosci* **2019**, *10*, 3108–3119.
- (48) Vidal, B.; Bolbos, R.; Redouté, J.; Langlois, J.-B.; Costes, N.; Newman-Tancredi, A.; Zimmer, L. Pharmacological MRI to Investigate the Functional Selectivity of 5-HT_{1A} Receptor Biased Agonists. *Neuropharmacology* **2019**, 107867.
- (49) Wang, C.; Jiang, Y.; Ma, J.; Wu, H.; Wacker, D.; Katritch, V.; Han, G. W.; Liu, W.; Huang, X.-P.; Vardy, E.; McCorvy, J. D.; Gao, X.; Zhou, X. E.; Melcher, K.; Zhang, C.; Bai, F.; Yang, H.; Yang, L.; Jiang, H.; Roth, B. L.; Cherezov, V.; Stevens, R. C.; Xu, H. E.

- Structural Basis for Molecular Recognition at Serotonin Receptors. *Science* **2013**, *340*, 610–614.
- (50) Bucki, A.; Marcinkowska, M.; Śniecikowska, J.; Więckowski, K.; Pawłowski, M.; Głuch-Lutwin, M.; Gryboś, A.; Siwek, A.; Pytko, K.; Jastrzębska-Więsek, M.; Partyka, A.; Wesołowska, A.; Mierzejewski, P.; Kołaczkowski, M. Novel 3-(1,2,3,6-Tetrahydropyridin-4-Yl)-1H-Indole-Based Multifunctional Ligands with Antipsychotic-Like, Mood-Modulating, and Procognitive Activity. *J. Med. Chem.* **2017**, *60*, 7483–7501.
- (51) Kołaczkowski, M.; Bucki, A.; Feder, M.; Pawłowski, M. Ligand-Optimized Homology Models of D1 and D2 Dopamine Receptors: Application for Virtual Screening. *J. Chem. Inf. Model.* **2013**, *53*, 638–648.
- (52) Daina, A.; Michielin, O.; Zoete, V. SwissADME: A Free Web Tool to Evaluate Pharmacokinetics, Drug-Likeness and Medicinal Chemistry Friendliness of Small Molecules. *Sci Rep* **2017**, *7*, 42717.
- (53) Obach, R. S. Prediction of Human Clearance of Twenty-Nine Drugs from Hepatic Microsomal Intrinsic Clearance Data: An Examination of in Vitro Half-Life Approach and Nonspecific Binding to Microsomes. *Drug Metab. Dispos.* **1999**, *27*, 1350–1359.
- (54) Latacz, G.; Lubelska, A.; Jastrzębska-Więsek, M.; Partyka, A.; Sobiło, A.; Olejarz, A.; Kucwaj-Brysz, K.; Satała, G.; Bojarski, A. J.; Wesołowska, A.; Kieć-Kononowicz, K.; Handzlik, J. In the Search for a Lead Structure among Series of Potent and Selective Hydantoin 5-HT₇R Agents: The Drug-Likeness in Vitro Study. *Chemical Biology & Drug Design* **2017**, *90*, 1295–1306.
- (55) Latacz, G.; Lubelska, A.; Jastrzębska-Więsek, M.; Partyka, A.; Kucwaj-Brysz, K.; Wesołowska, A.; Kieć-Kononowicz, K.; Handzlik, J. MF-8, a Novel Promising Arylpiperazine-Hydantoin Based 5-HT₇ Receptor Antagonist: In Vitro Drug-Likeness Studies and in Vivo Pharmacological Evaluation. *Bioorg. Med. Chem. Lett.* **2018**, *28*, 878–883.

- (56) Cruciani, G.; Carosati, E.; De Boeck, B.; Ethirajulu, K.; Mackie, C.; Howe, T.; Vianello, R. MetaSite: Understanding Metabolism in Human Cytochromes from the Perspective of the Chemist. *J. Med. Chem.* **2005**, *48*, 6970–6979.
- (57) Chen, X.; Murawski, A.; Patel, K.; Crespi, C. L.; Balimane, P. V. A Novel Design of Artificial Membrane for Improving the PAMPA Model. *Pharm. Res.* **2008**, *25*, 1511–1520.
- (58) Lipinski, C. A.; Lombardo, F.; Dominy, B. W.; Feeney, P. J. Experimental and Computational Approaches to Estimate Solubility and Permeability in Drug Discovery and Development Settings. *Adv. Drug Deliv. Rev.* **2001**, *46*, 3–26.
- (59) Hidalgo, I. J.; Raub, T. J.; Borchardt, R. T. Characterization of the Human Colon Carcinoma Cell Line (Caco-2) as a Model System for Intestinal Epithelial Permeability. *Gastroenterology* **1989**, *96*, 736–749.
- (60) Obach, R. S.; Baxter, J. G.; Liston, T. E.; Silber, B. M.; Jones, B. C.; MacIntyre, F.; Rance, D. J.; Wastall, P. The Prediction of Human Pharmacokinetic Parameters from Preclinical and in Vitro Metabolism Data. *J. Pharmacol. Exp. Ther.* **1997**, *283*, 46–58.
- (61) Banker, M. J.; Clark, T. H.; Williams, J. A. Development and Validation of a 96-Well Equilibrium Dialysis Apparatus for Measuring Plasma Protein Binding. *J Pharm Sci* **2003**, *92*, 967–974.
- (62) Stresser, D. M.; Blanchard, A. P.; Turner, S. D.; Erve, J. C.; Dandeneau, A. A.; Miller, V. P.; Crespi, C. L. Substrate-Dependent Modulation of CYP3A4 Catalytic Activity: Analysis of 27 Test Compounds with Four Fluorometric Substrates. *Drug Metab. Dispos.* **2000**, *28*, 1440–1448.
- (63) Ono, S.; Hatanaka, T.; Hotta, H.; Satoh, T.; Gonzalez, F. J.; Tsutsui, M. Specificity of Substrate and Inhibitor Probes for Cytochrome P450s: Evaluation of in Vitro Metabolism Using CDNA-Expressed Human P450s and Human Liver Microsomes. *Xenobiotica* **1996**, *26*, 681–693.

- (64) Polli, J. W.; Wring, S. A.; Humphreys, J. E.; Huang, L.; Morgan, J. B.; Webster, L. O.; Serabjit-Singh, C. S. Rational Use of in Vitro P-Glycoprotein Assays in Drug Discovery. *J. Pharmacol. Exp. Ther.* **2001**, 299, 620–628.
- (65) Mathes, C. QPatch: The Past, Present and Future of Automated Patch Clamp. *Expert Opin. Ther. Targets* **2006**, 10, 319–327.
- (66) Porsolt, R. D.; Anton, G.; Blavet, N.; Jalfre, M. Behavioural Despair in Rats: A New Model Sensitive to Antidepressant Treatments. *Eur. J. Pharmacol.* **1978**, 47, 379–391.
- (67) Detke, M. J.; Rickels, M.; Lucki, I. Active Behaviors in the Rat Forced Swimming Test Differentially Produced by Serotonergic and Noradrenergic Antidepressants. *Psychopharmacology (Berl.)* **1995**, 121, 66–72.
- (68) Kleven, M. S.; Assié, M. B.; Koek, W. Pharmacological Characterization of in Vivo Properties of Putative Mixed 5-HT_{1A} Agonist/5-HT_(2A/2C) Antagonist Anxiolytics. II. Drug Discrimination and Behavioral Observation Studies in Rats. *J. Pharmacol. Exp. Ther.* **1997**, 282, 747–759.

1
2
3
4
5
6
7
8
9
10
11
12
13
14
15
16
17
18
19
20
21
22
23
24
25
26
27
28
29
30
31
32
33
34
35
36
37
38
39
40
41
42
43
44
45
46
47
48
49
50
51
52
53
54
55
56
57
58
59
60

TABLE OF CONTENTS GRAPHIC

